CHAPTER 4

Contaminant Distribution

4.1 Introduction

This chapter is organized by contaminant category, beginning with semi-volatile organic compounds (SOCs), and followed by mercury, trace metals, spheroidal carbonaceous particles (SCPs), and finally nutrients. Atmospheric transport is also addressed. The SOCs include current- and historic-use pesticides (CUPs and HUPs), and industrial compounds such as polychlorinated biphenyls (PCBs) and combustion tracers (polycyclic aromatic hydrocarbons; PAHs). Within each section, data are discussed by medium—snow, air, vegetation, fish, and lake sediments. Lake water concentrations were generally very low and often below detection limits (see Figure 3-1 in Chapter 3). As such, lake water data are not reported in this chapter.

The contaminants found in greatest general abundance within each category are discussed with respect to both their spatial and their temporal distributions. Spatial distributions include the horizontal differences in contaminants among parks, as well as the elevational gradients. Whenever possible, study-wide data are displayed in order of decreasing latitude. Throughout each section, source attribution of individual contaminants is discussed. A separate section details the principal airsheds of each park.

4.2 Semi-Volatile Organic Compounds (SOCs)

For all results reported in this chapter, SOC compounds are grouped by compound classes, as listed in Table 4-1.

Table 4-1. Compound Groupings Used in Chapter 4.

Term Used	Definition
PCBs[1] or "sum PCBs"	Sum of 5 PCB congeners (118, 138, 153, 183, 187)
PBDEs[1] or "sum PBDEs"	Sum of 5 PBDE congeners (47, 99, 100, 153, 154)
PAHs[1] or "sum PAHs"	Sum of 16 PAHs (fluorene, anthracene, phenanthrene, fluoranthene, pyrene, retene, benzo(a)anthracene, chrysene/triphenylene, benzo(b)fluoranthene, benzo(k)fluoranthene, benzo(e)pyrene, benzo(a)pyrene, indeno(1,2,3-cd)pyrene, dibenz(a,h)anthracene, and benzo(ghi)perylene)
Endosulfans or "sum Endosulfans"	Sum of 3 endosulfans (I, II and sulfate)
Chlordanes or "sum Chlordanes"	Sum of 4 chlordanes (cis- and trans-chlordane, cis- and trans-nonachlor, excludes oxy-chlordane)
DDTs or “sum DDTs”	Sum of p,p′-DDT, o,p′-DDT, p,p′-DDE, o,p′-DDE, p,p′DDD, and o,p′-DDD
Total Pesticide	Sum of endosulfans, chlorpyrifos, dacthal, HCB, g-HCH, a-HCH, dieldrin, DDTs, and chlordanes

[1]PCBs = polychlorinated biphenyls; PBDEs = polybrominated diphenyl ethers; PAHs = polycyclic aromatic hydrocarbons

Figures 4-1 to 4-6 show key SOC compounds across all WACAP parks and in each medium—snow, air, lichen, conifer, fish, and surficial sediment (top-most sediment layer). The plots present average (arithmetic mean) concentrations or fluxes and their standard deviations. Polybrominated diphenyl ethers (PBDEs) were measured only in sediment and fish samples. Sections 4.2.1 to 4.2.5 discuss each medium separately. To minimize species differences, SOC concentrations in fish and lichens are reported per gram of lipid, rather than weight. Data are often presented on a log scale.

4.2.1 SOCs in Snow

Figures 4-1 to 4-5 show both concentrations and fluxes of SOCs in snow. Fluxes, in ng/m^2/yr, represent the total SOC input to the watershed from the accumulated springtime snowpack. The fluxes are calculated by multiplying the SOC concentration in the melted snow water (ng/L) by the accumulated amount of snow at the time of sampling, in liters water per m^2 per year (this is simply related to the height of the snowpack and its density or water equivalence). In general, CUPs, including endosulfans, chlorpyrifos, and dacthal, were detected in more than 90% of the snow samples (see Figure 4-1). Both a- and g-HCH (hexachlorocyclohexane) show similar spatial trends for snow (see Figure 4-2). NOAT and GAAR have higher a- and g-HCH fluxes than DENA, and the fluxes in the sites in the conterminous 48 states fall into a close range between 40 and 90 ng/m^2/yr. Within this range, g-HCH at GLAC has the highest flux and concentration. Hexachlorobenzene (HCB), dieldrin, and sum chlordanes are frequently detected in snow, even in the Alaska parks (see Figure 4-3). NOAT and GAAR have the highest measured snow concentrations for HCB and sum chlordane, at 0.023 and 0.057 ng/L, respectively.

Within each WACAP watershed, snow samples were collected at the same site for 3 consecutive years, providing important insight into the variability associated with contaminant deposition via snow. Samples collected at the same site at the same time (site replicates) show less than 20% relative standard deviation (RSD) in concentrations. Within one park, for the same year, the inter-site variability was 40-60%. Combined, inter-site and inter-annual variability within a park was much larger, at 80-120% RSD, for parks in the conterminous 48 states. For the Alaska parks, variability was even higher, approaching 140% RSD for the 3 years of sampling. The higher variability in snow concentrations and deposition in Alaska probably reflects the lower concentrations and lower snow amounts. The high variability among sampling years within a park highlights the importance of using same-year data to make inter-park comparisons and the importance of multi-year sampling to understand contaminant inputs to the park ecosystems.

Figure 4-7 shows the distribution of pesticides in snow observed at SEKI and MORA in the 3 years of sampling. For these parks, the concentration of pesticides in snow showed substantial year-to-year variability. For example, total pesticide concentrations at SEKI ranged from a low of 3.5 ng/g to a high of 10 ng/g. At MORA, total pesticides ranged from 0.38 ng/g to 0.63 ng/g. Despite this result, the pattern of SOCs at each park is clearly different from the other and is consistent for each park from year to year. At MORA, endosulfans have the highest concentration in all 3 years, whereas at SEKI, dacthal is highest in all 3 years. So, despite significant year-to-year variations in total concentrations, the pattern of pesticides deposited to each park is consistent for all 3 years of the WACAP study. This finding implies that the sources of pesticides to each park do not change significantly from year to year. It also implies that the sources influencing MORA and SEKI are different, given the different patterns of pesticides deposited. The year-to-year variation in snowpack concentration and flux implies that the SOC inputs to the ecosystem, via annual snowpack, vary substantially from year to year.

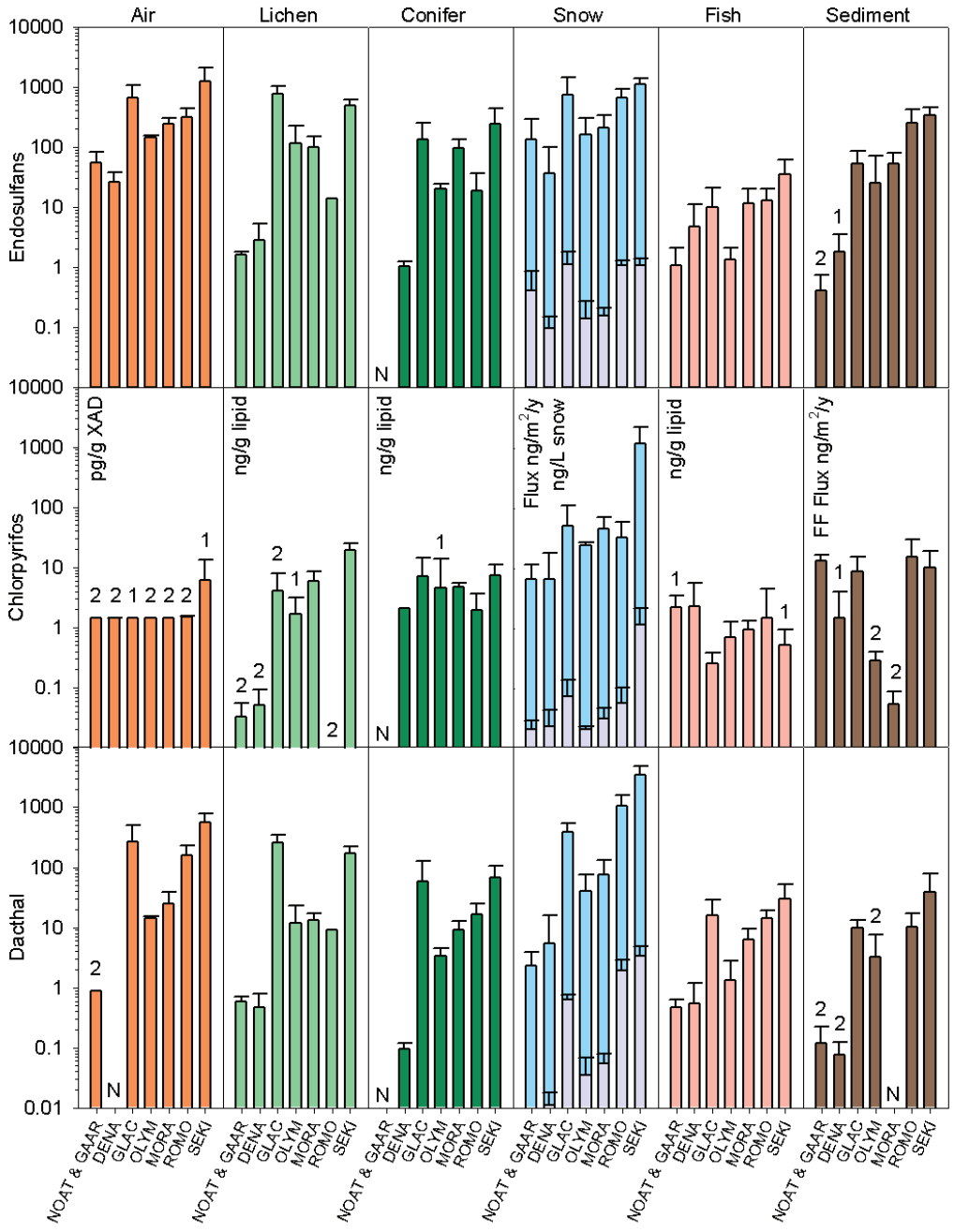

Figure 4-1. Current-Use Pesticides (CUPs): Average Concentrations and Fluxes of Sum Endosulfans, Chlorpyrifos, and Dacthal across Parks and Media. Snow data include fluxes in blue and concentrations in gray. Sediment data are reported as focusing factor-corrected (FF) flux for surficial sediment (top-most sediment layer) only. Conifer samples were not collected at NOAT and GAAR. If no label is present at the top of a bar, the component was detected in at least 70% of the samples. Below detection limit (BDL) values were replaced with half the estimated detection limit (EDL). 1 indicates that the analyte was detected in 50-70% of the samples and BDL values were replaced with half the EDL. 2 indicates that the analyte was detected in <50% of the samples and the value on the graph is half the EDL. N = no data.

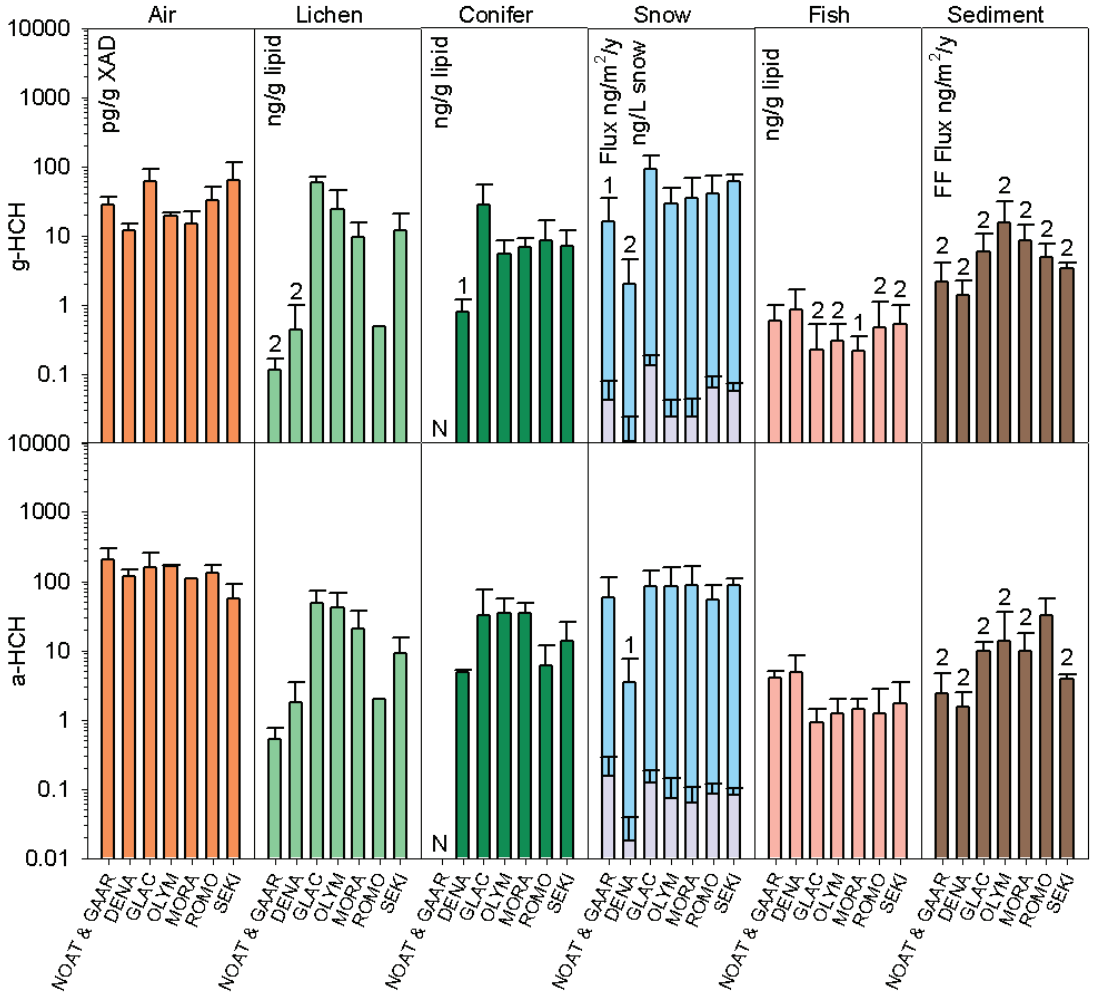

Figure 4-2. HCHs: Average Concentrations and Fluxes of a-HCH and g-HCH across Parks and Media. Snow data include fluxes in blue and concentrations in gray. Sediment data are reported as focusing factor-corrected (FF) flux for surficial sediment only. Conifer samples were not collected at NOAT and GAAR. 1, 2, and N codes are the same as for Figure 4-1.

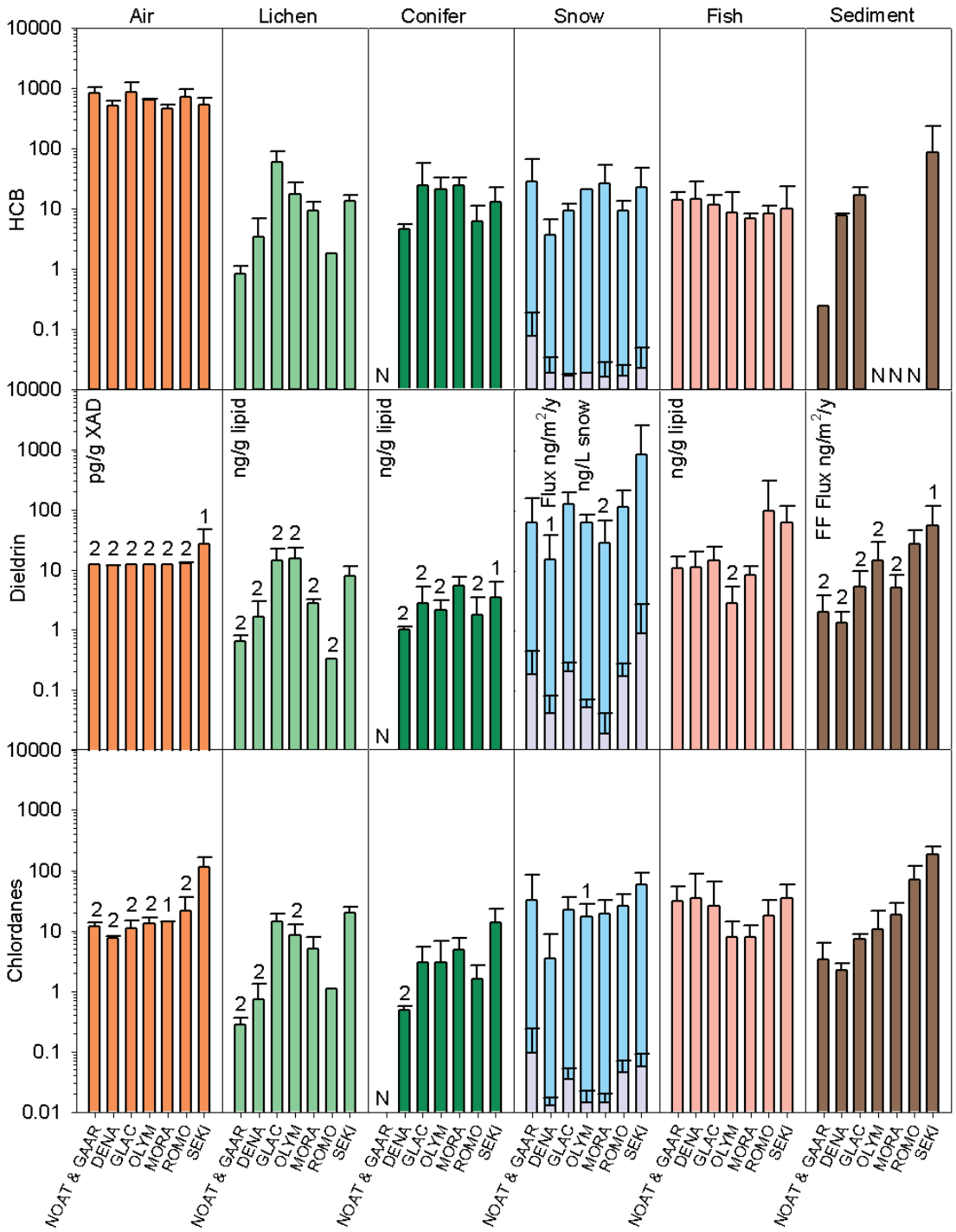

Figure 4-3. Historic-Use Pesticides (HUPs): Average Concentrations and Fluxes of HCB, Dieldrin, and Sum Chlordanes across Parks and Media. Snow data include fluxes in blue and concentrations in gray. Sediment data are reported as focusing factor-corrected (FF) flux for surficial sediment only. Conifer samples were not collected at NOAT and GAAR. 1, 2, and N codes are the same as for Figure 4-1.

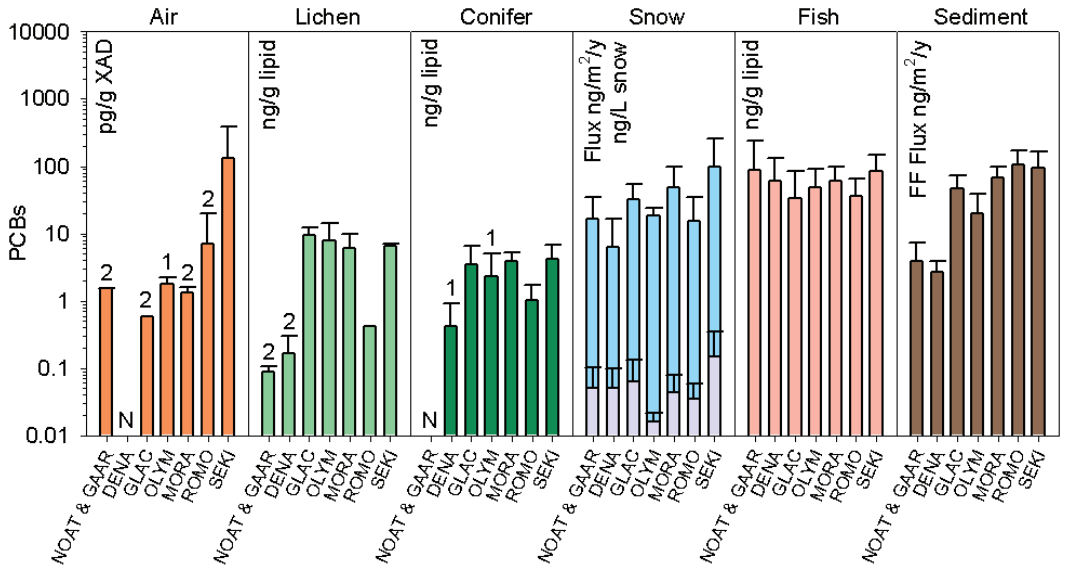

Figure 4-4. PCBs: Average Concentrations and Fluxes of Sum PCBs across Parks and Media. Snow data include fluxes in blue and concentrations in gray. Sediment data are reported as focusing factor-corrected (FF) flux for surficial sediment only. Conifer samples were not collected at NOAT and GAAR. 1, 2, and N codes are the same as for Figure 4-1.

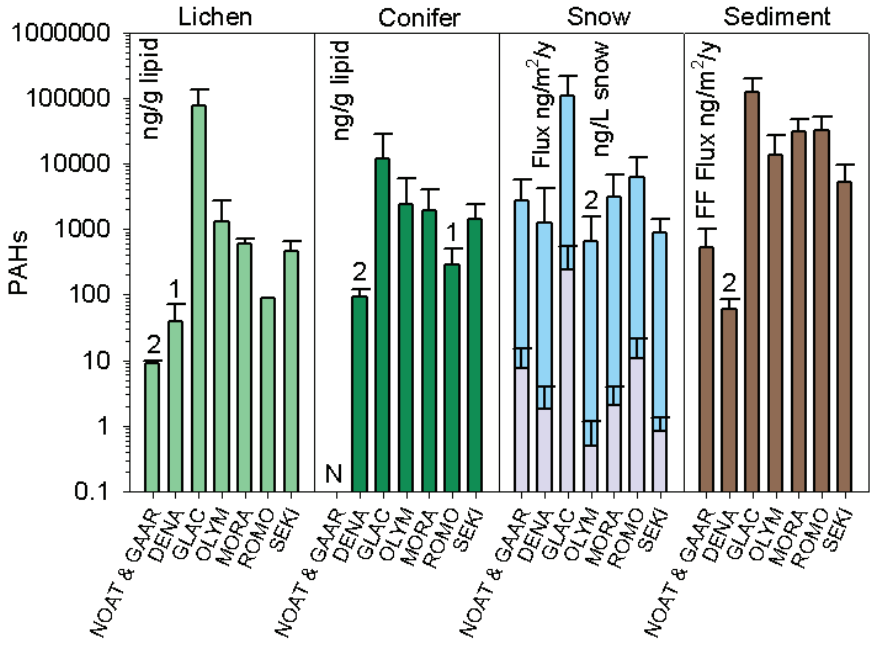

Figure 4-5. PAHs: Average Concentrations and Fluxes of Sum PAHs across Parks and Media. Snow data include fluxes in blue and concentrations in gray. Sediment data are reported as focusing factor-corrected (FF) flux for surficial sediment only. Conifer samples were not collected at NOAT and GAAR. 1, 2, and N codes are the same as for Figure 4-1.

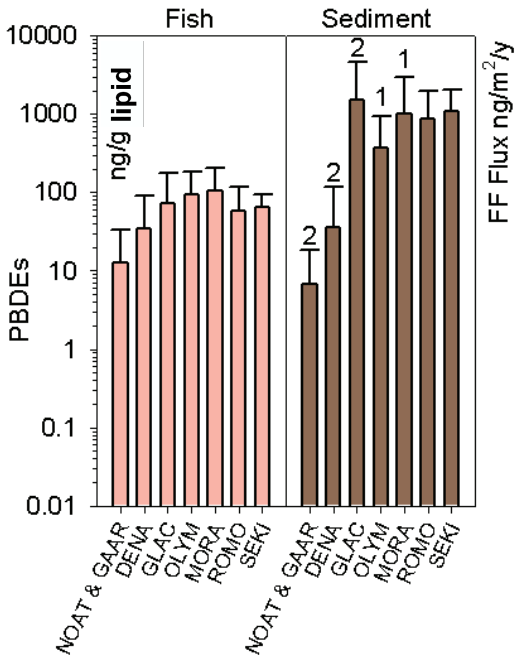

Figure 4-6. PBDEs: Average Concentrations and Fluxes of Sum PBDEs in Fish and Sediments across Parks. Sediment data are reported as focusing factor-corrected (FF) flux for surficial sediment only. 1, 2, and N codes are the same as for Figure 4-1.

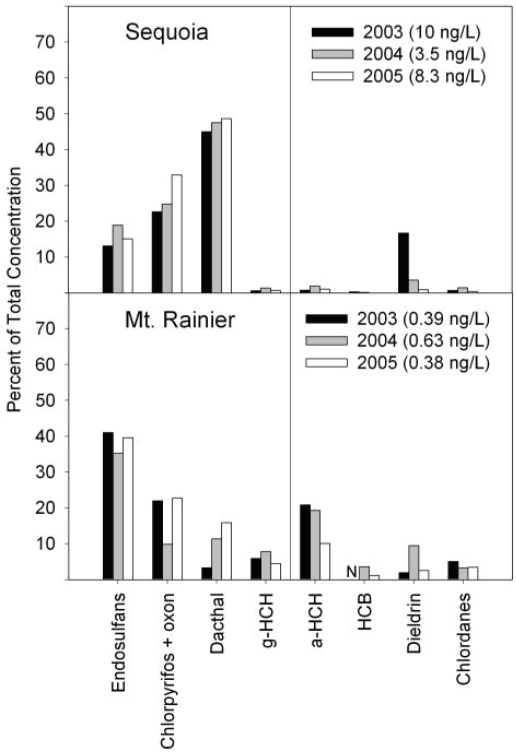

Figure 4-7. Annual Percent of Total Concentration in Snow for Current- and Historic-Use Pesticides at SEKI and MORA (after Hageman et al., 2006).

4.2.2 SOCs in Air

As described in Chapter 3, PASDs (passive air sampling devices) were deployed at both core and secondary parks for one year (± 2 weeks) to give a qualitative picture of atmospheric contamination. Following collection, the PASDs were analyzed to indicate regional patterns of SOC concentrations in ambient air.

The SOCs detected in air were similar to those detected in other media for each park, e.g., snow and vegetation (Figure 3-1 in Chapter 3); however, the concentrations of SOCs were generally much lower in the PASD sampling material, XAD (pg/g dry XAD), compared with concentrations in vegetation (ng/g lipid lichens or conifer needles; see Figures 4-1 to 4-4). Current-use pesticides, especially dacthal and endosulfans, were highest in parks in the conterminous 48 states (Figure 4-8), notably at SEKI. Of the historic-use pesticides, HCB and chlordanes appeared similar across all parks, whereas HCHs were as high in some Alaska parks as they were in parks in the conterminous 48 states (Figure 4-8). A few SOCs were detected primarily in the air of only one or two parks: chlorpyrifos (almost entirely as the degradation product Chlorpyrifos-oxon) at NOCA and SEKI; PCBs at SEKI; and p,p'-DDE at CRLA, SEKI, and BIBE (Figure 4-8). The fact that these contaminants occur at only a few parks suggests a regional source.

Simple linear regression of individual SOCs by latitude (Figure 4-9) yielded convincing evidence ($p < 0.003$) that concentrations of a-HCH *increase* and that concentrations of dacthal, endosulfans, and chlordanes *decrease* in the air with increasing latitude. There was suggestive evidence ($p < 0.1$) that PAHs and g-HCH also *decrease* with increasing latitude; p,p′-DDE was detected only at a few sites, all in the conterminous 48 states. The latitudinal increase of a-HCH in air in North America has been reported previously (Shen et al., 2005; Simonich and Hites, 1995) and is generally attributable to greater fractionation and lower revolatilization of this compound at colder temperatures. In Europe, HCB has been shown to increase with latitude (Meijer et al., 2003); however, this result was not observed in the WACAP data.

4.2.3 SOCs in Vegetation

4.2.3.1 Spatial Patterns of SOCs in Vegetation

4.2.3.1.1 Regional Patterns of Pesticide Accumulation in Lichens

Average total pesticide concentrations (Figure 4-10) in lichens were lowest (~5-10 ng/g lichen lipid) in parks in the Arctic and interior Alaska (GAAR, NOAT, and DENA), and increased southward with decreasing latitude. Mean park total pesticide concentrations were ~100 ng/g lipid in southern coastal Alaska (KATM, WRST, GLBA, and STLE) and were up to two orders of magnitude higher than concentrations in parks in the Arctic and interior Alaska (500-1,000 ng/g lipid) in some parks in the conterminous 48 states, notably YOSE, SEKI, GLAC, and GRSA. Pesticide concentrations in much of the central and southern Rockies (GRTE, ROMO, BAND, and BIBE) were comparable to the concentrations in the Pacific Northwest (200-300 ng /g lichen lipid). Means concentration comparisons are provided in Table 4-2.

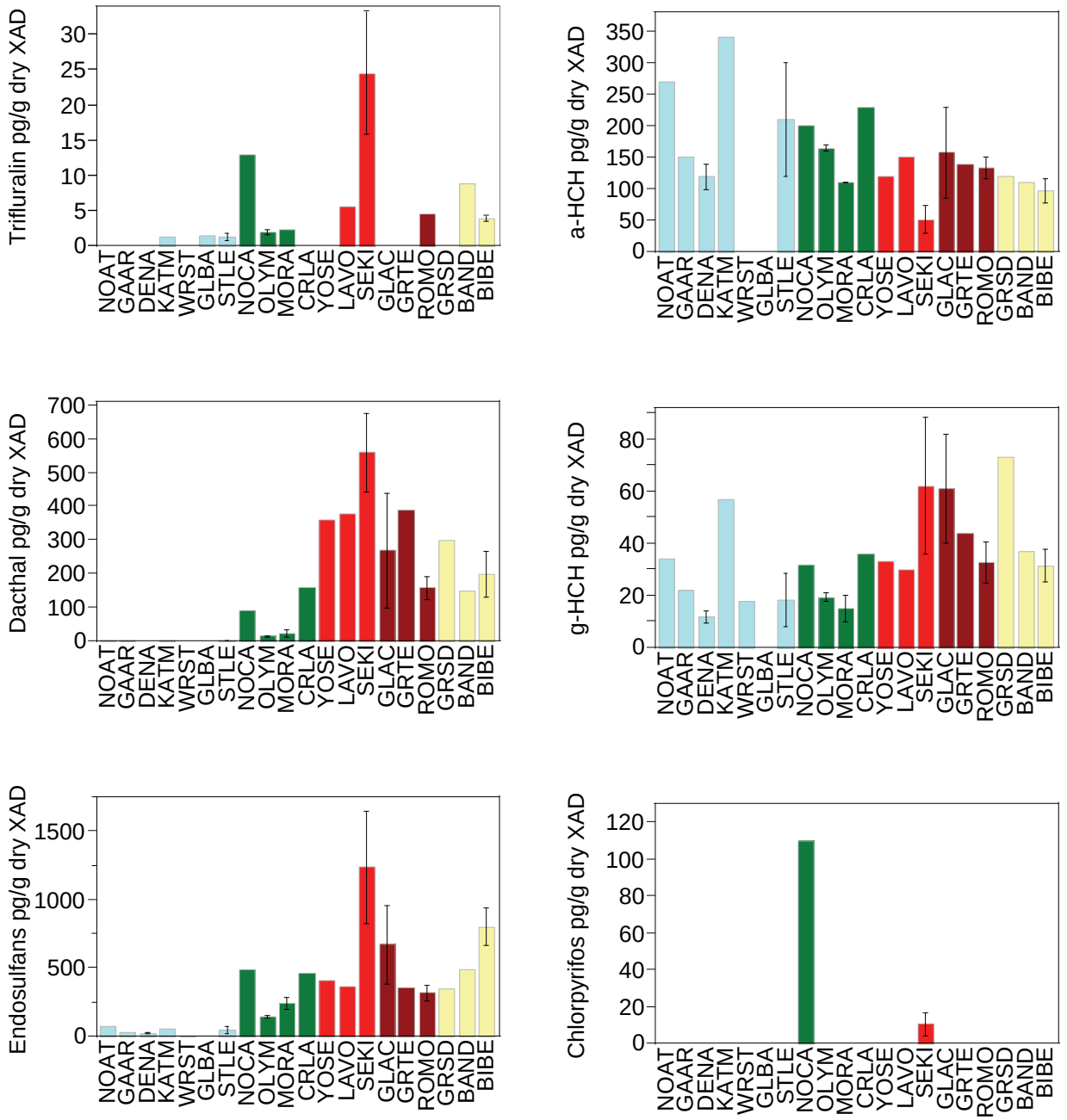

Figure 4-8. Regional Patterns of SOCs in Ambient Air as Indicated by Concentrations Accumulated in XAD Resin in Suspended Passive Air Sampling Devices (PASDs). From one to four PASDs were deployed in each WACAP park for one year beginning July 2005. Parks are listed from north to south from Alaska (light blue) through the Pacific Northwest (green) to California (red) and from the northern (brown) to southern (pale yellow) Rocky Mountains. Error bars indicate one standard error. (Figure continued on page 4-10.)

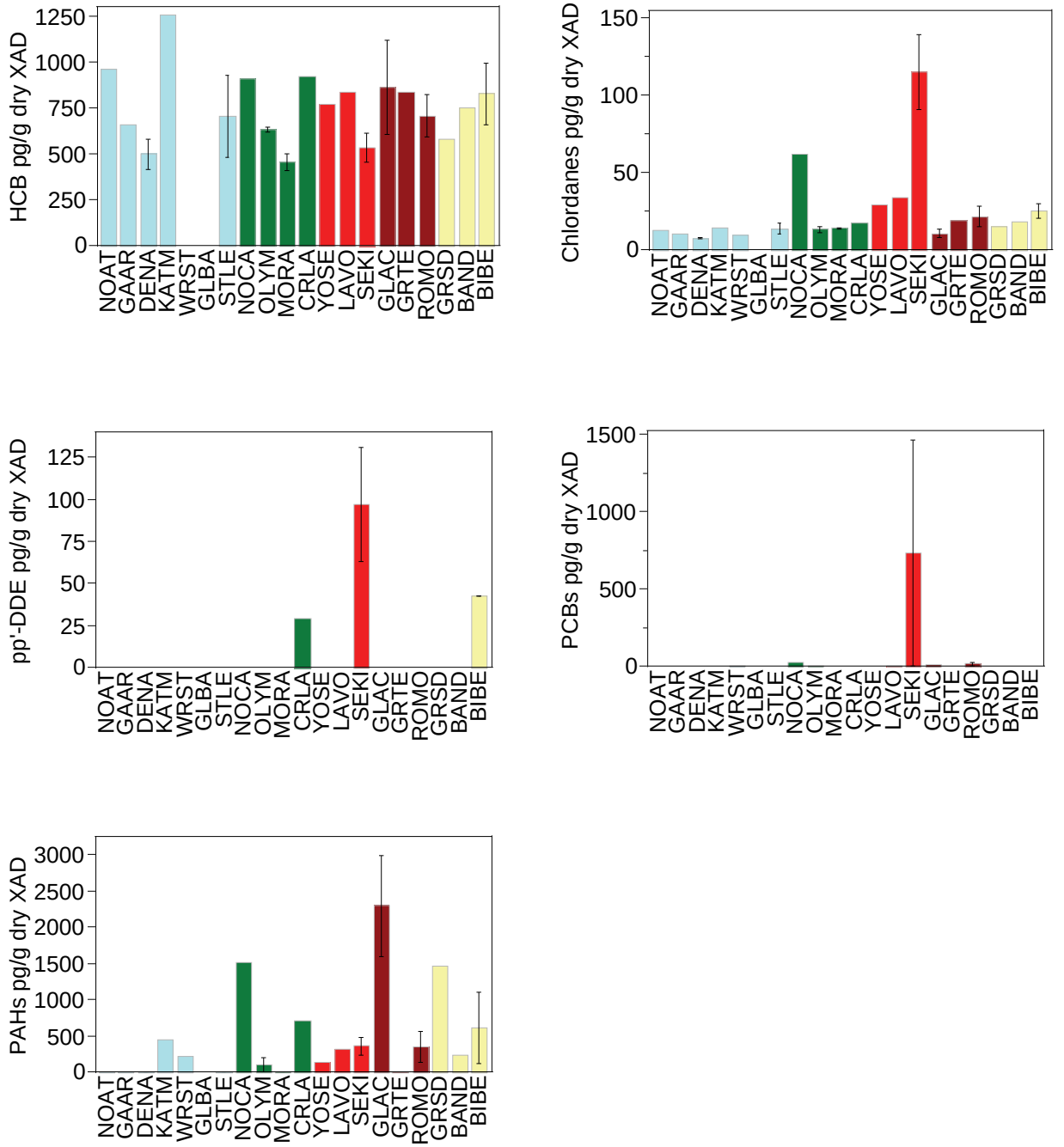

Figure 4-8 (continued).

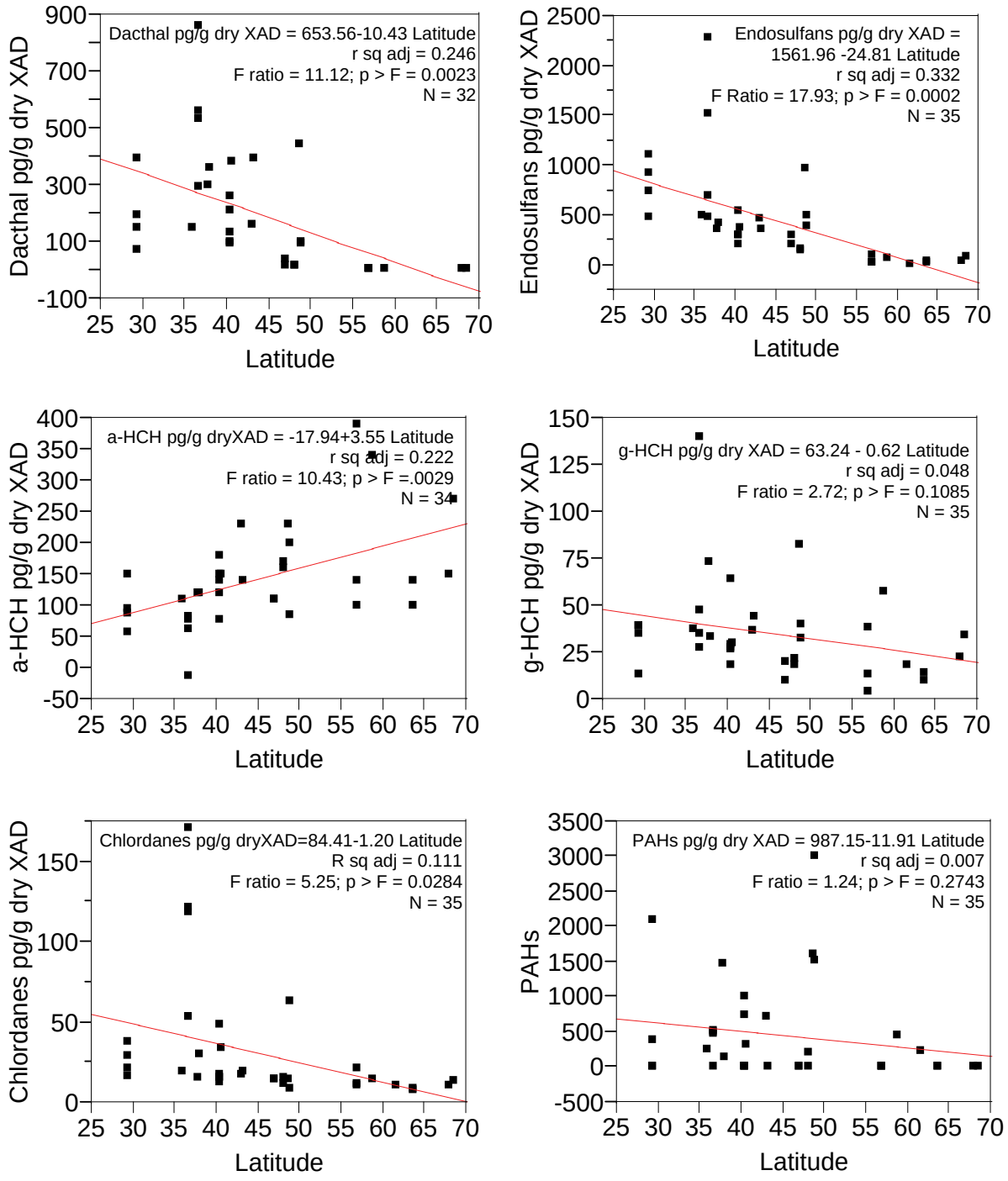

Figure 4-9. Simple Linear Regression of Individual SOCs Determined in the XAD Resin by Latitude.

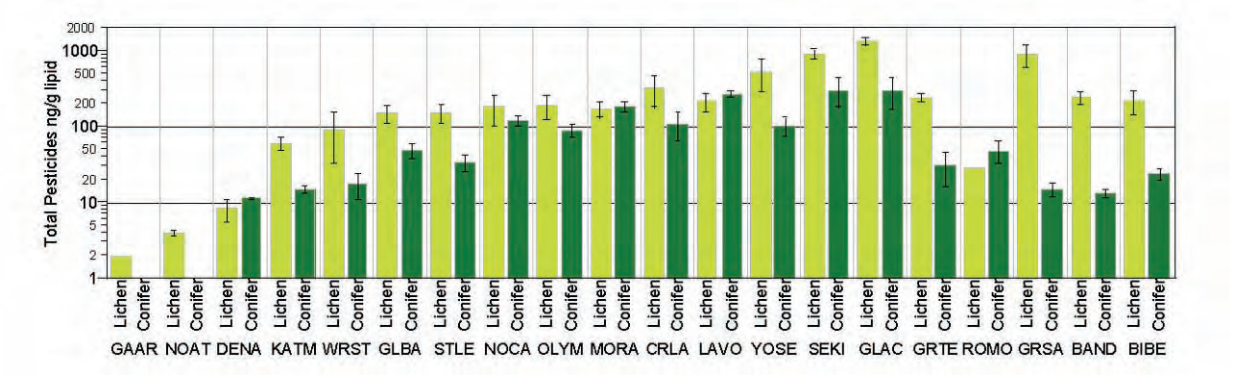

Figure 4-10. Comparison of Total Pesticide Concentrations in Lichen and Conifer Needle Vegetation from WACAP Parks in the Arctic (NOAT, GAAR), Interior Alaska (DENA), Coastal Alaska (KATM, WRST, GLBA, STLE), the Pacific Northwest (NOCA, OLYM, MORA, CRLA), California (LAVO, YOSE, SEKI), the Northern Rocky Mountains (GLAC, GRTE), and the Southern Rocky Mountains (ROMO, GRSA, BAND, BIBE). Note log scale; error bars indicate one standard error. No conifer samples were collected in the Arctic. Lichen concentrations increased more than 2 orders of magnitude from Arctic Alaska to the conterminous 48 states. Conifer concentrations increased about 1 order of magnitude from interior Alaska to the conterminous 48 states (excluding the central and southern Rocky Mountains, which were similar to coastal Alaska.

One might ask whether the very low SOC concentrations in the Arctic and interior Alaska lichen samples (NOAT, GAAR, DENA) occurred because these parks are most remote from source regions, or whether the low concentrations are an artifact of species differences, or, in the case of tundra lichens, snow burial. The answer appears to be mixed: lichen species can differ as accumulators of organic contaminants, and snow burial can enhance these differences. Specifically:

1. In DENA, where the tundra lichens (*Flavocetraria cucullata* and *Masonhalea richardsonii*) were both collected at multiple elevations, total pesticide concentrations in *F. cucullata* were 12 times higher than those in *M. richardsonii* (see DENA5 in Appendix 4A.1; paired t-tests, equal variances, $p < 0.05$), but did not differ from total pesticide concentrations in *F. cucullata* from WRST or KATM (Appendix 4A.2; Tukey-Kramer multiple means comparison, $\alpha = 0.05$). Similarly, total pesticide concentrations in *M. richardsonii* samples from DENA did not differ from those from NOAT and GAAR (where no *F. cucullata* was collected) (Appendix 4A.2; Tukey-Kramer multiple means comparison, $\alpha = 0.05$). Inductive reasoning indicates that total pesticide concentrations would have been comparable in all Alaska parks, had the same species been collected. Figure 4-11 depicts these patterns.

2. In KATM (Appendix 4A.3), where both tundra and epiphytic lichens were sampled, the epiphyte, *Hypogymnia physodes*, had higher concentrations of all SOCs except chlordanes and dacthal (not different) than the tundra lichen, *Flavocetraria cucullata* (t-test, equal variances, $p < 0.05$), as one would expect, assuming the tundra lichens are buried under snow in winter. SOC concentrations in the epiphyte were 1.5- to 4.6-fold higher, depending on the SOC, which is not large enough to account for concentration differences between tundra lichens in Alaska and epiphytic lichens from some parks of the conterminous 48 states, notably GLAC, SEKI, and GRSA, but is large enough to account for differences between tundra lichens in Alaska and epiphytic lichens from southern coastal Alaska parks and parks of the Pacific Northwest.

Table 4-2. Mean SOC Concentrations in Lichens and Conifer Needles (ng SOC/g lipid in vegetation) from Each WACAP Park. For each contaminant (i.e., within columns), concentrations that do not share a T-K letter are significantly different. The T-K letter indicates grouping derived from the Tukey-Kramer multiple means comparison test, α = 0.05). Blank cells indicate that all samples were below laboratory detection limits.

Lichens	**Current-Use Pesticides**					**Historic-Use Pesticides**						**Total Pesticides**				
Park	Trifluralin	Triallate	Chlorpyrifos	Dacthal	Endosulfans	HCB	a-HCH	g-HCH	Chlordanes	Dieldrin	DDTs	CUPs	HUPs	%CUPs	PCBs	PAHs
NOAT, GAAR				0.60 d	1.61 c	0.84 ab	0.53 bc		0.03 e			2.2 e	1.4 c	61 abcd	0.03 c	3 b
DENA				0.54 d	2.83 c	3.56 b	1.85 c	0.45 c				3.4 e	5.9 c	37 cd		87 b
KATM				0.58 d	19.72 c	25.17 ab	9.65 abc	2.61 bc	2.42 cde			20.3 e	39.9 c	34 e	1.79 c	262 b
WRST				1.34 d	25.21 c	50.06 ab	20.28 abc	5.32 bc	1.77 de			26.6 de	77.4 bc	26 e	1.97 bc	1258 b
GLBA	1.51 a				60.70 c	48.75 ab	28.00 abc	6.96 bc	4.91 cde			62.2 de	88.6 bc	41 de	7.08 abc	1264 b
STLE		0.60 b	0.60 b	6.09 d	76.66 c	40.86 ab	30.67 abc	7.60 bc	2.50 de			84.0 de	81.6 bc	51 de	2.70 bc	780 b
NOCA	0.17 a	5.20 b	5.20 b	15.44 d	119.30 c	18.74 ab	12.92 abc	5.50 bc	2.19 cde		5.72 c	145.3 de	45.1 bc	76 a	4.07 abc	1960 b
OLYM	0.89 a	1.57 b	1.57 b	12.91 d	117.92 c	21.31 ab	43.33 ab	23.47 b	3.04 cde			134.9 de	91.2 bc	60 bcd	7.84 abc	2175 b
MORA	6.00 a		6.00 b	13.21 d	101.14 c	9.27 ab	20.84abc	9.67 bc	5.14 cde		2.96 c	126.4 de	47.9 bc	73 ab	6.18 abc	764 b
CRLA		4.37 b	4.37 b	57.63 bcd	205.38 bc	18.35 ab	14.98 abc	4.69 bc	12.04 bcd		10.88 c	271.8 cde	60.9 bc	82 abc	5.91 abc	1103 b
LAVO				75.00 bcd	101.98 c	10.90 ab	10.73 abc	3.58 bc	11.14 bcde	3.14 a	31.08 bc	177.0 de	70.6 bc	71 ab	4.04 abc	315 b
YOSE	1.88 a	19.83 a	19.83 a	204.67 a	227.57 bc	16.80 ab	6.93 abc	4.00 bc	13.85 abc		34.80 bc	473.8 bcd	76.4 bc	86 a	5.49 abc	2096 b
SEKI	0.94 a	19.33 a	19.33 a	169.75 ab	487.75 b	13.33 ab	9.24 abc	12.16 bc	19.84 ab	8.01 a	159.95 a	697.1 ab	222.5 a	76 a	6.48 abc	814 b
GLAC	1.00 a	5.28 b	5.28 b	242.61 a	775.34 a	55.06 a	45.00 a	65.06 a	9.15 cde		113.40 ab	1029.5 a	287.7 a	78 a	9.39 a	72758 a
GRTE	0.13 a	4.10 ab	4.10 ab	39.75 bcd	144.25 bc	11.85 ab	9.00 abc	5.30 bc	4.51 cde	1.45 a	16.50 bc	192.3 bcde	48.6 bc	80 ab	2.87 abc	571 b
ROMO				9.00 bcd	14.00 c	1.83 ab	2.01 abc	0.49 bc	1.12 cde			23.0 cde	5.5 bc	81 abc	0.42 abc	100 ab
GRSA	0.63 a			175.00 abc	536.00 ab	65.50 ab	32.00 abc	11.00 bc	28.25 a		71.79 abc	711.6 abc	208.5 ab	77 ab	11.60 ab	667 b
BAND	0.51 a	5.10 ab	5.1 ab	39.80 cd	138.35 c	10.99 ab	10.37 abc	5.78 bc	7.433 cde		29.98 bc	188.9 de	64.6 bc	75 ab	4.734 abc	190 b
BIBE				9.8d	190.00 bc	3.45 ab	2.50 abc	2.68 bc	2.06 cde		12.40 bc	199.8 bcde	23.1 bc	90 a	1.97 abc	484 b
Conifers	**Current-Use Pesticides**					**Historic-Use Pesticides**						**Total Pesticides**				
Park	Trifluralin	Triallate	Chlorpyrifos	Dacthal	Endosulfans	HCB	a-HCH	g-HCH	Chlordanes	Dieldrin	DDTs	CUPs	HUPs	%CUPs	PCBs	PAHs
DENA			0.86 b	0.09 bcd	0.69 bc	4.53 a	4.82 ab	0.80 a	0.15 bc			1.6 d	10.3 b	14 h	0.56 ab	96b
KATM			0.63 b	0.26 d	1.68 c	7.76 a	4.44 ab	1.15 a	0.17 bc			2.6 d	13.5 b	16 gh	0.13 b	59 b
WRST			0.61 b		1.16 c	6.15 a	1.93 b	7.42 a	0.15 bc			1.8 d	15.7 b	10 h		40b
GLBA			2.35 b	0.10 d	1.63 bc	7.40 a	5.38 ab	32.76 a	0.44 bc			4.1 d	46.0 ab	8 h		131b
STLE			0.81 b	0.44 d	1.66 c	9.09 a	4.69 ab	16.63 a	0.33 bc			2.9 d	30.7 ab	9 h	0.18 b	227b
NOCA				9.36 bcd	42.52 b	26.00 a	31.80 ab	5.74 a	2.22 bc		6.61 ab	51.9 cd	72.4 ab	42 fe	1.66 ab	2429b
OLYM	2.31 a		1.62 b	3.36 d	19.99 bc	20.80 a	34.20 a	5.38 a	2.57 bc			27.3 d	63.0 ab	30 cde	2.33 ab	2462 b
MORA			1.68 b	9.11 bcd	93.57 abc	23.83 a	34.87 a	6.71 a	4.94 bc	5.56 a	2.13 b	104.4 bcd	78.0 ab	57 fg	3.89 a	1955 b
CRLA	0.27 a			21.12 bc	42.27 bc	21.36 a	16.58 ab	3.71 a	1.45 bc			63.7 bcd	43.1 ab	60 de	0.84 ab	826 b
LAVO			2.00 b	85.80 a	136.28 ab	14.60 a	16.80 ab	4.28 a	6.00 b		4.85 ab	224.1 ab	46.5 ab	83 a	1.31 ab	2170 b
YOSE			7.45 a	53.20 abcd	19.23 bc	14.63 a	6.30 ab		3.15 bc			79.9 bcd	24.1 ab	77 ab	1.10 ab	3787 b
SEKI			2.48 b	66.42 ab	191.72 a	12.61 a	13.79 ab	6.99 a	13.81 a	3.83 a	19.03 a	260.6 a	70.1 ab	79 ab	4.19 a	3255 b
GLAC		13.73 a	2.39 b	58.20 abc	132.09 abc	24.11 a	31.78 ab	27.45 a	2.28 bc		7.46 ab	206.4 abc	93.1 a	69 abc	3.46 ab	20044 a
GRTE		4.13 a	1.01 b	10.35 bcd	8.01 bc	6.91 a	5.80 ab	0.80 a	0.36 bc			23.5 d	13.9 b	63 bcd	0.73 ab	186b
ROMO			0.80 b	16.39 bcd	15.12 b	6.24 a	6.17 ab	8.36 a	1.12 bc		1.51 b	32.3 d	23.4 ab	58 cd	1.04 ab	242 b
GRSA				4.08 cd	6.06 bc	3.42 a	1.45 b					10.1 d	4.9 b	68 abcd	1.22 ab	134b
BAND				4.99 cd	2.69 c	3.26 a	2.22 b		0.09 c			7.7 d	5.6 b	58 cd	1.08 ab	221 b
BIBE			1.63 b	2.17 bcd	12.05 bc	5.27 a	2.47 ab		0.30 bc			15.9 cd	2.8 ab	85 abcd	0.12 ab	20 b

3. Pesticide concentrations in tundra lichens (*Cladina arbuscula* and *Flavocetraria cucullata*) collected at WRST and STLE appeared to be comparable to those in the non-buried lichen epiphyte, *Alectoria sarmentosa*, indicating that some tundra lichen species accumulate pesticides as well as some epiphtyes. *Alectoria sarmentosa* appears to be as poor an accumulator among the epiphytic lichens as *M. richardsonii* is among the tundra lichens (Figure 4-11; Appendix 4A.4).

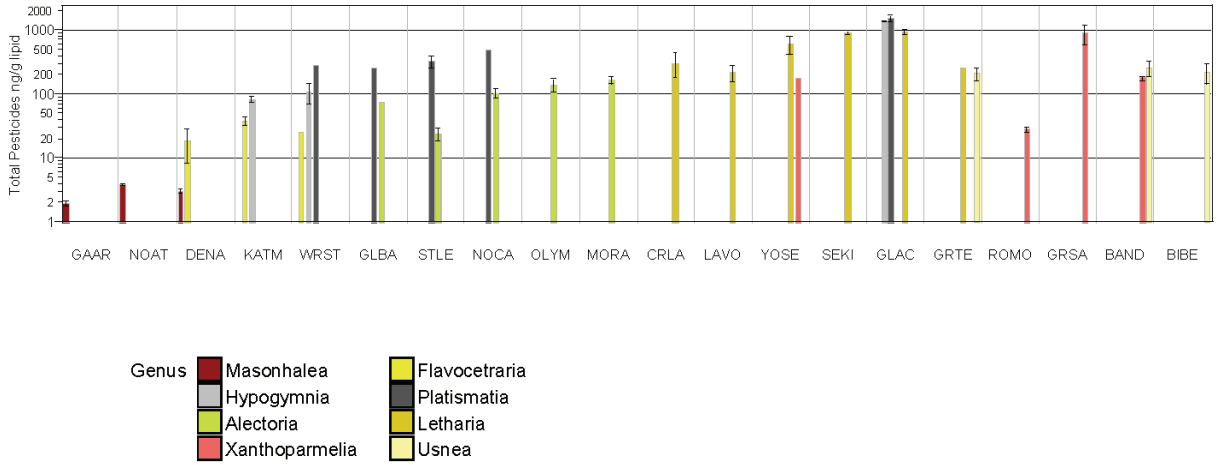

Figure 4-11. Comparison of Total Pesticide Accumulation in Lichen Species by Park from North to South along the Pacific Coast (GAAR to SEKI) and from North to South in the Rocky Mountains (GLAC to BIBE). Pesticide concentrations generally increased from north to south along the Pacific Coast and decreased from north to south in the Rocky Mountains (with the exception of GRSA, where intensive local agriculture might have influenced accumulation). Some lichens are better accumulators than others; of the tundra lichens, *Flavocetraria* accumulated more pesticides than *Masonhalea*; of the epiphytes, *Platismatia* accumulated more pesticides than *Alectoria*. Standardizing species can reduce noise in contaminant data.

In conclusion, inter-species differences in accumulation rates, and possibly snow burial, appear to account to some extent for low concentrations of pesticides in lichens from northern Alaska parks compared to those in lichens from parks in coastal Alaska and many conterminous 48 states. However, in any analysis disregarding (Table 4-2) or accounting for species differences (Appendix 4A.2), lichens from GLAC, SEKI, and sometimes YOSE and GRSA had higher pesticide concentrations than lichens in other parks.

4.2.3.1.2 Regional Patterns of Pesticide Accumulation in Conifer Needles

Regional patterns of pesticide accumulation in conifer needles were similar to patterns in lichens, except that the difference between samples from parks with lowest and highest concentrations was only about one order of magnitude (Appendices 4A.4 and 4A.7). Parks in the Arctic are largely treeless, and no conifer needles were collected there. The average total pesticide concentration in conifer needles from DENA was 11 ng/g lipid in needles. Concentrations of pesticides in conifer needles increased with southerly latitudes, maximizing in the Pacific Northwest and California and in GLAC in the northern Rockies at 100-200 ng/g lipid. Average total pesticide concentrations in conifer needles from parks of the central and southern Rockies were comparable to those in the Canadian Rockies (Davidson et al., 2003; Davidson et al., 2004) and coastal Alaska (20-30 ng/g lipid). Mean comparison tests disregarding (Table 4-2) or

accounting for species differences between parks (Appendix 4A.5) support lichen data, in that conifer needles from SEKI, GLAC, and YOSE were most likely to have higher concentrations of SOCs than conifer needles in other parks.

The main discrepancy between vegetation sample types is the low concentration of total pesticides in conifer needles, compared to lichens, in the central and southern Rockies. The genus *Pinu*s, the only species collected in parks from the central and southern Rocky Mountains, appears to accumulate lower concentrations of nearly all SOCs than other coniferous species in parks (Appendix 4A.6). For example, if fir had been sampled instead of pine, SOC concentrations in needles in the southern Rockies parks (GRSA, BAND, and BIBE) might have been closer to concentrations in needles in the Pacific Northwest, as they were in lichens. It is also possible that the drier, warmer climates of the southern Rockies affect lichen and conifer uptake differently. Pine was also collected exclusively at YOSE, where needle SOC concentrations might otherwise have been intermediate to LAVO and SEKI (see subsection 4.2.3.2.3). Finally, it seems unlikely that snow burial can account for the magnitude of difference between northern Alaska and other WACAP parks, because SOC concentrations in conifer needles at the lowest elevations in DENA were substantially smaller than concentrations in samples from the highest elevation sites in other parks, which presumably are also buried under snow for many months of the year.

4.2.3.1.3 General Observations Regarding Pesticides in WACAP Vegetation

The current-use pesticides, endosulfans and dacthal, dominated total pesticide loading in vegetation samples from the conterminous 48 states (Figures 4-12 and 4-13, Table 4-2). This observation is consistent with the proximity of parks in the conterminous 48 states to large-scale agriculture, compared with Alaska parks. Agricultural intensity within 150 km of a park is strongly correlated with concentrations of these CUPs in vegetation. The Spearman's Rho correlation for dacthal and agricultural intensity was 0.873 for conifer needles and 0.849 for lichens; the Spearman's Rho correlation for endosulfan and agricultural intensity was 0.777 for conifer needles and 0.743 for lichens (see Table 5-15 in Chapter 5). Average regional concentrations of dacthal and endosulfans in lichens were 2 and 31 ng/g lipid, respectively, in Alaska parks and 82 and 243 ng/g lipid, respectively, in parks of the conterminous 48 states. Trifluralin and triallate in conifer needles and chlorpyrifos in lichens were below detection limits at all Alaska parks.

Historic-use pesticides, especially HCB, a-HCH, and g-HCH, comprised a larger fraction of the total contaminant concentration in Alaska parks, compared to parks in the conterminous 48 states, and concentrations were similar across parks, varying about one order of magnitude between lowest (NOAT, GAAR, DENA, ROMO, BIBE) and highest (GRSA, GLAC) measurements in both types of vegetation (Figures 4-12 and 4-13, Table 4-2). Endosulfan and dacthal comprised less than half of total pesticide concentrations in vegetation from Alaska parks, in contrast to parks in the conterminous 48 states. Dieldrin and DDTs were not detected in any Alaska parks in either conifer needles or lichens. Where they were detected in parks in the conterminous 48 states, mean dieldrin concentrations were < 20 ng/g lipid; DDT ranged up to 110 and 160 ng/g lipid at SEKI and GLAC, respectively.

Agricultural intensity, nitrogen availability as indicated by ammonium nitrate in fine particulates sampled by park IMPROVE monitors, and population density were positively correlated with SOC concentrations in vegetation. Many of the SOCs were also correlated with each other (i.e.,

parks with high concentrations of one SOC tended to have high concentrations of other SOCs). Agricultural intensity and population density were confounded (Spearman's Rho = 0.63 to 0.68), probably because many major western cities are built in valleys and at lower elevations where conditions are optimal for both habitation and agriculture (compare backgrounds of Figure 4-12 or 4-13 with Figure 4-19 later in this chapter). For lichens, stronger correlations were observed between SOC concentrations and agricultural intensity, but for conifer needles, correlation strength was comparable between agricultural intensity and population density. See Chapter 5 for a table (Table 5-15) and a discussion of strongest correlations.

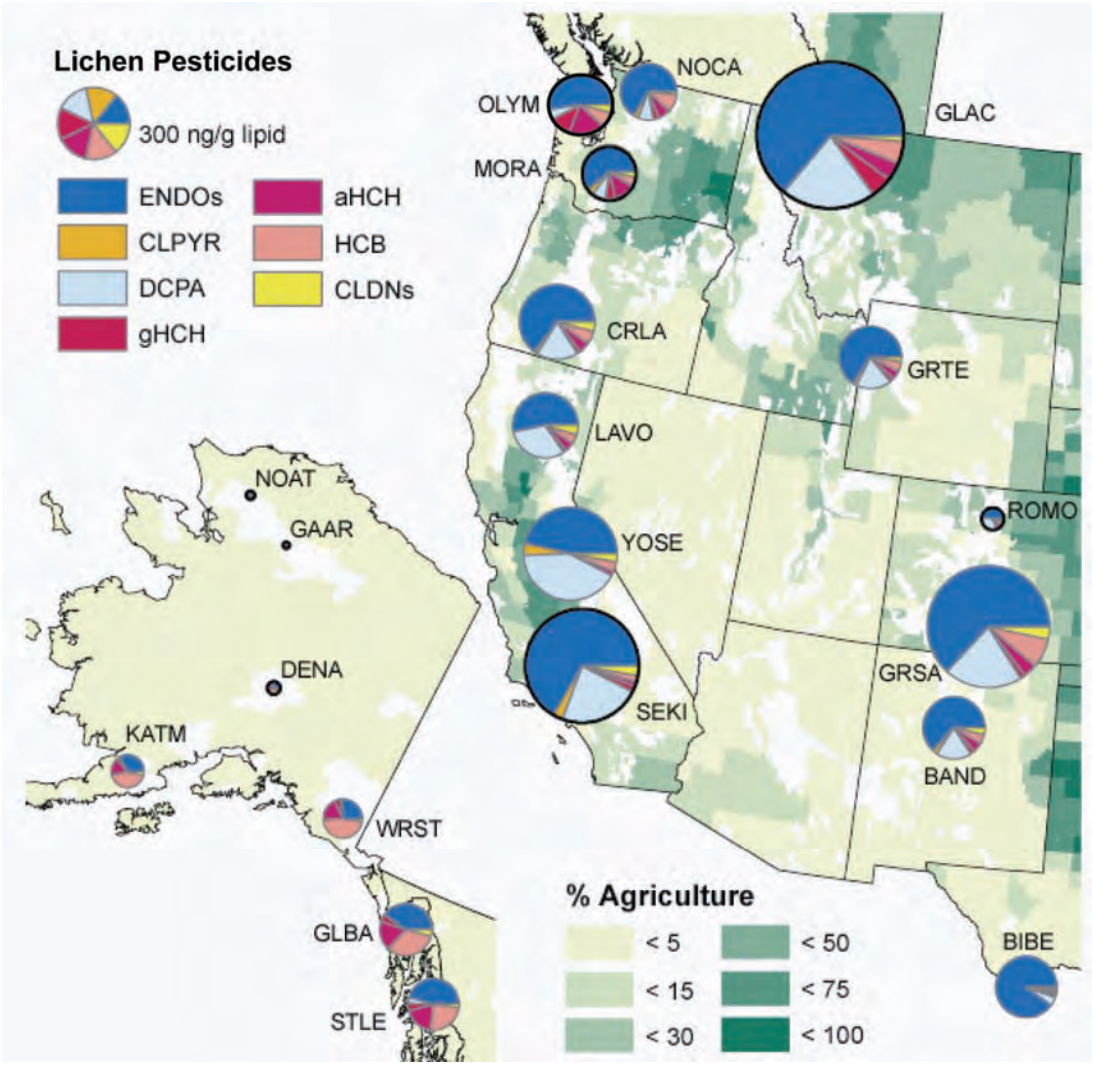

Figure 4-12. Pesticide Concentrations (ng/g lipid) in Lichens from Core and Secondary WACAP Parks Overlaid on a Map of Agricultural Intensity (US Department of Agriculture, National Agriculture Statistics Service, 2002). Circle area is proportional to total pesticide concentration. Light to dark green shading indicates increasing agricultural intensity. White shading indicates national forests or parks. Current-use pesticides endosulfan and dacthal dominate pesticide concentrations in parks in the conterminous United States, where most agriculture occurs. Historic-use pesticides comprise a relatively larger fraction of total pesticide concentrations in Alaska. Sites outlined in black are the core parks. Pesticide groups are endosulfans (ENDOs), chlorpyrifos (CLPYR), dacthal (DCPA), g-HCH and a-HCH (gHCH and aHCH), HCB, and chlordanes (CLDNs).

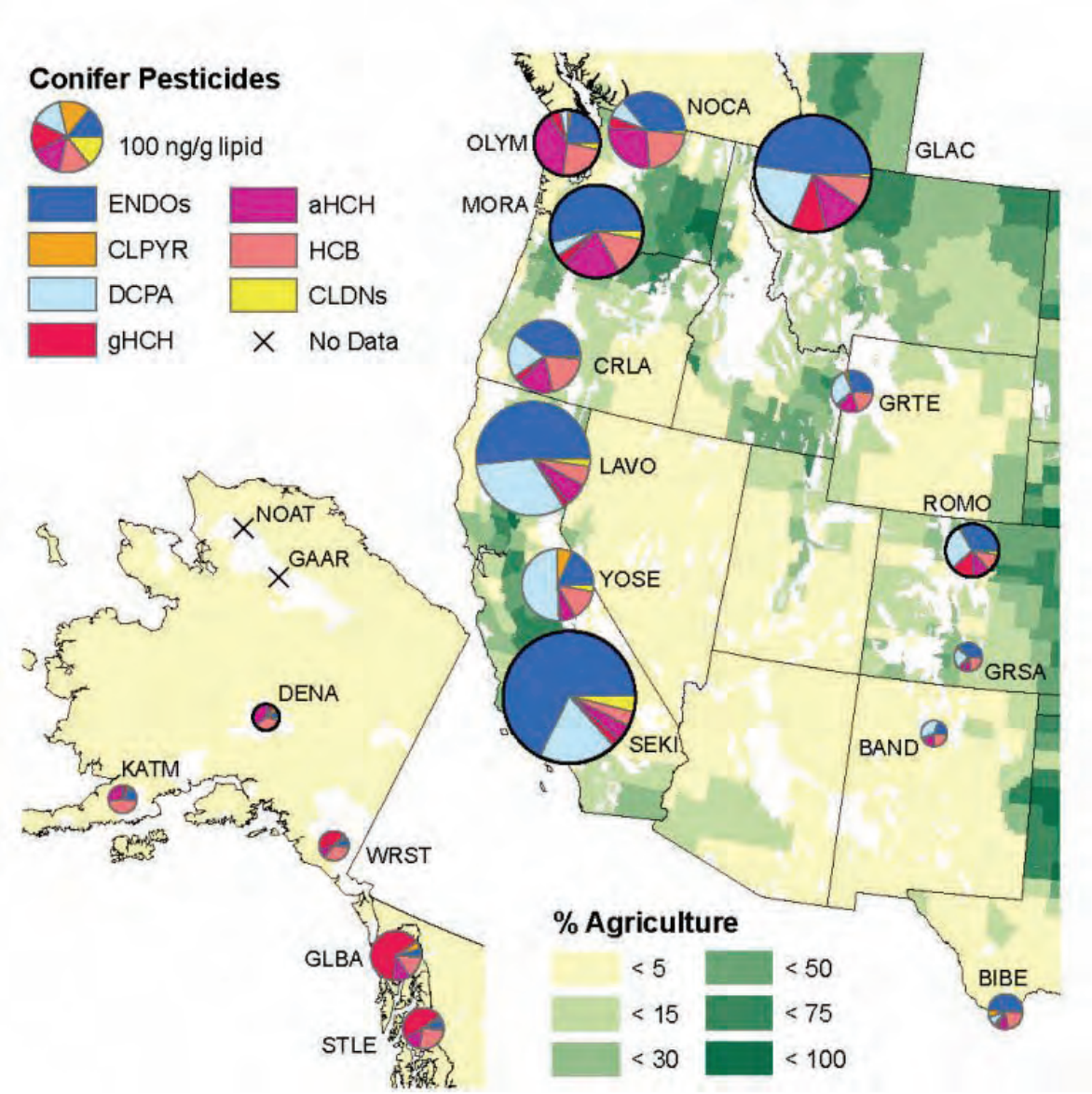

Figure 4-13. Pesticide Concentrations (ng/g lipid) in Conifer Needles from Core and Secondary WACAP Parks Overlaid on a Map of Agricultural Intensity (US Department of Agriculture, National Agriculture Statistics Service, 2002). Circle area is proportional to total pesticide concentration. Light to dark green shading indicates increasing agricultural intensity. White shading indicates national forests or parks. Current-use pesticides endosulfan and dacthal dominate pesticide concentrations in parks in the conterminous United States, where most agriculture occurs. Historic-use pesticides are relatively more important in Alaska, although total contaminant concentrations are lower. Conifers were not present in NOAT and GAAR. Sites outlined in black are the core parks. Pesticide coding is identical to that in Figure 4-12.

Concentrations of individual current-use pesticides in park vegetation appear to be markedly influenced by local usage. Because different types of crops are grown in different parts of the country, application rates (g/ha) of crop-specific insecticides and herbicides vary regionally across the United States. A visual comparison among maps of application rates of chlorpyrifos (Figure 4-14), dacthal (Figure 4-15), endosulfans (Figure 4-16), triallate (Figure 4-17), and trifluralin (Figure 4-18) in the western United States, with concentrations detected in vegetation, shows good agreement, especially if back trajectories are considered. In vegetation, application rate does not necessarily correspond with concentrations. For example, chlorpyrifos are applied at higher rates than endosulfans and dacthal but concentrations in vegetation were fairly low.

PAHs. Total PAH concentrations were lowest in the Arctic (<10 ng/g lipid) and in parks in central Alaska (<500 ng/g lipid), increasing in concentration and number of compounds with decreasing latitude along the Pacific Coast from southeastern Alaska (<5,000) to southern California (<20,000), peaking in GLAC (up to 200,000 ng/g lipid) and lower in the rest of the Rockies (<1,100 ng/g lipid) (see also Figure 4-19). The number of PAH compounds detected generally increased with total PAH concentration from 2 in the arctic to 17 in GLAC.

The PAHs detected in greatest concentrations (10 to 10,000 ng/g lipid) and in most or all parks were fluorene, phenanthrene, fluoranthrene, pyrene, retene, chrysene/triphenylene, and benzo(a) anthracene. The other PAHs detected in vegetation—acenaphthylene, acenapthene, anthraxcene, benzo(b)fluoranthene, benzo(a)pyrene, indeno(1,2,3-cd)pyrene, dibenz(a,h)anthraxcene, and benzo(ghi)perylene—were detected in fewer parks, usually at concentrations < 100 ng/g lipid. One exception is the west side of the Continental Divide in GLAC, where concentrations of these PAHs were higher, but decreased with distance and elevation from Columbia Falls, Montana. Total PAH concentrations in vegetation reported in this document could be overestimated because of the co-elution of matrix interferences.

PCBs. Compared to the major herbicides and PAHs, concentrations of PCBs were very low in both lichens and conifer needles, and no discernable regional patterns were observed, either in total accumulation of PCBs or the relative proportions of PCBs detected (Table 4-2).

4.2.3.2 Effects of Species on SOC Concentrations in Vegetation

4.2.3.2.1 Conifer Needles vs. Lichens

The relative contribution of individual SOCs to the total contaminant concentration in vegetation of the 20 WACAP parks was similar in conifer needles and lichens: PAHs > endosulfans > dacthal > HCB and a-HCH (Table 4-2). However, SOC concentrations were usually higher in lichens than in conifer needles, even after lipid normalization. Specifically, paired t-tests of conifer vs. lichen SOC concentrations at 69 WACAP sites where both vegetation types were collected provided evidence that mean concentrations of chlorpyrifos, dacthal, endosulfans, HCB, chlordanes, DDTs, PCBs, and PAHs were 2.6 to 9.0 times higher in lichens than in conifer needles (Prob > t < 0.05; see Appendix 4A.7). Only a-HCH and g-HCH concentrations did not differ among the vegetation types, and no compounds were higher in conifer needles than in lichens. Although there was no evidence that dieldrin, trifuralin, and triallate concentrations differed between vegetation types, statistical power was low because only 3, 1, and 7 of the 69 sites, respectively, had detectable concentrations of SOCs in both media.

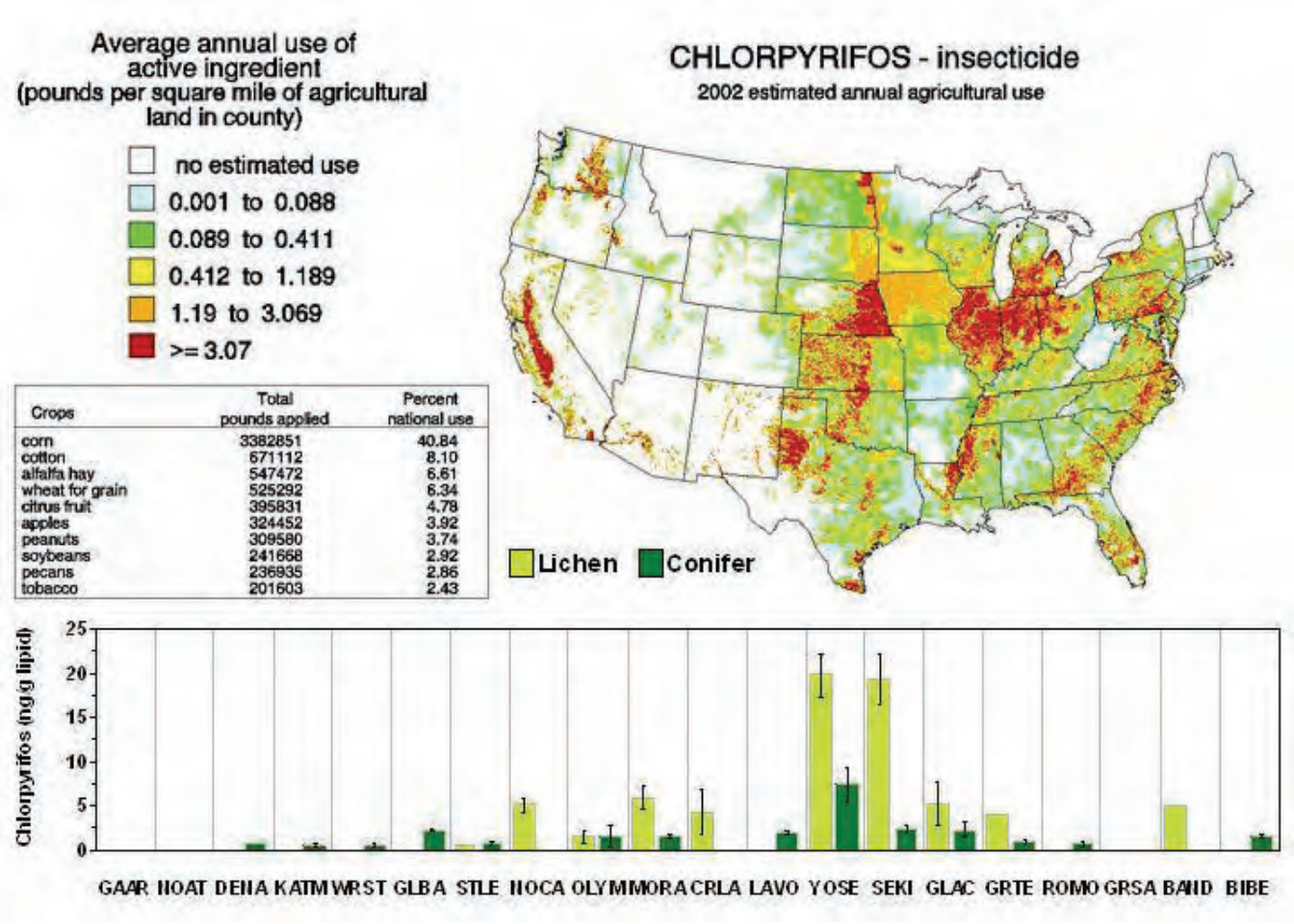

Crops	Total pounds applied	Percent national use
corn	3382851	40.84
cotton	671112	8.10
alfalfa hay	547472	6.61
wheat for grain	525292	6.34
citrus fruit	395831	4.78
apples	324452	3.92
peanuts	309580	3.74
soybeans	241668	2.92
pecans	236935	2.86
tobacco	201603	2.43

Figure 4-14. Uses and Estimated Application Intensity in 2002 of the Current-Use Insecticide Chlorpyrifos in the Conterminous 48 States vs. Mean Concentration in Vegetation (ng chlorpyrifos/g lipid conifer needles or lichens) from WACAP Parks. Chlorpyrifos were detected in vegetation in all parks except NOAT and GAAR, but highest concentrations were observed in SEKI and YOSE, close to the San Joaquin Valley in California, a particularly high use area. Error bars indicate one standard error.

Source of chlorpyrifos data:
http://ca.water.usgs.gov/pnsp/pesticide_use_maps/show_map.php?year=02&map=m6009.

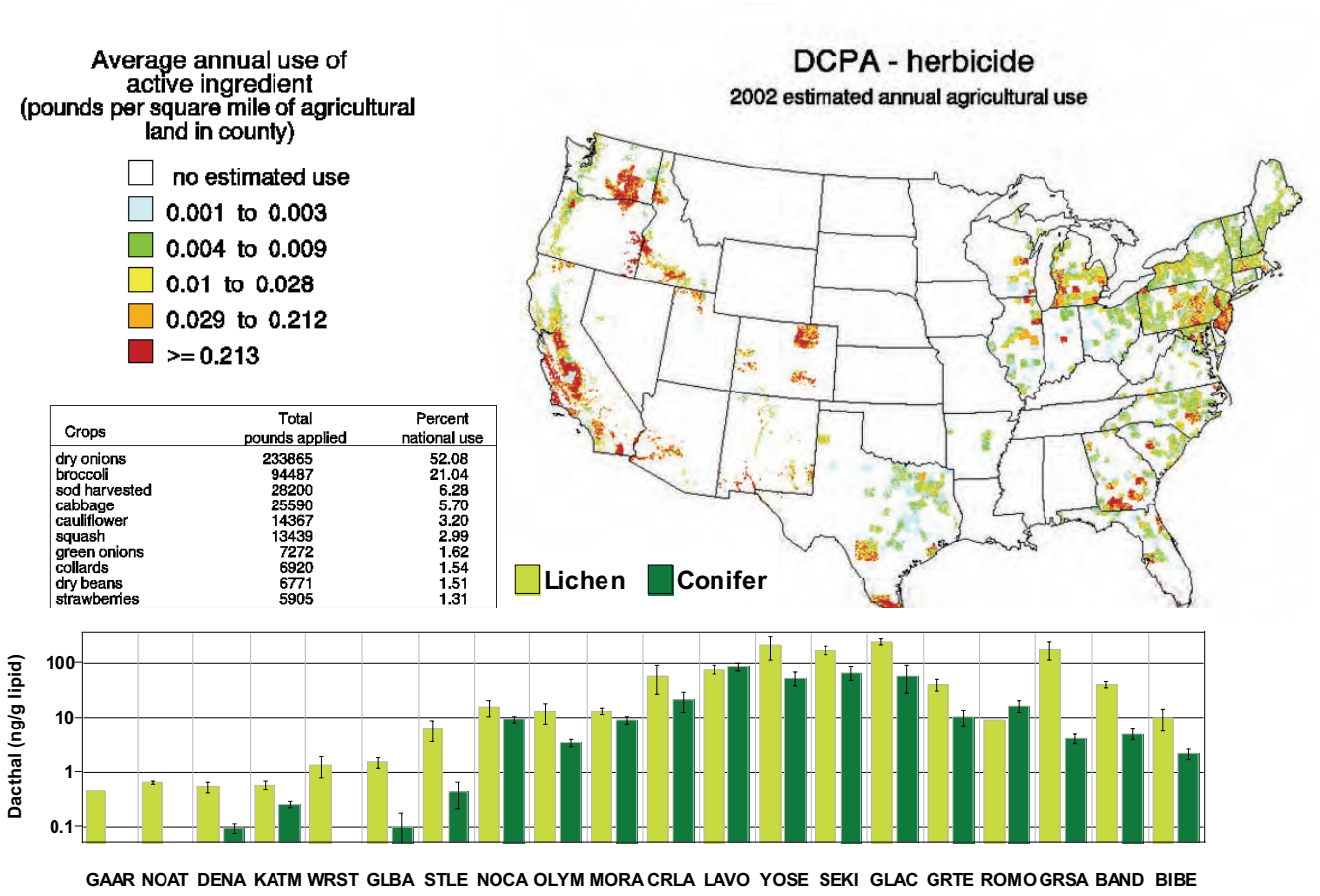

Crops	Total pounds applied	Percent national use
dry onions	233865	52.08
broccoli	94487	21.04
sod harvested	28200	6.28
cabbage	25590	5.70
cauliflower	14367	3.20
squash	13439	2.99
green onions	7272	1.62
collards	6920	1.54
dry beans	6771	1.51
strawberries	5905	1.31

Figure 4-15. Uses and Estimated Application Intensity in 2002 of the Current-Use Herbicide Dacthal in the Conterminous 48 States vs. Mean Concentration in Vegetation (ng dacthal/g lipid conifer needles or lichens) from WACAP Parks. Dacthal was detected in vegetation in all parks, but the three parks with highest concentrations were YOSE and SEKI, downwind of the high-use San Joaquin Valley in California, and GRSA, in Alamosa County, Colorado (red patch in southeast Colorado). GLAC also had high concentrations; no data are available for Montana and Wyoming, but high-use areas in western Washington and northern Idaho are upwind of GLAC. Error bars indicate one standard error.

Source of dacthal data:
http://ca.water.usgs.gov/pnsp/pesticide_use_maps/show_map.php?year=02&map=m1892.

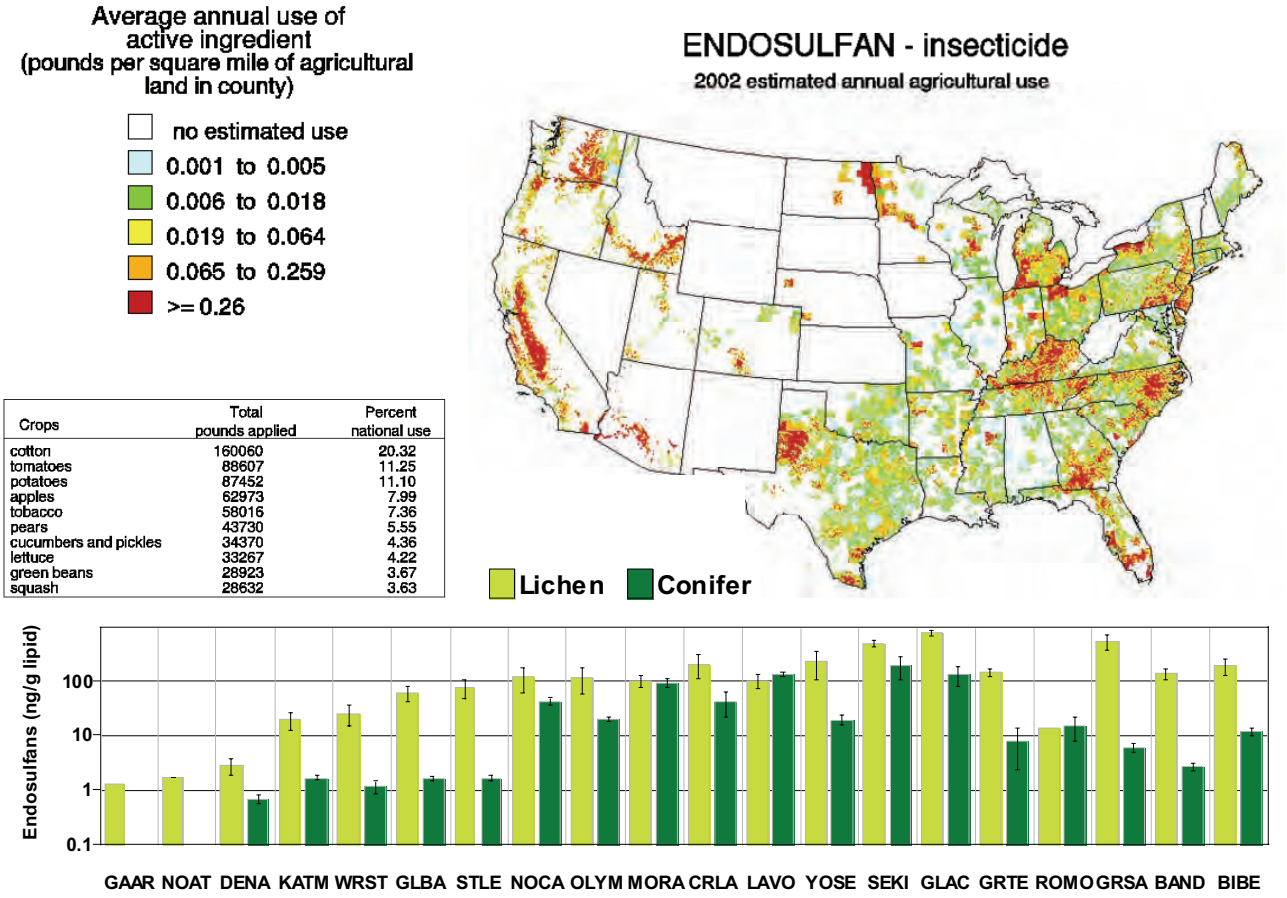

Crops	Total pounds applied	Percent national use
cotton	160060	20.32
tomatoes	88607	11.25
potatoes	87452	11.10
apples	62973	7.99
tobacco	58016	7.36
pears	43730	5.55
cucumbers and pickles	34370	4.36
lettuce	33267	4.22
green beans	28923	3.67
squash	28632	3.63

Figure 4-16. Uses and Estimated Application Intensity in 2002 of the Current-Use Insecticide Endosulfan in the Conterminous 48 States vs. Mean Concentration in Vegetation (ng endosulfan/g lipid conifer needles or lichens) from WACAP Parks. Endosulfans were detected in vegetation in all parks. No use data are available for Montana, Wyoming, New Mexico, or Mexico, hindering interpretation of results for GLAC, GRTE, BAND, and BIBE. But proximity to high-use areas appears to affect relative concentrations of endosulfans in other parks (NOCA, OLYM, MORA, CRLA, LAVO, YOSE, SEKI, ROMO, and GRSA). Error bars indicate one standard error.

Source of endosulfan data:
http://ca.water.usgs.gov/pnsp/pesticide_use_maps/show_map.php?year=02&map=m6019.

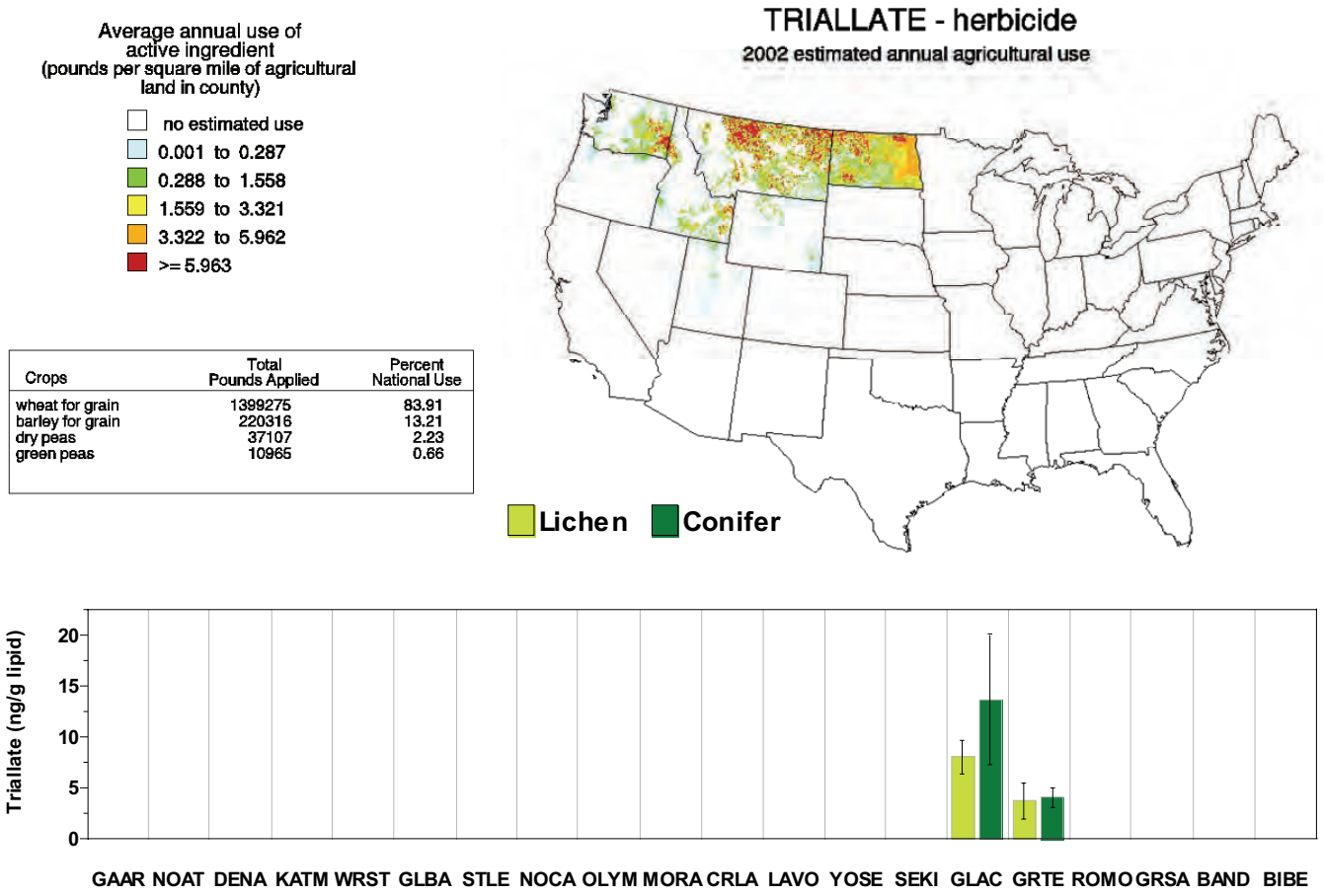

Crops	Total Pounds Applied	Percent National Use
wheat for grain	1399275	83.91
barley for grain	220316	13.21
dry peas	37107	2.23
green peas	10965	0.66

Figure 4-17. Uses and Estimated Application Intensity in 2002 of the Current-Use Herbicide Triallate in the Conterminous 48 States vs. Mean Concentration in Vegetation (ng triallate/g lipid conifer needles or lichens) from WACAP Parks. Triallate is used most intensively in the northern states and was detected, correspondingly, only in vegetation from GLAC and GRTE. Error bars indicate one standard error.

Source of triallate data:
http://ca.water.usgs.gov/pnsp/pesticide_use_maps/show_map.php?year=02&map=m1790.

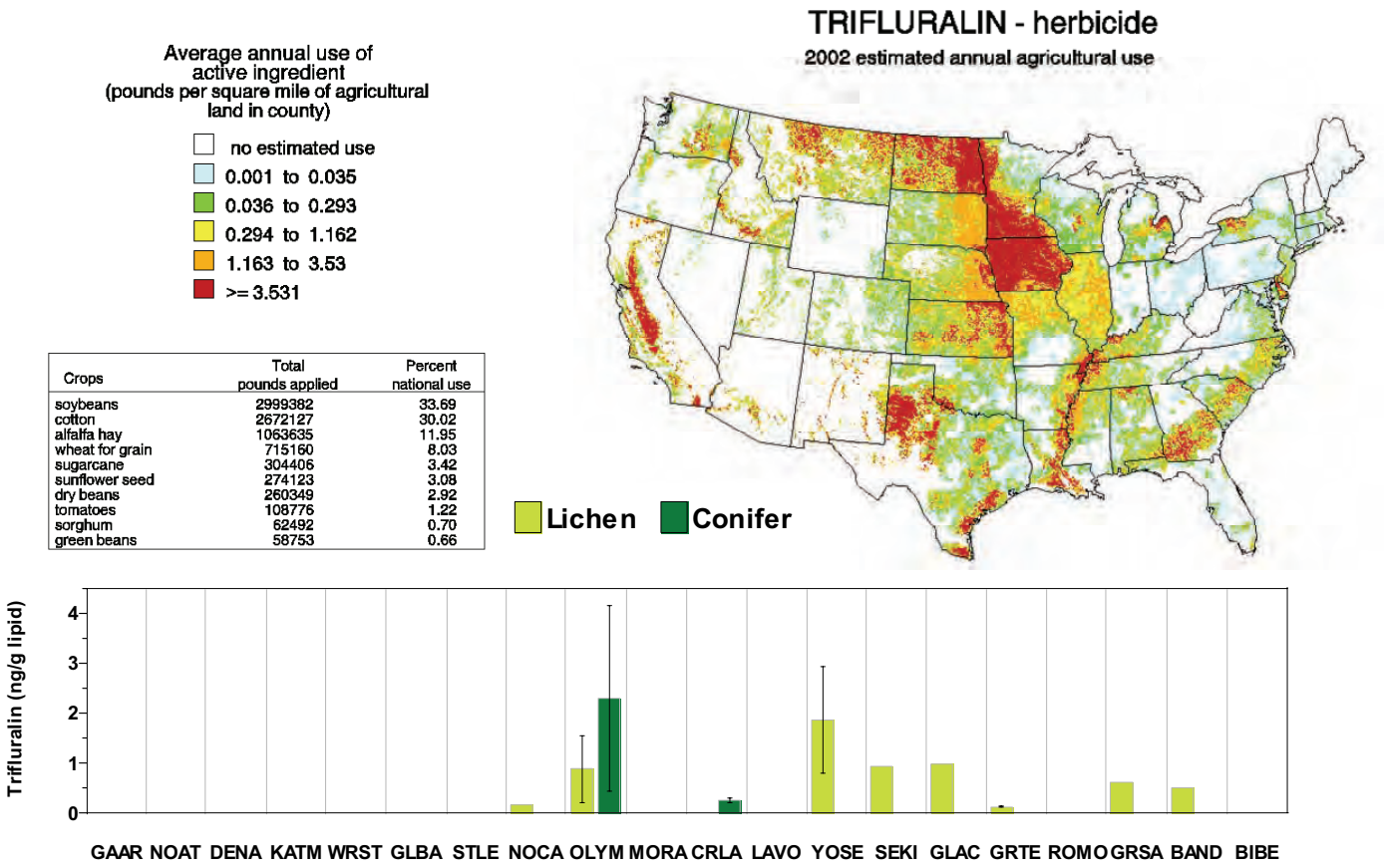

Figure 4-18. Uses and Estimated Application Intensity in 2002 of the Current-Use Herbicide Trifluralin in the Conterminous 48 States vs. Mean Concentration in Vegetation (ng trifluralin/g lipid conifer needles or lichens) from WACAP Parks. Trifluralin was detected in vegetation at low concentrations in nine parks, primarily in lichens. Parks where it was detected are downwind of high-use areas. Trifluralin was detected in OLYM (only at OLYM1) on the outskirts of Port Angeles, Washington. Error bars indicate one standard error.

Source of trifluralin data:
http://ca.water.usgs.gov/pnsp/pesticide_use_maps/show_map.php?year=02&map=m1361.

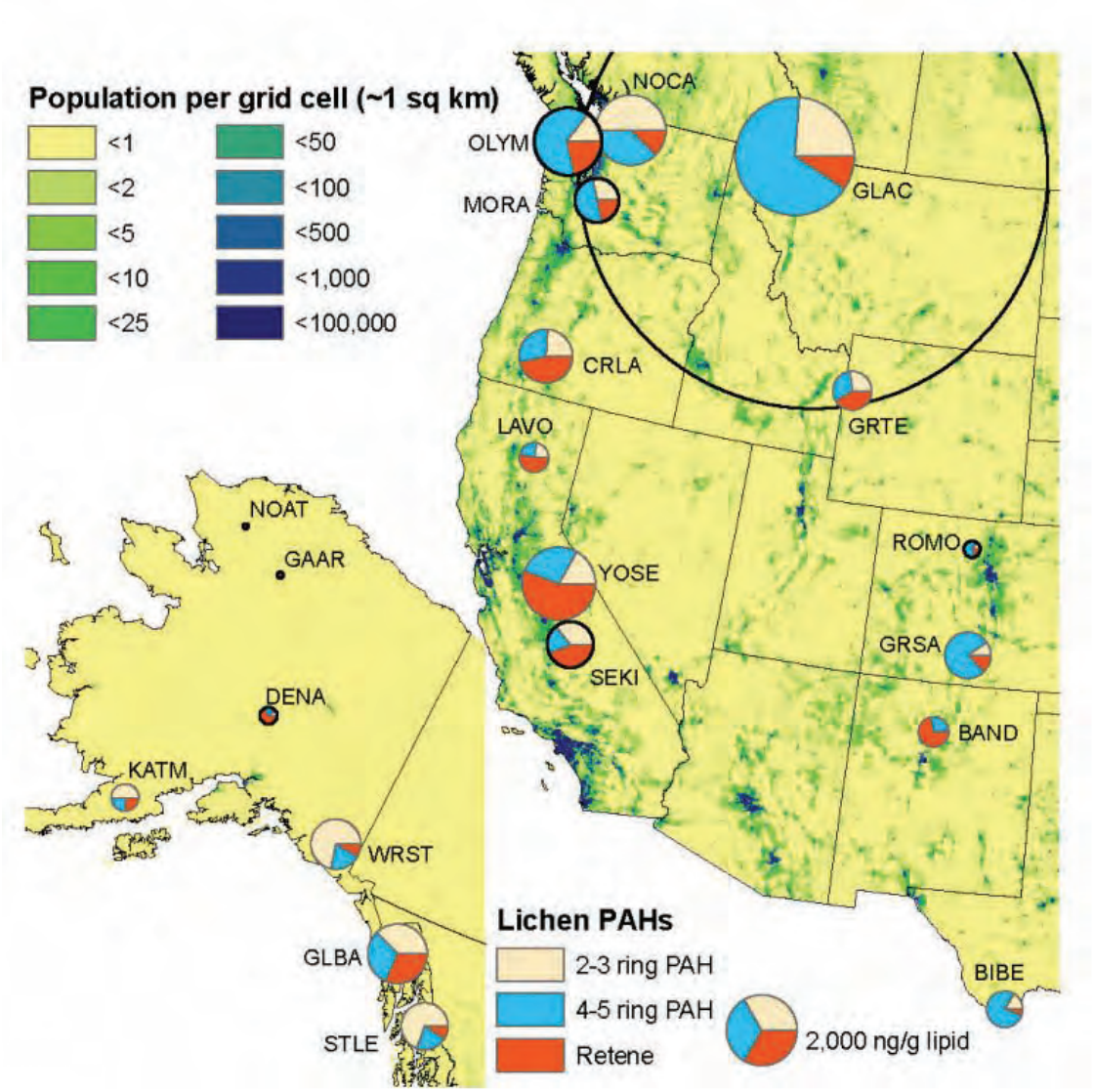

Figure 4-19. Concentrations (ng/g lipid) of PAHs in Lichens from Core and Secondary WACAP Parks Overlaid on a Map of Population Density. Circle area is proportional to total PAH concentration. Total PAH concentrations were lowest in Arctic Parks (< 10 ng/g lipid) and parks in central Alaska (< 500 ng/g lipid), increasing in concentration with decreasing latitude along the Pacific Coast from southeastern Alaska to southern California. Highest concentrations were in GLAC, where the black circle represents the true size of the total PAH concentration. Sites outlined in black are the core parks.

Possible explanations for greater SOC accumulations in lichens are:

1. Lichen material was on average older than conifer needles. Conifer needles were all sampled in the summer of their second year, whereas lichen samples were collected to represent the population on the site. Therefore, lichen samples, after homogenization in the laboratory, had a longer exposure and accumulation period than conifer needle samples. This explanation is valid only if SOCs in vegetation never equilibrate but continue to increase year after year; there is limited literature to suggest otherwise (see discussion in Chapter 5).
2. Epiphytic lichens were not buried under snow in wintertime, whereas conifer needles at higher elevation and higher latitude sites could be buried under snow from several weeks to many months of the year, reducing total exposure compared to lichens. The "lichen line" on trees demarcates the winter snow line; unlike conifer needles, epiphytic lichens usually do not survive extended burial.
3. Some physiochemical properties between lichens and conifer needles differed (e.g., surface chemistry or texture), predisposing lichens to more effectively accumulate some compounds or some forms of compounds (e.g., particulate vs. gas phase forms).

The chief advantage of sampling conifer needles is that their age is known and therefore, unless they are buried under snow in winter, their exposure period is also known. In contrast, lichen concentrations represent average concentrations in the lichen population that was sampled at the site, within which some individuals could be decades old and others only a few years old. Because coniferous forests cover an extensive land area in western North America and because the biomass of needles on a kg/ha basis is usually very much larger than lichen biomass, from an ecological perspective, conifer needle data are likely to be more relevant than lichen data. To the extent that contaminants concentrated in needles are deposited in litterfall or washed out in leachates, conifer needles must play a greater role than lichens in transferring contaminants to soils and soil organisms.

The chief advantage of sampling lichens is that their SOC concentrations are more likely to be above detection limits (e.g., PAHs at WACAP sites in GLAC) which makes it easier to detect differences between sites in mapping local contamination or elevation effects. In arctic and alpine ecosystems, where coniferous trees are absent, lichens can be a dominant component of the ecosystem and a good sampling choice. Analytically, the clean-up process was faster and instrument output was more readily interpretable for lichens than for conifer needles.

4.2.3.2.2 Differences in SOC Accumulation between Lichen Species

One of the assumptions of WACAP was that, within biological media types (i.e., lichens, conifer needles, or fish), differences between species could be minimized by lipid normalization. Although WACAP was not designed to specifically test this assumption, at the conclusion of the laboratory analyses, there were six sites (DENA5, WRST1, WRST5, OLYM5, and GLAC5) where SOC concentrations had been determined in multiple replicates of more than one species of lichen. A comparison of within-site means across species by one-way analysis of variance provided evidence that lipid normalization (i.e., reporting SOC concentration on a gram lipid basis) was largely successful in minimizing differences across species. Most comparisons showed no differences between species. However, significant differences between some species combinations for some SOCs did occur and the concentration differences were usually between 2- and 10-fold (Appendix 4A.1). For example, at WRST1, mean concentrations of HCBs and

PAHs were 2.5 times higher in the leafy epiphyte, *Platismatia glauca*, than in the leafy epiphyte, *Hypogymnia apinnata*. At WRST5, concentrations of dacthal, endosulfans, HCBs, a-HCH, g-HCH, chlordanes, PCBs, and PAHs were 5-17 times higher in *P. glauca* than in the pendant epiphyte, *Alectoria sarmentosa*. At OLYM5, concentrations of dacthal, endosulfans, and PCBs were 2.5-5 times higher in *Bryoria,* another pendant epiphyte, than in *A. sarmentosa.* Most notably, of the leafy tundra lichens, SOC concentrations were 7-50 times higher in *Flavocetraria cucullata* than in *Masonhalea richardsonii* for all SOCs except dacthal, which was not different. *Masonhalea* appears to be a very poor accumulator of SOCs.

When SOCs differed between species, they were usually consistently higher in one species than in another, but exceptions did occur. At GLAC5, concentrations of HCB, g-HCH ($p > F = 0.06$), chlordanes, DDTs, PCBs, and PAHs were 2-10 times higher in the leafy epiphyte, *Hypogymnia physodes*, than in the shrubby epiphyte, *Letharia vulpine*. However, *L. vulpina* had 2 times more g-HCH than *H. physodes*, and it also had detectable concentrations of chlorpyrifos, which was not detected in *H. physodes* at that site. Therefore, using the same species reduces error between sites by up to an order of magnitude. Because error among field replicates of the same species is fairly low (Appendix 4A.1), using the same species is an inexpensive way to improve detection of between-site differences. Based on WACAP results, *Masonhalea* should be avoided in future sample efforts. It is not a good accumulator of SOCs, nutrients, or metals, possibly because of its dense, glossy surface. *Flavocetraria cucullata* and *Cladina arbuscula* are better accumulators and could be comparable to epiphytes that are poor accumulators, such as *Alectoria sarmentosa* (Appendix 4A.8). *Flavocetraria cucullata* is readily recognizable and widespread in Alaska and in some moist, alpine areas of the northern conterminous 48 states.

In general, epiphytes are the best choice for sampling, but in dry, treeless areas of the conterminous 48 states, the rock lichen, *Xanthoparmelia,* appears to accumulate SOCs at concentrations similar to those in the epiphyte, *Usnea (*Appendix 4A.9). However, a higher proportion of total dry weight will be in soil mineral particles trapped between overlapping lobes of the lichen, some of which can be very time consuming, if not impractical, to remove. In addition, the burden of soil particulates in *Xanthoparmelia* might be magnified in windy or dusty sites, which might have happened in GRSA, because overlapping lobes trap soil particulates as the lichen grows.

4.2.3.2.3 Differences in SOC Accumulation between Conifer Species

The working assumption for the WACAP study design was that lipid normalization would minimize inter-species differences in SOC accumulation among conifers, as with lichens and fish. Unlike lichens (multiple species collected at some sites), only one species of conifer was collected at each site. Because conifer needles did not show elevation trends within parks, even when the same species were compared, mean SOC concentrations of different species from different sites within parks were compared. These means comparison tests (Appendix 4A.6) indicated that spruce (*Picea*), true fir (*Abies*), and Douglas-fir (*Pseudotsuga*) had fairly similar accumulation capacities, whereas western hemlock (*Tsuga*) was somewhat higher and pine (*Pinus*) was substantially lower, compared to the firs and spruce. See Figure 4-20 for a visual representation of these patterns.

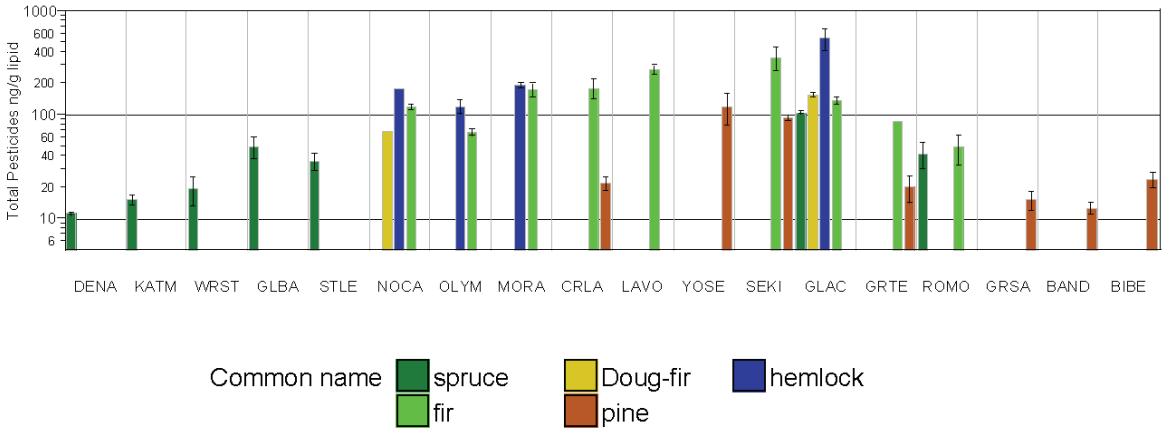

Figure 4-20. Comparison of Total Pesticide Accumulation in Conifer Needles by Species and Park. Although data were lipid normalized, intra-park differences among species indicate that some species are better accumulators than others (e.g., spruce and fir are comparable, hemlock is a somewhat better accumulator, and pine is the poorest accumulator). These differences might be attributable to needle morphology (see text for discussion). Mean concentrations in YOSE, GRSA, BAND, and BIBE would probably have been higher, had fir been sampled there instead of pine. Bar height indicates the mean; error bars indicate one standard error.

Specifically, firs usually accumulated substantially higher concentrations of SOCs than did pines, especially endosulfans (~10 × higher), dacthal (~2-5× higher), and historic-use HCHs and HCB (~ 3-5× higher). Western hemlock SOC concentrations were higher than those in fir by 1/3- to 3-fold. Douglas-fir was similar to true firs for most SOCs but was often 2-3 times lower in endosulfans and dacthal. Spruce was similar to fir and hemlock but tended to be ~5-10 times lower in endosulfans. These differences make sense from a needle morphology and tree architecture point of view (i.e., spruce, fir, and Douglas-fir needles have a similar flattened shape and size, whereas hemlock needles are shorter and pine needles are round and longer. Compared to fir and spruce needles, hemlock needles are more densely packed on the branches and pine needles are more loosely packed. All these factors could affect air circulation and needle surface area, and, together with differences in surface wax chemistry, affect absorption rates. Komp and McLachlan (1997) and Collins et al. (2006) have discussed these and other factors leading to interspecies variability. Figure 4-21 presents photos of the most commonly collected species of fir, spruce, and Douglas-fir in WACAP, compared with western hemlock and the most commonly collected pine.

The three genera that were most widely collected in national parks in the western United States were spruce in Alaska, fir in the Pacific Northwest, California, and northern Rocky Mountains, and pine in the southern Rocky Mountains. Although species differences after lipid normalization were lower (usually none to 5-fold) than park-to-park differences (up to 10-fold), species can nevertheless be an important source of error. To improve detection of differences among sites or parks, future researchers might choose to limit collections to a single genus, or to collect enough within-site replicates of multiple species to calculate a compensation factor for cross-species comparisons.

Figure 4-21. Needles of (A) Subalpine Fir, (B) Sitka Spruce, (C) Douglas-fir, (D) Western Hemlock, and (E) Lodgepole Pine. Similar morphology and arrangement on branches might help explain why SOC concentrations were usually similar among fir, spruce, and Douglas-fir. Hemlock tended to have higher concentrations of SOCs and pine had substantially lower concentrations of SOCs compared to spruce and fir; differences in needle length and density might partially explain this effect. Photos ©Susan McDougall (hemlock) and J.S. Peterson (all others) @ USDA-NRCS PLANTS database.

4.2.3.3 Elevational Gradients of SOCs in Vegetation

Several reasons explain why we might expect altitudinal gradients in SOC concentrations. First, many contaminants are present primarily because of regional sources (see Section 4.2.6). For such compounds, we would expect the greatest air concentrations, and therefore ecosystem exposure, to occur at the lowest altitudes. For contaminants associated with trans-Pacific/Asian sources (Jaffe et al., 2003; Killin et al., 2004), we would expect air concentrations and ecosystem exposure to occur at altitudes greater than 2,000 meters, because of the greater occurrence of transport at these altitudes (Jaffe et al., 2003). Finally, for contaminants that can undergo cold fractionation, we would expect an altitude gradient with highest concentrations at the highest and coldest elevations (Wania and Mackay, 1993; Blais et al., 1998; Simonich and Hites, 1995; Davidson et al., 2003; Davidson et al., 2004). It is also likely that several of these processes can operate simultaneously, thus complicating interpretation of the data.

Regression analysis of the combined WACAP lichen data provided strong evidence ($p \leq 0.014$) that concentrations of PCBs and the pesticides chlorpyrifos, dacthal, endosulfans, HCB, a-HCH, g-HCH, and chlordanes increased with elevation averaged across WACAP parks (Table 4-3). There was suggestive evidence ($p = 0.0875$) that DDT concentrations also increased with elevation.

Table 4-3. Linear Regression Model Results. Data are from all WACAP parks that met criteria*, for the fit of lichen SOC concentrations to increasing elevation after accounting for differences between parks.

SOC	Slope	SE	P-value	R^2	Estimated Ave. % Change in Concentration from 500 to 1,000 m
Chlorpyrifos	0.0035	0.0013	0.0117	0.5338	218
Dacthal	0.0010	0.0002	0.0001	0.9654	165
Endosulfans (sum)	0.0009	0.0002	0.0001	0.9541	157
Endosulfan I	0.0009	0.0001	0.0001	0.9454	157
Endosulfan II	0.0008	0.0002	0.0011	0.9297	149
Endosulfan sulfate	0.0009	0.0002	0.0001	0.9541	157
HCB	0.0012	0.0002	0.0001	0.9368	124
a-HCH	0.0013	0.0002	0.0001	0.8793	192
g-HCH	0.0016	0.0002	0.0001	0.8970	153
Chlordanes (sum)	0.0009	0.0002	0.0003	0.7878	156
Trans-Chlordane	0.0018	0.0005	0.0005	0.7684	217
Cis-Nonachlor	0.0009	0.0002	0.0001	0.7595	364
Trans-Nonachlor	0.0017	0.0005	0.0007	0.6971	236
DDTs (sum)	0.0004	0.0002	0.0875	0.9321	122
PCBs (sum)	0.0030	0.0009	0.0009	0.6174	165
PCB 118	0.0006	0.0002	0.0141	0.3786	135
PCB 138	0.0011	0.0003	0.0007	0.6589	161
PCB 153	0.0006	0.0002	0.0042	0.5345	150
PCB 183	0.0002	0.0001	0.0049	0.4552	178
PAHs (sum)	-0.0009	0.0002	0.0007	0.9374	-64
Fluorene	-0.0007	0.0002	0.0001	0.9479	-70
Phenanthrene	-0.0006	0.0001	0.0001	0.9754	-74
Retene	0.0015	0.0001	0.1443	0.4881	n.s.
Chrysene/Triphene	-0.0005	0.0002	0.0219	0.9271	-78
Benzo(a)anthracene	-0.0014	0.0003	0.0001	0.8998	-50

*Parks in models: BAND, CRLA, DENA, GLAC, KATM, LAVO, MORA, NOCA, SEKI, and STLE. Values for concentration change represent the average across all parks in the models. See Chapter 3 and Appendix 4A.11 for regression model details.

n.s. = not significant

By contrast, all the PAHs tested, except retene, decreased with elevation ($p \leq 0.0219$) (Table 4-3). The absolute change in ng/g lipid (non-transformed data) or percentage change (natural log transformed data) per 500 m increase in elevation varied by park, contaminant, and lichen species within park (Table 4-4). The bar charts in Figure 4-22 and Appendix 4A.10 show the concentration increases (or decreases) from lowest to highest elevations within each park and portray the magnitude and consistency of concentration changes across vegetated elevations of the WACAP parks.

Table 4-4. Simple Linear Regression Results of Lichen SOCs on Park and Elevation. Values represent concentration changes per 500 m elevation increment in ng/g lipid (non-transformed data) or percent change (natural log-transformed data) calculated for individual parks.

Compound	PARKS											
	BAND	CRLA	DENA	GLAC	KATMF[1]	KATMH[2]	LAVO	MORA	NOCA	SEKI	STLEA[3]	STLEP[4]
Chlorpyrifos	ND	7.20	ND	-1.40	ND	ND	ND	3.10	1.40	ND	ND	ND
Dacthal	156%	547%	128%	212%	332%	105%	182%	149%	165%	128%	192%	191%
Endosulfans	201%	386%	223%	182%	192%	547%	173%	192%	135%	116%	157%	105%
Endosulfan I	173%	521%	223%	173%	142%	234%	173%	157%	122%	142%	192%	128%
Endosulfan II	192%	426%	ND	259%	ND	ND	182%	149%	128%	111%	100%	173%
Endosulfansulfate	212%	349%	223%	182%	234%	605%	173%	223%	142%	111%	142%	100%
HCB	0.81	10.24	1.69	0.12	0.49	-0.42	0.12	0.64	0.00	0.16	0.06	0.56
a-HCH	192%	406%	300%	165%	165%	-90%	173%	300%	135%	182%	192%	100%
g-HCH	0.64	2.72	0.20	2.10	0.04	0.06	0.12	1.56	0.09	1.00	0.16	0.06
Chlordanes	0.01	8.41	ND	1.69	0.06	1.96	0.72	0.56	0.00	0.16	0.02	-0.06
t-Chlordane	0.10	6.30	ND	2.70	0.00	0.70	1.55	1.05	0.05	0.90	0.10	-0.50
c-Nonachlor	0.40	2.35	ND	1.55	0.10	0.60	0.55	0.35	0.10	0.50	0.10	-0.05
t-Nonachlor	0.35	5.60	ND	3.25	-0.20	1.20	1.25	0.80	-0.05	0.95	0.10	-0.75
DDTs	NS	NS	NS	NS	NS	NS	NS	NS	NS	NS	NS	NS
PCBs	1.25	11.3	ND	0.15	0.35	1.95	1.95	4.85	0.75	0.5	0.8	-0.25
PCB 118	NS	NS	NS	NS	NS	NS	NS	246%	NS	NS	NS	NS
PCB 138	0.35	4.40	ND	0.05	0.10	0.50	0.80	1.60	0.40	0.15	0.20	0.05
PCB 153	0.25	2.60	ND	0.20	0.20	0.60	0.50	1.20	-0.10	0.10	0.15	-0.15
PCB 183	0.15	0.20	ND	0.00	0.00	0.05	0.05	0.30	0.05	0.05	0.00	-0.05
PCB 187	0.30	1.25	ND	0.30	0.00	0.30	0.30	0.50	0.10	0.15	0.05	0.00
PAHs	-19.2%	-74.1%	-52.2%	-60.6%	-315.8%	-77.9%	-23.5%	-86.1%	-54.9%	-95.1%	-30.1%	-81.9%
FLO	ND	ND	ND	-74%	ND	-17.4%	-30%	105%	-52%	-86%	-44%	-74%
PHE	ND	-0.74	38.47	-0.70	1.16	-0.95	-0.33	1.00	-0.58	-0.78	-0.50	1.05
Retene	NS	NS	NS	NS	NS	NS	NS	NS	NS	NS	NS	NS
CHR/TRI	-60.6%	-90.5%	-182.2%	-60.6%	-258.6%	-28.7%	-5.0%	-81.87%	-81.9%	-81.9%	-22.3%	-60.6%
B(a) A	-40.7%	-33.3%	-173.3%	-54.9%	ND	ND	-36.8%	-19.2%	-60.6%	-74.1%	-9.07%	-35.0%

Note: Negative trends indicate decreasing concentration with increasing elevation. See Methods chapter and Appendix 4A.11 for model details. ND = no data, all samples below EDLs; NS = fitted line not a significantly better fit than the mean for this park ($p > 0.05$).

[1]KATMF = KATM *Flavocetraria cuculata*. [2]KATMH = KATM *Hypogymnia physodes*. [3]STLEA = STLE *Alectoria sarmentosa*. [4]STLEP = STLE *Platismatia glauca*.

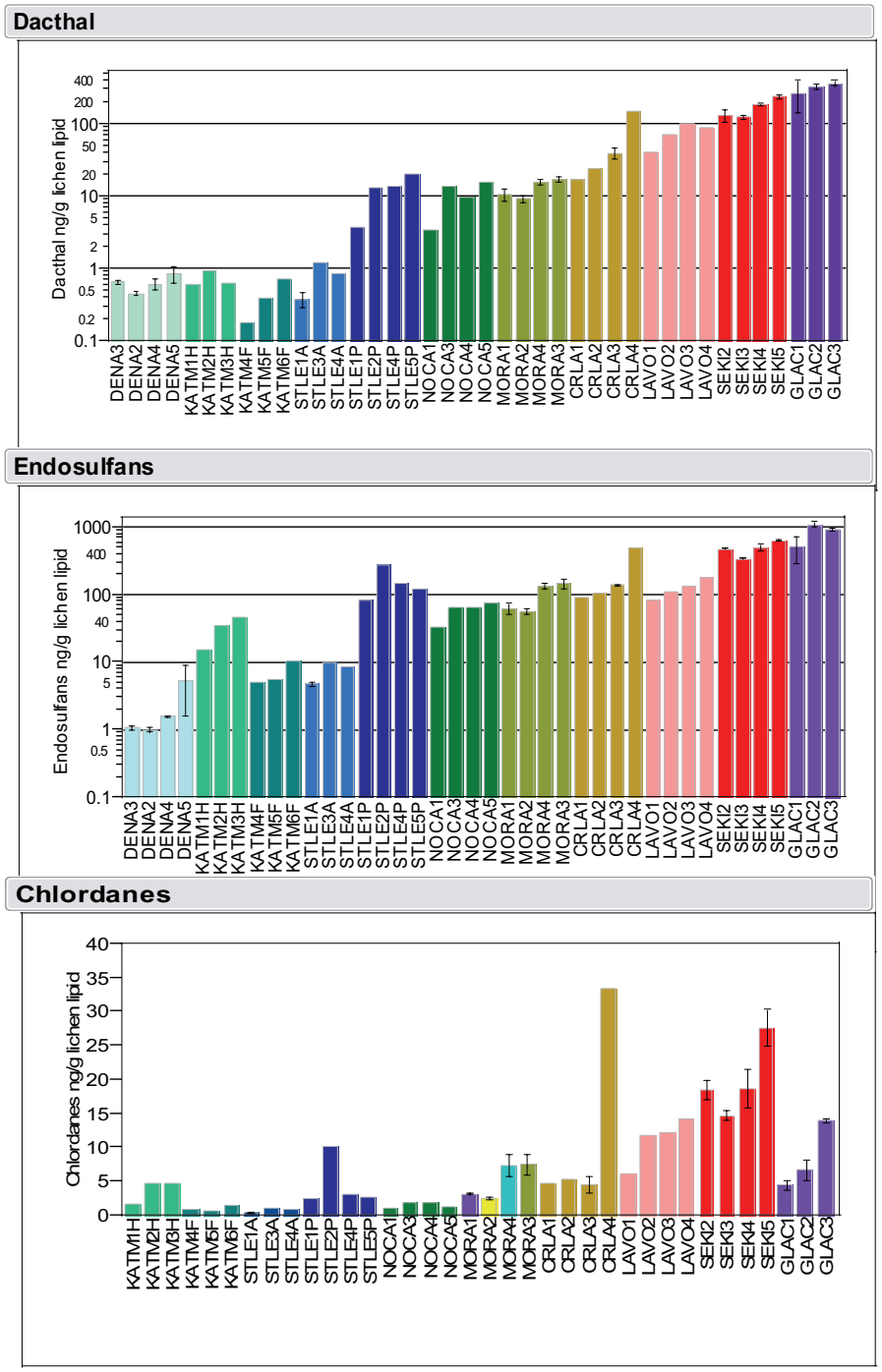

Figure 4-22. Elevational Gradients for Sum Dacthal, Sum Endosulfan, and Sum Chlordane Concentrations in Lichens. Within each park, sites are listed in order of increasing elevation. Codes H, F, A, and P refer to lichen species sampled (see Table 4-4). Bars show the standard error. Statistical analyses of elevational gradients are reported in Tables 4-3 and 4-4. Additional graphic displays for other SOCs are given in Appendix 4A.10. See Chapter 3 for data selection criteria for elevational trends analyses.

In general, changes in SOC concentration per unit change in elevation were within the same order of magnitude across parks (Table 4-4). Parks with similar percentage increases might have different absolute increases in SOC concentrations per unit increase in elevation. For example, endosulfan concentrations in the lichen *Flavocetraria cucullata* from KATM increased 192% per 500 m, with the lowest elevation averaging 0.13 ng/g lipid, whereas endosulfans in GLAC lichens increased nearly the same percentage, 182%; however, samples from the lowest elevation averaged ~ 500 ng/g lipid (Table 4-4, Figure 4-22). Doubling the latter concentration is more likely to have adverse ecological effects, especially if the total quantities of contaminants accumulated in vegetative biomass/ha are considered (see discussion in Chapter 5).

For the two parks, KATM and STLE, where two species were collected, the change in SOC concentration per unit elevation increase was as variable across species as it was between parks (Table 4-4). In KATM, we expected smaller SOC concentration changes in the tundra lichen, *Flavocetraria cucullata* (KATMF), compared to the epiphytic lichen *Hypogymnia physodes* (KATMH). Presumably the ground lichen would be buried under snow more days per year, whereas the epiphyte would be exposed to the air a greater number of days per year. Concentrations of SOCs were consistently higher in *H. physodes* (Figure 4-22, Appendix 4A.10), whereas elevational differences were often larger in *F. cucullata* (Table 4-4). Similarly, in STLE, *Platismatia glauca* (STLEP) appeared to be a better accumulator of SOCs than *Alectoria sarmentosa* (STLEA) (Figure 4-22; Appendix 4A.10) but changes in concentration per unit elevation increase were consistently larger for *A. sarmentosa*.

It is important not to over-interpret Table 4-4 because the slopes used to calculate percent change within individual parks are based on only 3-5 elevations; also, in the secondary parks, only one sample (three for the core parks) was collected per elevation. In contrast, the general models shown in Table 4-3 were developed from the combined WACAP dataset, providing better statistical power. Very high R-squared values and low standard errors for many compounds (e.g., dacthal, endosulfans, HCB, PAHs) indicate that concentrations of these important SOCs can be predicted accurately from elevation with general models (see Appendix 4A.11 for regression model details). For most PCBs and pesticides, concentrations at 1,000 m were 150-220% of concentrations at 500 m. PAHs were 50% to 80% lower at 1,000 m, compared with 500 m.

4.2.4 SOCs in Fish

Figures 4-1 to 4-4 and 4-6 show the concentrations of SOCs in fish; the data are reported in ng/g lipid. The dominant SOCs in fish were p,p′-DDE, dieldrin, PBDE 47, PBDE 99, PCB 153, PCB 138, dacthal, trans-nonachlor, HCB, and endosulfan sulfate. Dieldrin, p,p′-DDE, dacthal, and endosulfan sulfate concentrations were highest in fish from SEKI, ROMO, and GLAC. PBDE concentrations in fish across the WACAP parks (Figure 4-6) varied less than most other SOCs, both within and between lakes, and were highest in MORA fish, and lowest in fish in the Alaska national parks. Concentrations of the five major PCB congeners were comparable among fish from Alaska and Pacific coast parks (SEKI, OLYM, and MORA), and lower in fish from the Rocky Mountains (GLAC, ROMO) (Figure 4-4). Dacthal concentrations were highest in fish from SEKI, followed by ROMO and GLAC (Figure 4-1), and lower in parks in the Pacific Northwest (OLYM, MORA) and Alaska (DENA, NOAT). For most compounds, the variation in fish SOC concentrations within lakes was as large as the variations between lakes.

When compared to similar fish species collected from high-elevation lakes throughout Europe (Vives et al., 2004a), PBDE concentrations measured in fish in national parks in the western United States were, on average, approximately three times higher in concentration, after adjusting for differences between muscle and whole tissue concentrations (USEPA, 2000). Concentrations of most historic-use SOCs (HCB, DDTs, and HCHs) in fish in the western United States were comparable to or 2- to 9-fold lower than those in European mountain fish (Vives et al., 2004b). Because the European mountain fish and the WACAP fish studied included similar fish species collected from cold, oligotrophic lakes, within 3 years time, it is unlikely that the observed differences in the SOC concentrations are a result of fish accumulation differences or rapidly changing SOC emissions. Even a rapid PBDE doubling time of 6 years could not account for the 3-fold higher PBDE concentrations in fish in the western United States. This finding suggests that fish in national parks in the western United States are exposed to higher PBDE concentrations than similar European mountain fish, which is consistent with PBDE concentrations measured in other North American and European environmental compartments (Hites, 2004), and more recent European fish samples (Gallego et al., 2007).

Compared to fish collected from several alpine lakes in Canada (Demers et al., 2007), WACAP fish were significantly lower in HCHs and chlordanes (only ~ ¼ of the concentration) and comparable in concentrations of DDTs and HCB; dieldrin concentrations were approximately 3 times higher. Because the fish sampled in Canada and the western United States were of similar species and the lakes had similar productivity, these differences probably reflect differences in SOC exposure. Other than these, there are few observations of broad-ranging mountain fish DOC loads (particularly for CUPs) with which we can compare the WACAP fish data.

4.2.5 SOCs in Sediments

4.2.5.1 Spatial Distribution of SOCs in Sediments

Sediment cores provide information on the temporal changes of contaminant loadings in WACAP parks over the last ~150 years. Cores were collected from the lake sites in each core park by means of the methods described in Section 3.4.6.1. Because sediment data reflect an annual accumulation of material, they are reported as a flux (ng/m^2/yr), rather than a concentration. The sediment flux data have been corrected by lake "focusing factor," as described in Section 3.4.6.2, which adjusts for differences in sediment accumulation for each watershed.

Figures 4-1 to 4-6 show the SOC fluxes in the WACAP lake surficial sediments corrected for sediment focusing. In these figures, we used the most recent year of sediment data to represent the surficial flux. Figures 4-23 to 4-29 show the temporal trends in SOC fluxes.

The most common CUPs detected in the surficial sediments were the endosulfans and dacthal. Endosulfans have the highest recent sediment flux of all CUPs. GLAC, OLYM, and MORA all had fluxes near 60 ng/m^2/yr. ROMO and SEKI were a factor of 5-7 higher at 290 and 420 ng/m^2/yr, respectively. Endosulfans at NOAT, GAAR, and DENA were at or below detection limits (see Figure 4-1). The most frequently detected groups of HUPs in the WACAP lake surficial sediments were the chlordanes and dieldrin (see Figure 4-3). Chlordanes were detected in every park, and concentrations were a factor of 40 higher at SEKI than at NOAT and GAAR. Sum DDTs were frequently detected at ROMO and SEKI. Surficial sediment fluxes of DDTs at these parks were 2,500 and 760 ng/m^2/yr, respectively.

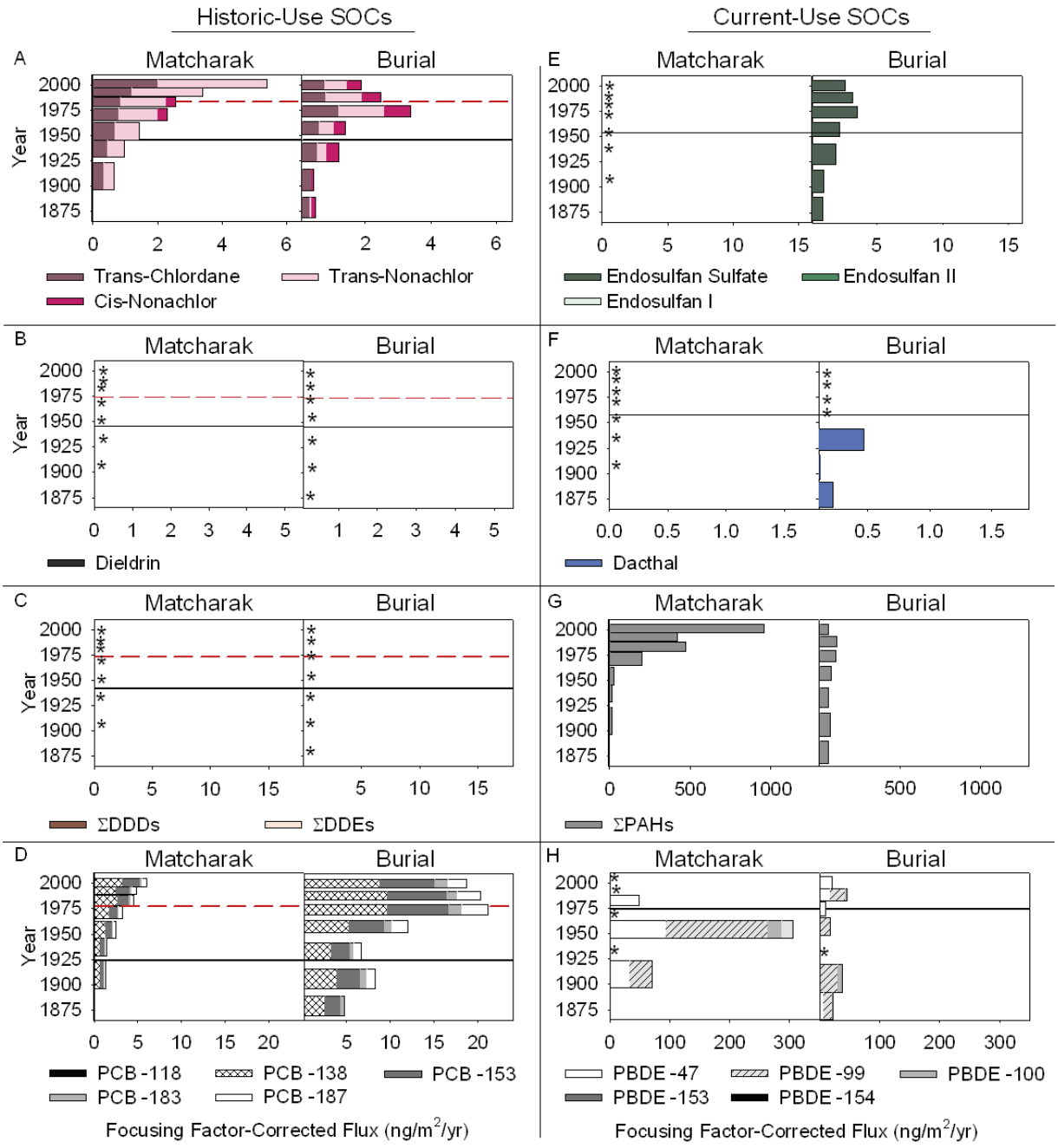

Figure 4-23. Focusing Factor-Corrected Flux (ng/m^2/yr) Profiles of Current- and Historic-Use SOCs in Matcharak Lake and Burial Lake Sediment Cores at GAAR and NOAT. Solid lines (——) indicate US registered use dates, dashed lines (– – –) indicate US restriction dates, and asterisks (∗) indicate below method detection limit.

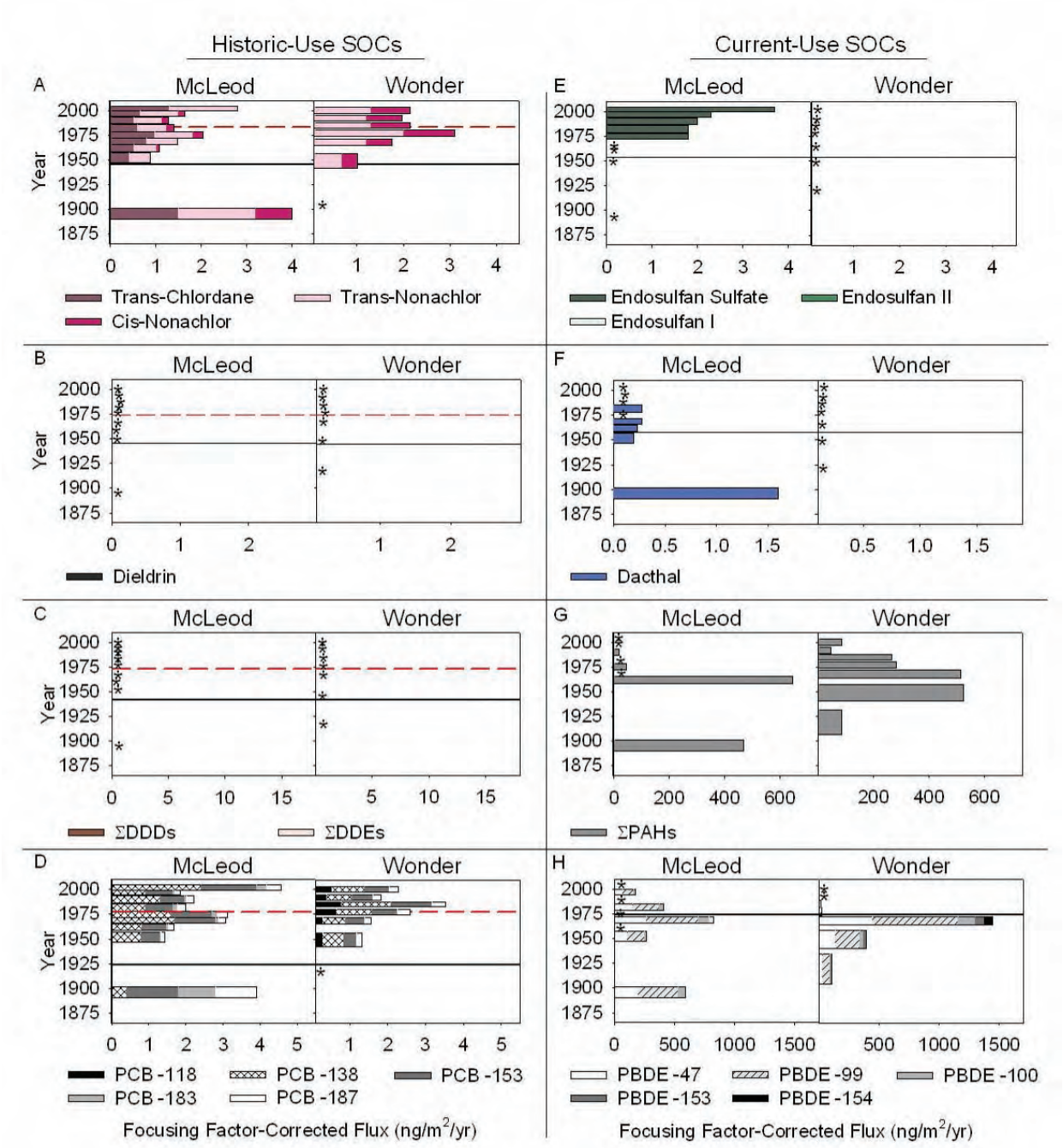

Figure 4-24. Focusing Factor-Corrected Flux (ng/m^2/yr) Profiles of Current- and Historic-Use SOCs in McLeod Lake and Wonder Lake Sediment Cores at DENA. Solid lines (——) indicate US registered use dates, dashed lines (– – –) indicate US restriction dates, and asterisks (∗)indicate below method detection limit.

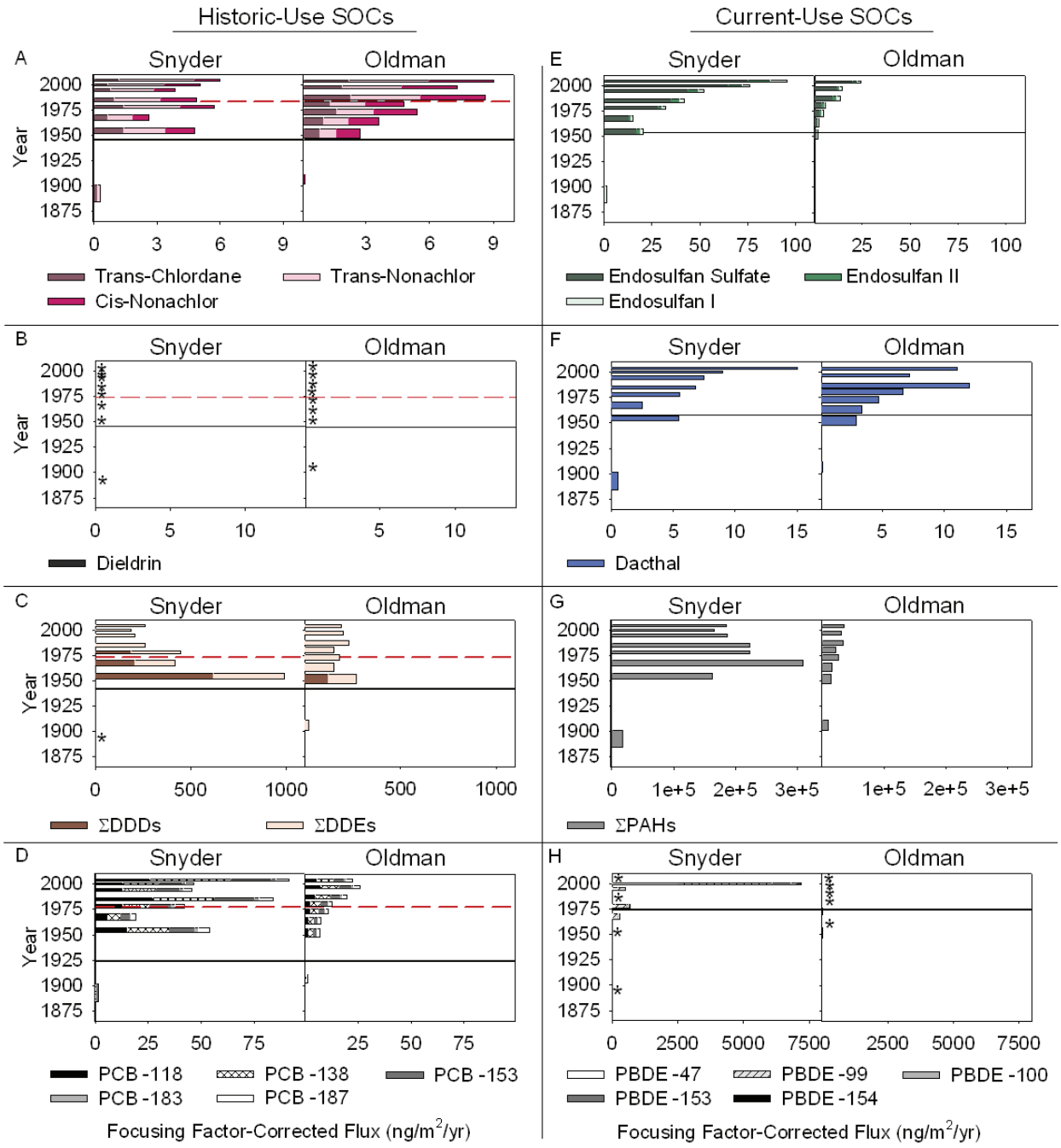

Figure 4-25. Focusing Factor-Corrected Flux (ng/m^2/yr) Profiles of Current- and Historic-Use SOCs in Snyder Lake and Oldman Lake Sediment Cores at GLAC. Solid lines (——) indicate US registered use dates, dashed lines (– – –) indicate US restriction dates, and asterisks (∗)indicate below method detection limit.

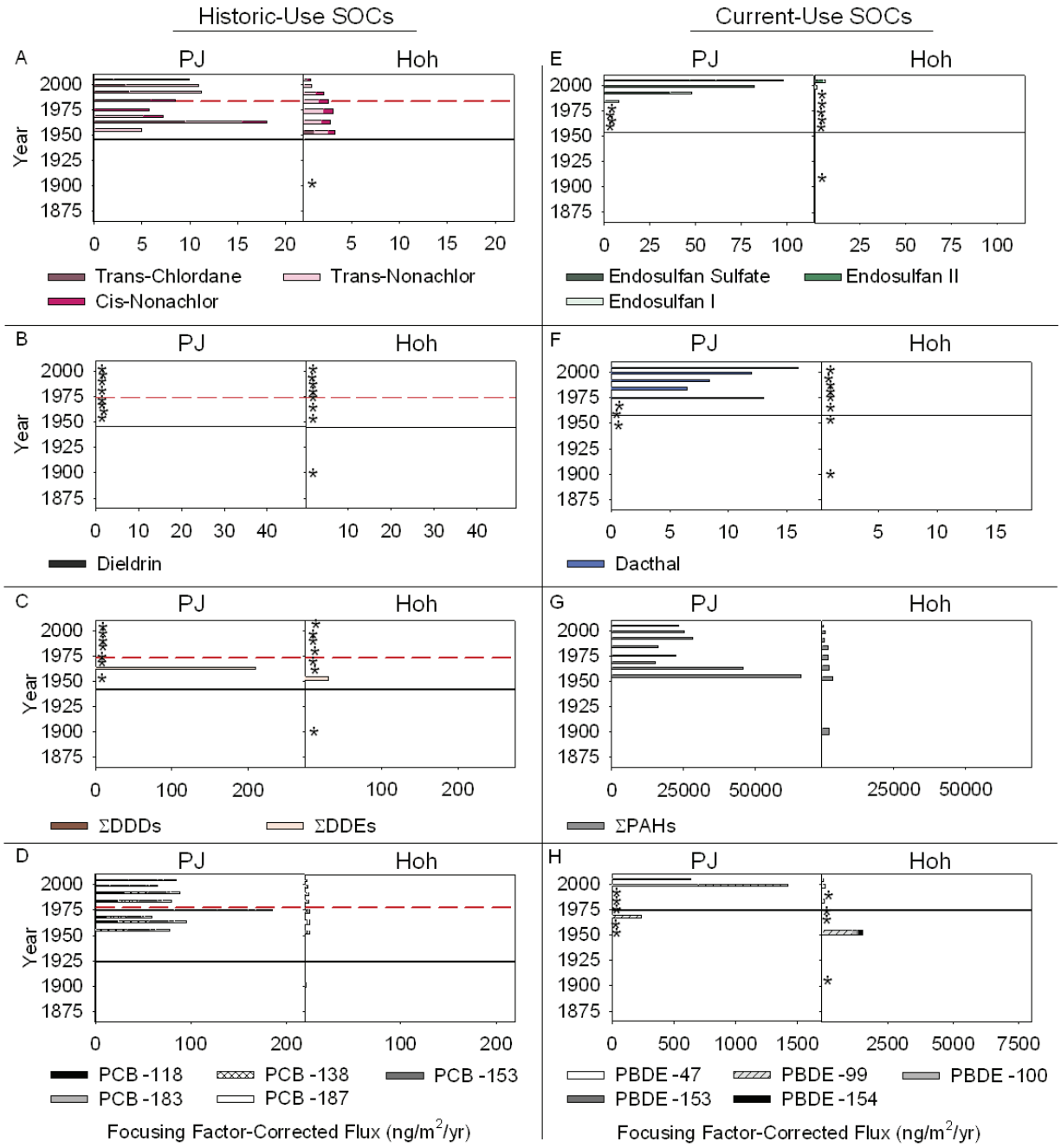

Figure 4-26. Focusing Factor-Corrected Flux (ng/m^2/yr) Profiles of Current- and Historic-Use SOCs in PJ Lake and Hoh Lake Sediment Cores at OLYM. Solid lines (——) indicate US registered use dates, dashed lines (– – –) indicate US restriction dates, and asterisks (∗)indicate below method detection limit.

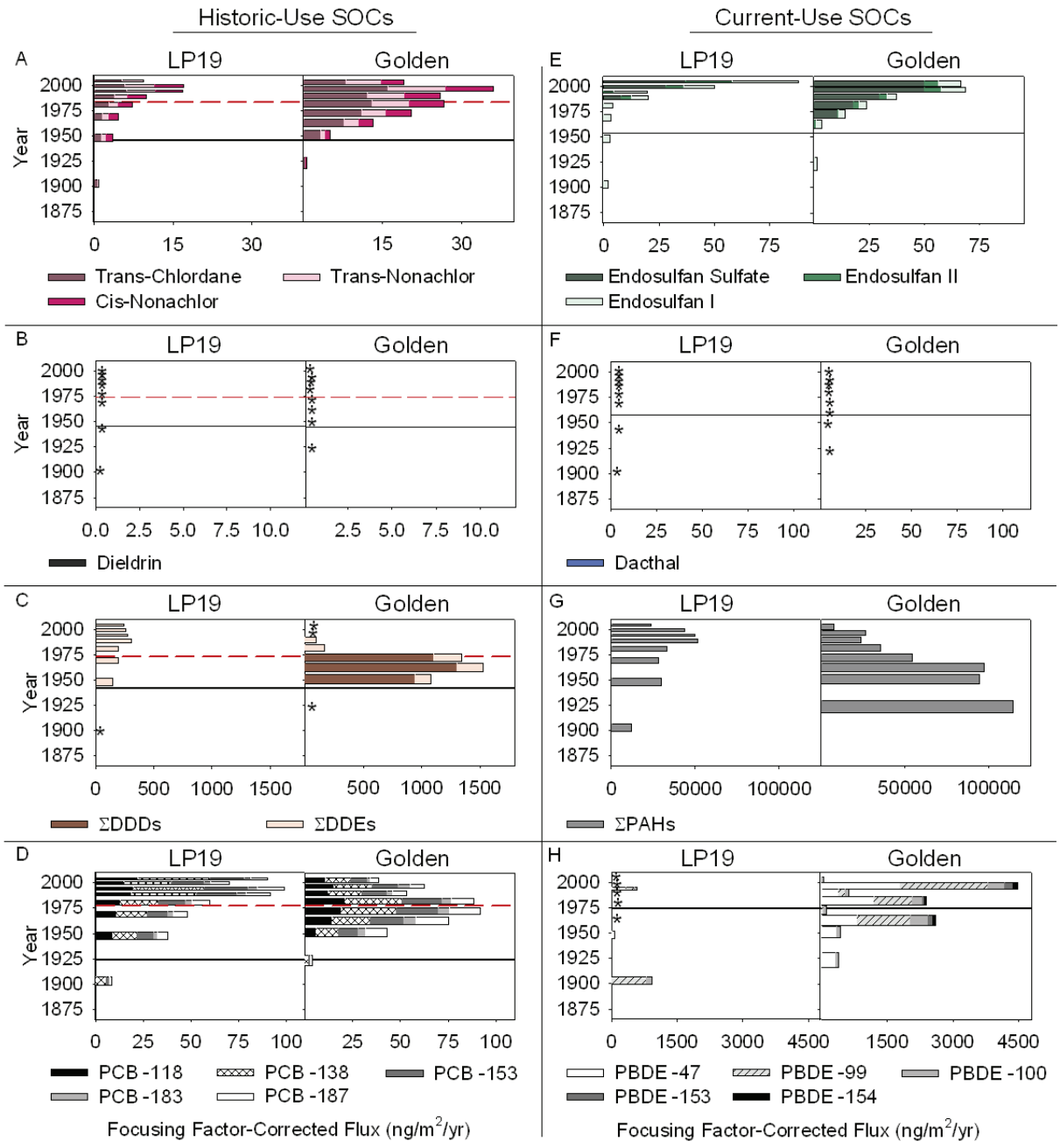

Figure 4-27. Focusing Factor-Corrected Flux (ng/m^2/yr) Profiles of Current- and Historic-Use SOCs in LP19 and Golden Lake Sediment Cores at MORA. Solid lines (——) indicate US registered use dates, dashed lines (– – –) indicate US restriction dates, and asterisks (∗)indicate below method detection limit.

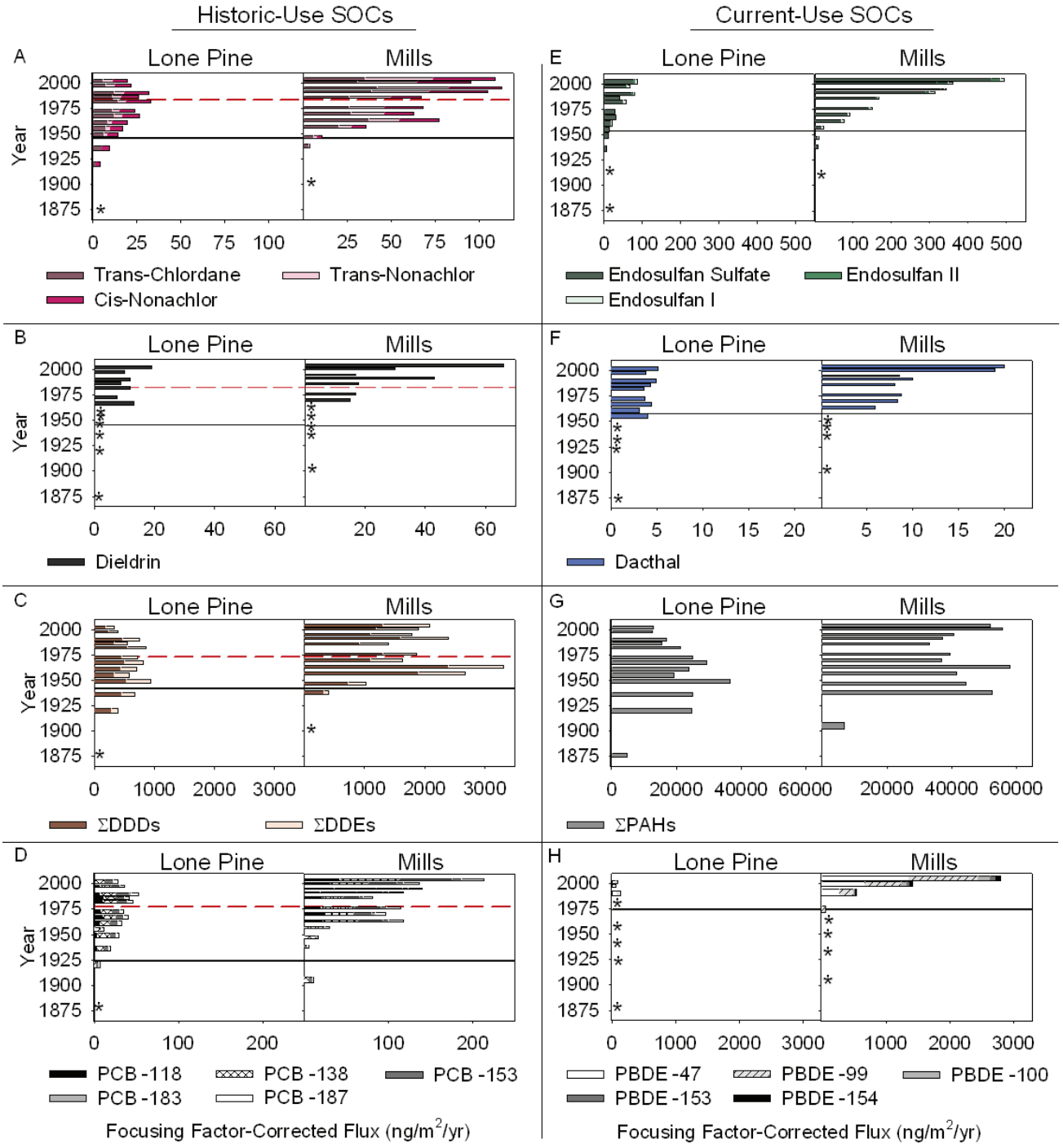

Figure 4-28. Focusing Factor-Corrected Flux (ng/m^2/yr) Profiles of Current- and Historic-Use SOCs in Lone Pine Lake and Mills Lake Sediment Cores at ROMO. Solid lines (——) indicate US registered use dates, dashed lines (– – –) indicate US restriction dates, and asterisks (∗)indicate below method detection limit.

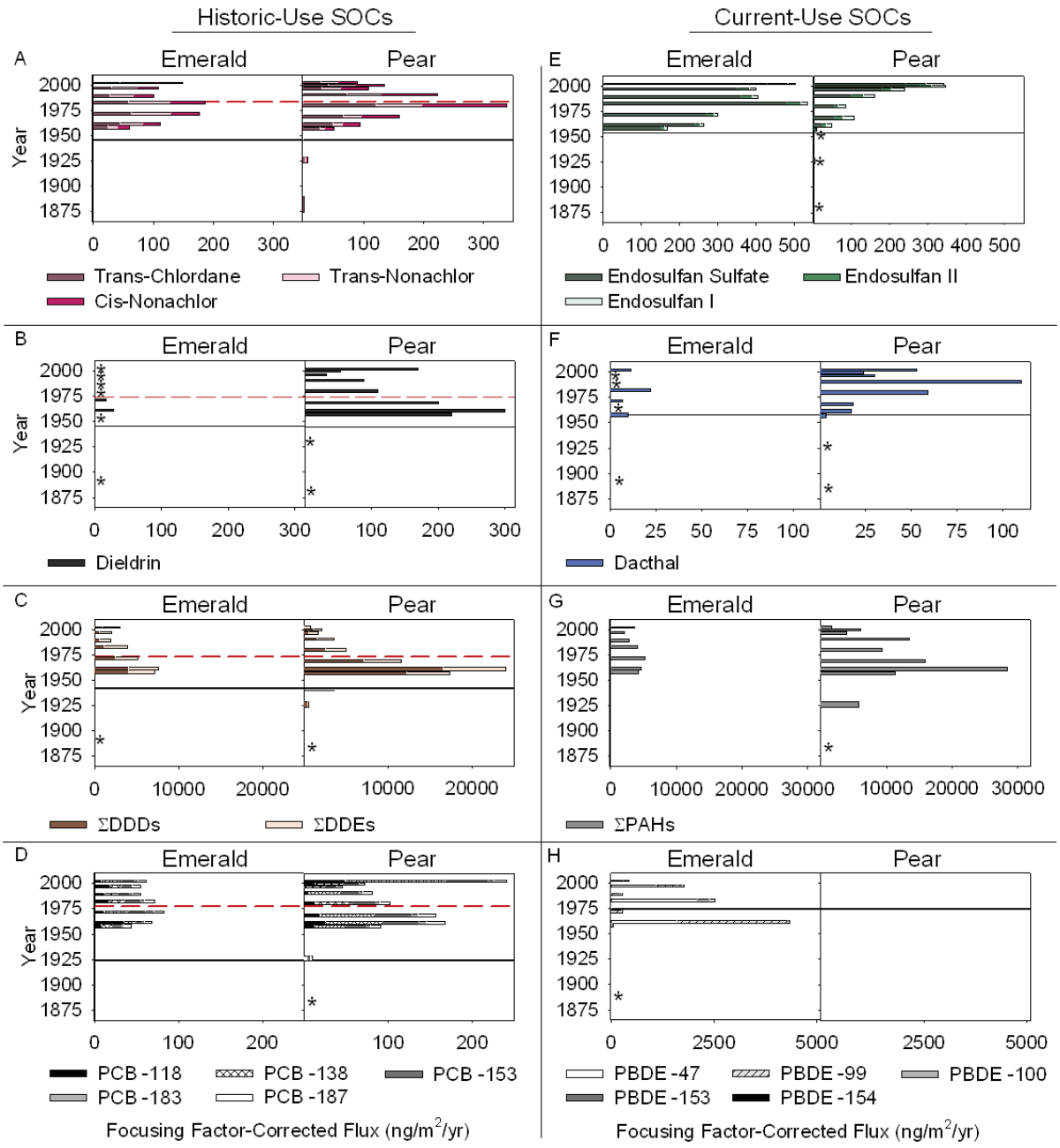

Figure 4-29. Focusing Factor-Corrected Flux (ng/m^2/yr) Profiles of Current- and Historic-Use SOCs in Emerald Lake and Pear Lake Sediment Cores at SEKI. Solid lines (——) indicate US registered use dates, dashed lines (– – –) indicate US restriction dates, and asterisks (∗)indicate below method detection limit.

PCBs were detected in all surficial sediments, and were highest at low latitude sites. The lowest focusing factor-corrected fluxes were at DENA, NOAT, and GAAR. The highest fluxes were found at SEKI and ROMO (see Figure 4-4).

PBDE fluxes were above the method detection limits in the surficial sediment only from ROMO. Within ROMO, Mills Lake, located on the east side of the Continental Divide, had PBDE focus-corrected flux an order of magnitude greater than Lone Pine Lake, which is located on the west side of the Continental Divide. This finding is discussed further in Section 4.2.6.3.

PAHs had the highest surficial sediment flux of all SOCs in the WACAP sites. As it did for the vegetation and snow samples, GLAC (Snyder Lake) had the highest surficial sediment PAH flux. This finding is discussed further in Section 4.2.6.2.

4.2.5.2 Temporal Distribution of SOCs in Sediments

Lake sediment analysis can be an extremely useful tool for evaluating the history of contaminant loading to a lake, but its utility is dependent upon several key assumptions: (1) the constituent of interest is stable (i.e., the compound is persistent and does not move appreciably as a result of diagenesis within the sediment) and (2) the sediment dating profile can be reasonably established through appropriate isotopic dating techniques. The WACAP sediment analysis meets both of these objectives for the target contaminants (both SOCs and selected elements). The fairly short gravity cores that were obtained from each lake typically penetrated to a depth going back to at least 1850. Some cores from lakes with very slow sedimentation rates penetrated much further back in time. We collected two cores from each lake, and if the first core dated out well with the radioisotope techniques, we accepted it for further analyses. If the first core could not be clearly dated, or if other concerns were apparent, we examined the second core and then selected the most appropriate of the two for further analysis. In all cases, one of the two cores displayed an acceptable dating profile.

For SOCs, given the expense of the analytical measurement, we carefully selected the exact slices of sediment for which we would perform analyses. These slices were selected and analyzed incrementally so that we would end up with a profile that maximized depiction of trends from pre-industrial times to the present. In general, we allocated approximately eight core slices per core for a complete SOC analyses. The results of this work are displayed in Figures 4-23 to 4-29). Each figure shows the pair of lakes for a particular WACAP park side by side, and the most prevalent SOCs are displayed by date. All figures use focus-corrected flux, so that comparisons among the lakes can readily be made. The solid horizontal lines in each figure represent the registration date for the specific SOC and the dashed lines represent the date of US restriction, if appropriate. The asterisks (*) indicate values below the method detection limit.

In most cases, the sediment SOC profiles are as expected with regard to the history of SOC use and regulation in the United States. Most do not appear in the sediment profiles until the date (sediment depth) that they were registered. After US restriction, most SOC concentrations began to decline; however, they have not reached zero because of revolatilization from various ecosystem sinks (including agricultural soils) and subsequent atmospheric deposition. For those cases in which the compound appears before the time of registration, we suspect that bioturbation and/or diffusion of the chemical within the sediment profile are responsible.

An examination of all seven figures reveals three groupings, with respect to the overall flux of SOCs to the lake sediments: high (ROMO, GLAC, SEKI), intermediate (OLYM, MORA), and

low (DENA, NOAT, GAAR). Sediment profiles of SOCs from SEKI and ROMO have the highest flux for most SOCs. Most of the SOC profiles for these two parks show an increase in specific SOCs near the time of registration. For SEKI lakes, there is often a decrease after the time in which the use of the specific compounds was restricted in the United States. In the ROMO lakes, there is good agreement within the sediment cores concerning the appearance of the compounds with time of US registration, but there has been virtually no decrease in deposition since use was restricted in the United States. This pattern might be a result of SOCs re-volatilizing from historic sources and undergoing atmospheric transport and deposition to remote ecosystems. A similar result was observed by Donald et al. (1999).

The profiles for specific SOCs from the paired lakes from each park generally show the same temporal pattern; however, the magnitude of flux to the sediments is frequently quite different. The differences in flux between sites in the same park could result from a variety of factors, including actual differences in airborne concentrations and deposition, differences in precipitation type and rate, differences in the way the watershed processes these compounds, and differences in mobility and delivery from the watersheds to the lake sediments themselves. Examining these issues for all sites is beyond the scope of WACAP, but will be addressed for ROMO as part of this work (Usenko et al., in press).

Several of the SOC sediment profiles stand out with much higher concentrations. Endosulfans and chlordanes are much higher at Emerald Lake (SEKI) and Mills Lake (ROMO), compared with all other sediment profiles, even those for the other lake in the same park. PAHs are significantly greater at Snyder Lake (GLAC) compared with all other lake profiles. This finding is consistent with PAH results at GLAC in other media, and is discussed further in Section 4.2.6.2.

For other SOCs, some concentrations were below our detection limit. This was the case for the entire profile of dieldrin, and for sum DDD and sum DDE, for all six lakes in MORA, OLYM, and GLAC. PCBs were lower in the intermediate lakes than in the high group, but are detectable throughout all profiles. Trends in PCB concentrations appeared to be stabilized or declining in the intermediate lakes, whereas two of the four lakes in the high group clearly had the highest PCB value at the surface of the core, which suggests a recent increase in flux of PCBs to the highest group.

SOC fluxes were lowest at the sites in Alaska (DENA, NOAT, GAAR), throughout their profiles. This is undoubtedly a result of the fact that these sites are long distances from major urban, industrial, and agricultural activities, and that precipitation, an important vector of SOC deposition, is generally lower at these sites. Chlordane and its major constituents, along with PCBs, were detectable in all Alaska lake sediment profiles, but at very low concentrations.

The group of contaminants most abundant in the sediments differed from those most common in snow and fish, primarily because of the different affinities SOCs have to partition among water, particulates, and lipid. Snow typically contains hydrophilic compounds, and some hydrophobic compounds can be associated with particulate deposition. Fish tend to accumulate compounds that are lipophilic. Lake sediments are a mix of organic and inorganic particles. Therefore, the contaminant histories in the sediments are influenced strongly by the watershed and lake processes leading to sedimentation, and would not be expected to have the same dominant suite of SOCs as snow and fish. It is difficult to compare SOC patterns across matrices; nonetheless, the sediments give information on the temporal changes in exposure to these contaminants.

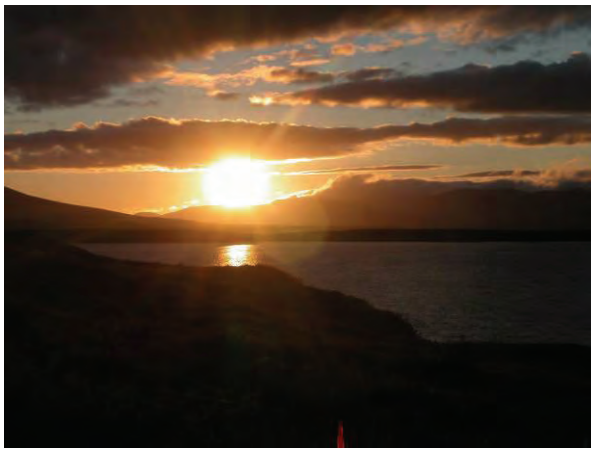

Lake Matcharak

McLeod Lake

Wonder Lake

Burial Lake

4.2.6 Source Attribution for SOCs

4.2.6.1 Sources of Pesticides

Some of the pesticides detected in both annual snowpack and in surficial sediment in WACAP lakes include dacthal, endosulfans, dieldrin, and chlordanes. SEKI, ROMO, and GLAC had the highest pesticide concentrations in 3 years of annual snowpack measurements and surficial sediment fluxes.

In an analysis of the first year of WACAP snow data (collected in 2003), Hageman et al. (2006) found a correlation between regional agricultural intensity and the concentration of several pesticides in WACAP snow, including both current-use and historic-use pesticides. They used the linear relationship between percent of regional agriculture and log concentration to estimate the fraction of each pesticide attributable to regional sources (within 75, 150, and 300 km). This model assumes that the amount of pesticide present in the snow in the Alaska parks was entirely from global sources and that the global contribution was constant at all parks. We have updated this analysis to include all 3 years of WACAP snow data. Figure 4-30 shows the percentage of pesticides related to regional sources, within 150 km of each park, by means of this method.

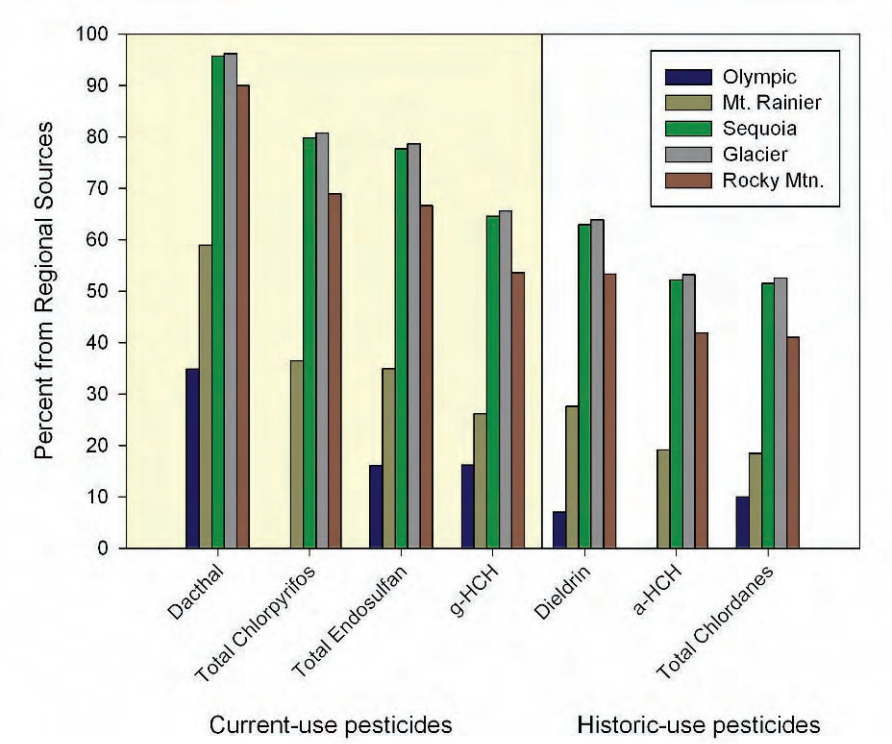

Figure 4-30. Percentage of Total Pesticide Concentration Related to Regional Sources. Regional is defined as within 150 km. Calculations use snow data collected from the springs of 2003-2005.

A small amount of agriculture occurs in Alaska, but for this analysis, the percentage of cropland intensity is insignificant. For GLAC and SEKI, the calculated contribution attributable to regional sources and transport is 80-100% for current-use pesticides, such as dacthal, total chlorpyrifos, and endosulfans. Even for some HUPs, such as dieldrin, a-HCH, and HCB, the pattern suggests a significant influence from historical regional agriculture. Presumably, this is a result of revolatilization of persistent SOCs that were applied to soils before the United States bans on agricultural usage.

Figures 4-12 and 4-13 show plots of SOC concentrations in lichens and conifer needles, respectively, overlaid on a map of agricultural intensity. For both lichens and conifer needles, the highest concentrations were measured in parks adjacent to the most intensive agricultural regions. In addition, parks with highest SOC concentrations were dominated by CUPs, usually endosulfans (see also Figure 4-31). At SEKI, the highest SOC concentrations in vegetation were endosulfans, but dacthal was the dominant SOC in snow (see Figures 4-1 and 4-7). This finding might reflect seasonality of sources, usage, or differences in uptake by snow and vegetation.

At parks with lowest overall concentrations of SOCs, HUPs made a larger contribution to total pesticide concentration. Concentrations of HUPs in Alaska parks were not very different from concentrations in parks in the conterminous 48 states. The results of Hageman et al. (2006) suggest that even for HUPs, regional agricultural sources are a good predictor for concentration in snow, presumably because the pesticide burden has revolatilized from soil and other sinks. For HUPs, regional agriculture explains 20-80% of the snow concentrations, with presumably global sources accounting for the remainder (see Figure 4-30).

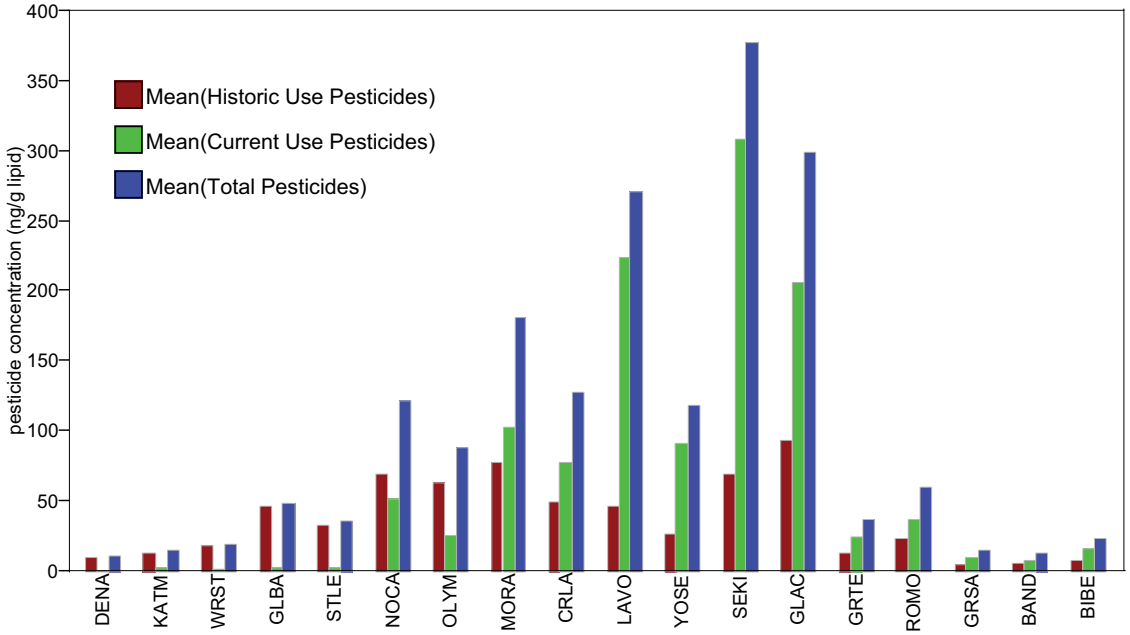

Figure 4-31. Mean Concentrations of Historic-Use (HCB, HCHs, Chlordanes, DDT, Dieldrin) and Current-Use (Trifluralin, Triallate, Chlorpyrifos, Dacthal, Endosulfans) Pesticides in Two-Year-Old Conifer Needles from WACAP Parks. Parks are ordered, left to right, from north to south along the Pacific Coast (DENA → SEKI), and from north to south in the Rocky Mountains (GLAC → BIBE). Current-use pesticides were not detected often in Alaska parks, comprised about one-third to one-half the total pesticide concentrations in northern Washington, and most of the pesticide burden elsewhere. Conifer needles were not sampled in NOAT and GAAR. Total pesticide burdens (current use + historic use) were highest in national parks of Washington, Oregon, California, and Montana.

Some specific pesticides in park vegetation could be influenced by regional and local application rates. Because different types of crops are grown in different parts of the United States, application rates of crop-specific insecticides and herbicides varies across the country.

Comparison of maps of application rates of chlorpyrifos, dacthal, endosulfans, triallate, and trifluralin in the western United States (Figures 4-14 to 4-18, respectively) and concentrations measured in vegetation suggest a relationship, especially if air mass back trajectories are considered (see Section 4.5).

Pesticide application rate does not correspond to pesticide concentrations in vegetation. For example, chlorpyrifos is applied at higher rates than endosulfans and dacthal, but concentrations in vegetation were low, probably as a result of the differences in the physico-chemical properties of these pesticides and their relative affinities to accumulate in vegetation. In addition, pesticide use data is missing for some western states and counties, limiting our ability to identify source regions.

4.2.6.2 Sources of PAHs at Glacier National Park

Previous studies have identified a relationship between PAH concentrations and proximity to urban regions (Garban et al., 2002; Hafner et al., 2005). Figure 4-5 shows the concentration of sum PAHs in vegetation, snow, and sediments. Concentrations of PAHs at GLAC were 1 to 2

orders of magnitude greater than at any other site, in these matrices. Figure 4-19 shows the concentration of sum PAHs in lichen at core and secondary parks, overlaid on a plot of population density. In contrast to the previous studies mentioned, a correlation with population is not present in the WACAP data, in large part because of the high PAH concentrations and low population density near GLAC.

However, the PAH concentrations in GLAC are not uniform across the park. Measurements in the watershed (Snyder Lake) closest to Columbia Falls showed significantly higher PAH concentrations. The sum PAH concentrations in snowpack, lichens, and surficial sediment were a factor of 7.7, 32.8, and 5.3 greater, respectively, in the Snyder Lake catchment (west of the Continental Divide) than in the Oldman Lake catchment (east of the Continental Divide). The PAH concentrations at Snyder Lake were the highest among all WACAP sites, whereas concentrations at Oldman Lake were comparable with those at sites in other parks. Referring to Figure 4-25, we see also that the PAHs in the Snyder Lake sediment core increased substantially in the early-mid 1950s. We believe the presence of high concentrations of PAHs at GLAC are related to the aluminum smelter in Columbia Falls, Montana, which came on-line in 1955 (Usenko et al., in press).

The electric-powered aluminum smelter in Columbia Falls operates with Söderberg aluminum smelting technology (Columbia Falls Aluminum Company, 2007). The smelter resides on the Flathead River (west of the Continental Divide), approximately 10 km southwest of GLAC and approximately 45 km southwest of Snyder Lake. Outflow from Snyder Lake forms a tributary of the Flathead River. Aluminum smelters that use Söderberg technology are known emitters of fluoride and PAHs, and can be significant local PAH sources in rural areas (Booth and Gribben, 2005; International Aluminum Institute, 2007). According to the USEPA, this specific smelter has been releasing hydrogen fluoride to the atmosphere at a rate of ~65 tons per year from 1999 to 2004 and PAHs to the atmosphere at a rate of ~14 tons per year from 1999 to 2005 (USEPA, 2007a). A previous study (National Park Service, 1998) suggests that fluoride, emitted to the atmosphere from the smelter, undergoes atmospheric transport and deposition to Snyder Lake catchment. These same upslope winds likely also transport PAHs from the aluminum smelter.

PAH ratios can be used to identify potential sources (Schauer et al., 2002; Yunker et al., 2002; Killin et al., 2004). The ratio of indeno[1,2,3-cd]pyrene concentration to indeno[1,2,3-cd]pyrene concentration + benzo[e]pyrene concentration (IcdP/(IcdP+BeP)) should remain fairly constant from emission sources to deposition in the environment, because these PAHs are typically sorbed to the particulate phase in the atmosphere and have similar physical and chemical properties. The IcdP/(IcdP+BeP) ratio from gasoline combustion in motor vehicles is 0.74 (Schauer et al., 2002), whereas the ratio from combustion of pine wood in a fireplace is 0.53 (Figure 4-32; Schauer et al., 2001). Aluminum smelters that use Söderberg aluminum smelting technology have been shown to emit an IcdP/(IcdP+BeP) ratio of 0.39 (Booth and Gribben, 2005; Sanderson et al., 2005).

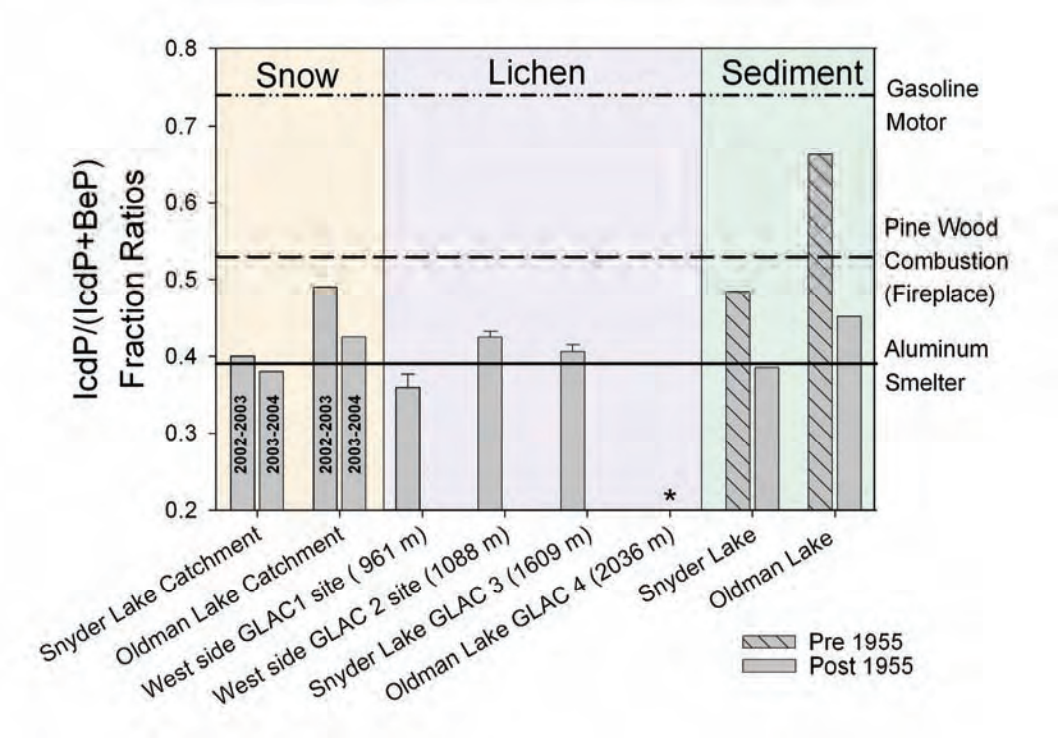

Figure 4-32. Fraction Ratios of IcdP/(IcdP+BeP) (average ± standard deviation) Calculated from Snow, Lichen, and Pre- and Post-1955 Sediment in Snyder and Oldman Lake Catchments in GLAC Compared to Measured Ratios. Measured ratios for gasoline motors from Schauer et al. (2002), pine wood combustion from Schauer et al. (2001), and an aluminum smelter from Sanderson and Farant (2005). " * " indicates values were below detection limits.

Figure 4-32 shows the measured IcdP/(IcdP+BeP) in snow, lichen, and sediment from the Snyder Lake and Oldman Lake catchments. The IcdP/(IcdP+BeP) ratio measured in the 2003 seasonal snowpack from Snyder Lake was 0.40, which closely matches the ratio previously seen for Söderberg aluminum smelter emissions; the ratio in the 2003 snowpack from Oldman Lake was 0.49. In addition, although the concentrations of PAHs in Snyder Lake vary considerably, the IcdP/(IcdP+BeP) ratio was fairly constant during the years of snow sampling.

The sum PAH flux in the Snyder Lake 2003-2004 snowpack was significantly lower than it was in the 2002-2003 snowpack. From March 2003 until 2007, the aluminum smelter reduced operations from 60% to 20% (Jamison, 2003). In 2002 (60% capacity), the aluminum smelter released 15.1 tons of PAHs to the atmosphere and in 2004 (20% capacity), the plant released 5.0 tons of PAHs (USEPA, 2007a). Although it is difficult to compare quantitatively, because a detailed timeline of smelter emissions is lacking, the reduction in PAH emissions is corroborated by a decline in PAH concentrations in the snowpack over this timeframe. The 2003-2004 snowpack PAH concentrations measured were approximately one-third of the 2002-2003 concentrations, similar to the reported emission reduction. At the same time the IcdP/(IcdP+BeP) ratios measured in the seasonal snowpack samples remained fairly constant from 2003 to 2004 (Figure 4-32), indicating that the smelter was still the dominant source of PAHs. BeP was not detected in lichens from Oldman Lake catchment, so the IcdP/(IcdP+BeP) ratio could not be calculated.

In the sediment cores at Snyder Lake, the IcdP/(IcdP+BeP) ratio was 0.49 before 1955, when the smelter came on line. From 1955 to the present, the IcdP/(IcdP+BeP) ratio has been fairly constant in the Snyder Lake sediment core, with an average and standard deviation of 0.35 ± 0.05. The IcdP/(IcdP+BeP) ratio measured in the Snyder Lake surficial sediment was 0.38. In Oldman Lake, IcdP was detected only in the 2005 (surficial sediment) and 1906 intervals. In 1906, the fraction ratio of IcdP/(IcdP+BeP) in the Oldman Lake sediment core was 0.66; in the surficial sediment of Oldman Lake, the IcdP/(IcdP+BeP) was 0.45 (Figure 4-32). In addition, the retene sediment flux over time was not significantly correlated with sum PAH, BeP, IcdP, or BghiP flux over time in Snyder Lake ($p > 0.05$), suggesting biomass combustion was not a major source of PAHs to the Snyder Lake catchment.

Taken together, we believe the data strongly suggest that the Snyder Lake watershed is influenced by the Columbia Falls aluminum smelter. The sources of PAHs for the Oldman Lake watershed are not as certain. The much lower concentrations and the IcdP/(IcdP+BeP) ratio are not consistent with an influence from the smelter, and the concentrations overall differ little from those in other parks.

4.2.6.3 Possible Urban/Regional Influences at Rocky Mountain National Park

At ROMO, a different issue emerges, related to observations at two sites across the Continental Divide. Mills and Lone Pine lakes are only 10 km apart, but they are on different sides of the Continental Divide. Mills Lake is on the east side and Lone Pine Lake is on the west side. Considering the impact that the Continental Divide has, it is possible that these two lakes receive different contaminant exposures.

Evidence of differences in atmospheric deposition within the Colorado Front Range has been reported in a number of studies (Burns, 2003, and references therein). Deposition of NO_3^- (nitrate) and NH_4^+ (ammonium) are greater on the east side of the Continental Divide than on the west side during summer. These two contaminants are associated with urban and agricultural sources. The elevated concentrations of these two contaminants might have resulted from summer upslope winds, or transport from the eastern lowlands up the Front Range of the Rocky Mountains, a wind pattern that is counter to the prevailing westerly winds (see Section 4.5).

Snow and sediment SOC data from ROMO suggest that these upslope winds might also be important in transporting PAHs and agricultural SOCs in higher concentrations to Mills Lake (Usenko et al., in press). Together, these matrices suggest year round differences in atmospheric concentrations between the two lakes. Figure 4-28 shows the SOC sediment flux profile for Mills and Lone Pine Lakes. For all compound classes, the sediment flux to Mills Lake was greater than the flux to Lone Pine (Usenko et al., in press).

A similar trend is true for the snow flux of SOCs. Table 4-5 shows the ratio of SOC fluxes, and concentrations, in the snowpack for Mills Lake compared with Lone Pine Lake for 2003 (Usenko et al., in press). The Mills Lake flux is always higher by a factor of from 1.6 to 4.1. However, much of the enhancement in snow flux at Mills Lake results from more snowfall in the Mills Lake basin, rather than higher atmospheric concentrations of contaminants. At Mills Lake, the 2003 snow water equivalent (SWE) was 90 cm; for Lone Pine Lake, it was 40 cm. The enhancement in snow concentrations between Mills and Lone Pine lakes is less than the fluxes. In fact, for dacthal, chlordanes, and PAHs, the snow concentrations are the same or greater in Lone Pine Lake than in Mills Lake (Usenko et al., in press).

SOC concentrations in air, conifer needles, and fish do not show a clear enhancement on the east side of ROMO. Conifers, in particular, do not provide evidence that the east side of ROMO has higher concentrations of pesticides than the west side. Although there is a suggestion of an east-west difference in SOC deposition at ROMO, not all of the WACAP data provide clear evidence for this effect. A more focused study, with many more sampling locations, would have to be conducted to address this question.

Table 4-5. Comparison of SOC Data from Mills and Lone Pine Lakes. The values in the table show the ratio of the Mills/Lone Pine Lake results for snow fluxes and snow concentrations.

	Mills to Lone Pine Ratio	
	Flux	**Concentration**
Endosulfans	3.2	1.4
Chlorpyrifos	NA	NA
Dacthal	2.5	1.0
g-HCH	4.1	1.8
a-HCH	4.1	1.8
HCB	NA	NA
Dieldrin	3.7	1.6
Chlordanes	1.6	0.7
PAHs	2.2	0.9

4.3 Trace Metals, Including Mercury

Figure 4-33 shows mean total mercury (Hg) concentrations in lichens, snow, fish, and sediments across all parks. Snow data are provided, both as concentrations and as fluxes. Hg concentrations in lichens are highest in parks in the conterminous 48 states. The same is true for Hg snow deposition fluxes. However, in fish, highest concentrations were found in samples taken in NOAT and GAAR. Detailed discussion of Hg concentrations in each medium follows.

4.3.1 Mercury and Trace Metals in Snow

Total Hg was measured in 60 snowpack samples, with park median concentrations ranging from 0.94 ng/L in MORA to 4.1 ng/L in GLAC. Mercury concentrations showed considerable spatial and temporal variability. Much of the Hg in snow is associated with particulate matter, which shows much greater variability at all scales, compared to dissolved constituents in melted snow (Turk et al., 2001). Hg was correlated with particulate carbon, and both were found at higher concentrations in snow samples from forested sites compared with samples from open meadows. In general, Hg concentrations in snow were lowest in the west coast parks, intermediate in the Alaska parks, and highest in the Rocky Mountain parks (Figure 4-33). The exception was OLYM, where concentrations and fluxes were fairly high. However, only a single year is represented because of poor snowpack conditions in 2003 and 2005.

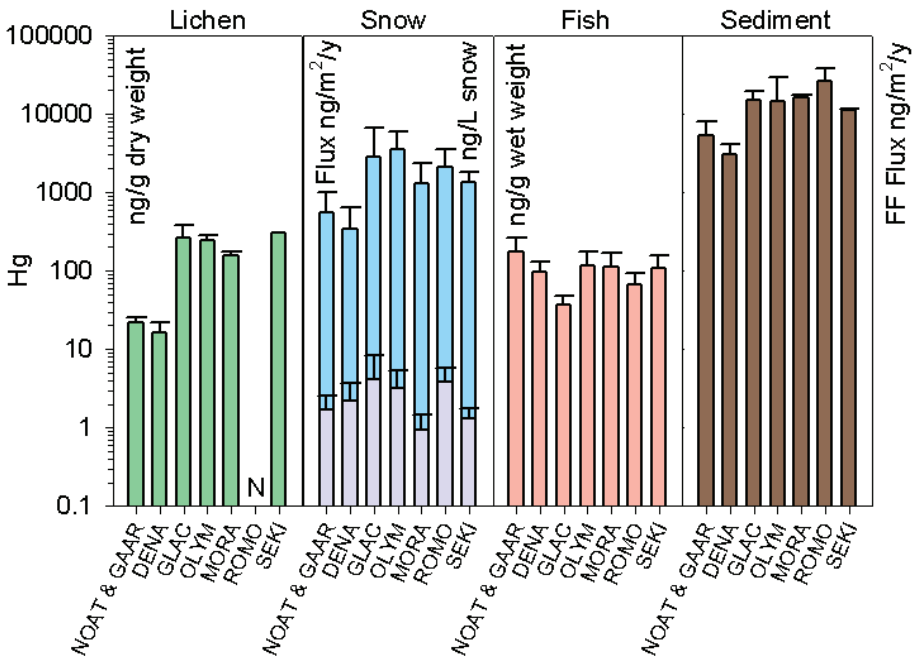

Figure 4-33. Average Concentrations and Fluxes of Mercury across Parks and Media. Snow data include fluxes (ng/m^2/yr) in blue and concentrations (ng/L) in gray. Fish data are for whole fish. Sediment data are reported as focusing factor-corrected (FF) flux for surficial sediment only. N = no data.

Deposition fluxes of Hg ranged from 336 ng/m^2/yr at DENA to 3,600 ng/m^2/yr at OLYM, with spatial and inter-annual variability driven largely by the variability in SWE. The Alaska parks had moderate concentrations but low SWE; OLYM had high concentrations and high SWE, and thus the highest Hg flux. MORA and SEKI had low concentrations and high SWE, and GLAC and ROMO had high concentrations and moderate SWE (see Figure 4-33). The Hg flux in OLYM was surprisingly high, but the median was calculated from only a few samples collected in a single year. Because warm-season deposition was not measured in this study, total annual deposition of mercury to the parks is higher than the snow fluxes reported here, especially in parks such as ROMO that receive substantial summer precipitation (Mast et al., 2005).

Concentrations of unfiltered methyl-mercury were measured in snowpack samples collected in 2005 only. Most values were below the detection limit of 0.04 ng/L; seven samples had values ranging from 0.05 to 0.59 ng/L; all of these had high particulate carbon concentrations as well.

Trace metals are often used as markers of source emissions types (see Section 4.2.6). We investigated the relationship between snow Hg concentrations and trace metals associated with coal combustion (Table 3-4). We found no significant correlations ($p < 0.1$) between Hg and these metals by linear regression or multiple linear regression, even if we accounted for the relationship between Hg and particulate carbon. We also analyzed the relationship between Hg and these metals by normalizing to Al concentrations to calculate an enrichment factor; again, we found no significant relationships. We hypothesize that the strong interaction between Hg and particulate carbon in snow overwhelms any relationship between Hg and other metals present in emissions from coal combustion.

4.3.2 Mercury and Particulate Carbon in Snow

We found a strong correlation ($R^2 = 0.63$, $p < .0001$) between total mercury and particulate carbon concentrations in the snowpack (Figure 4-34). The underlying mechanisms that control this relationship are uncertain. It is possible that mercury and particulate carbon become associated in the atmosphere and are deposited to the snowpack together. Or they could be deposited separately and become associated within the snowpack. This association could provide a mechanism to bind atmospherically deposited reactive mercury and prevent its reduction and subsequent evasion to the atmosphere (LaLonde et al., 2002). Thus, particulate carbon might act to sequester more of the deposited Hg from the winter deposition period, increasing the net flux of Hg to the watershed when the snowpack melts. Otherwise, Hg in the snowpack that is not bound to particulate carbon might be lost through revolatilization to the atmosphere. Thus, the WACAP Hg concentrations reflect complex biogeochemical cycling with natural and anthropogenic components.

Mercury in the snowpack is associated with particulate carbon

At Lake Irene in ROMO, snowpack sampling was conducted at paired sites approximately 200 m apart. The forest site was in a forest clearing about 10 m in diameter on a northwest-facing 20-degree slope; the meadow site was in an open meadow on a southeast-facing 5-degree slope (see photo). A single pair of samples (one from the forest site, one from the meadow site) was collected in 2002, 2004, and 2005, and two pairs were collected in 2003. Unfiltered total Hg averaged 2.7 ng/L greater (28%) at the forest site than at the meadow site for the five sample pairs. Particulate carbon was also higher at the forest site. Various processes could contribute to the difference. The greater surface area and more favorable depositional substrate of the forest canopy relative to the open snow-covered meadow probably enhances dry deposition of mercury and carbon in the forest (St. Louis et al., 2001). The northerly slope and shading from the canopy would also reduce solar radiation to the snowpack surface in the forest, limiting photo-reduction and evasion of mercury from the snowpack. The combined effects of particulate carbon and forest canopy on Hg concentrations in snow contribute to the large temporal and spatial variability in Hg deposition at all scales, as discussed in Section 4.3.1.

Higher mercury concentrations were found in the forest than in an adjacent meadow.

4.3.3 Trace Metals in Vegetation

Fifty-two lichen samples were analyzed for 45 elements, excluding nitrogen, representing 6 species for the 8 core parks. In addition, 105 samples representing 13 lichen genera from all 20 WACAP parks were analyzed for nitrogen. Because lichens differ in their elemental profiles, lichen element concentrations were considered separately by taxon (i.e., species when known, genus otherwise). Summary statistics for WACAP element concentrations by park and taxon are provided in Appendices 4A.12 and 4A.13.

Overall, metals were within expected background ranges in the WACAP parks.

To determine the enhancement of the nitrogen and sulfur nutrients and the toxic metals cadmium (Cd), nickel (Ni), and lead (Pb) in lichens of WACAP parks, relative to other remote sites in the western United States, we calculated the upper limit for the background range for public lands. To do this, we queried the national databases for the National Park Service [NPElement (Bennett, 2007)] and the US Forest Service [USFS Lichens and Air Quality Database (US Forest Service, 2007)] for lichen element concentrations from Montana, Wyoming, Colorado, New

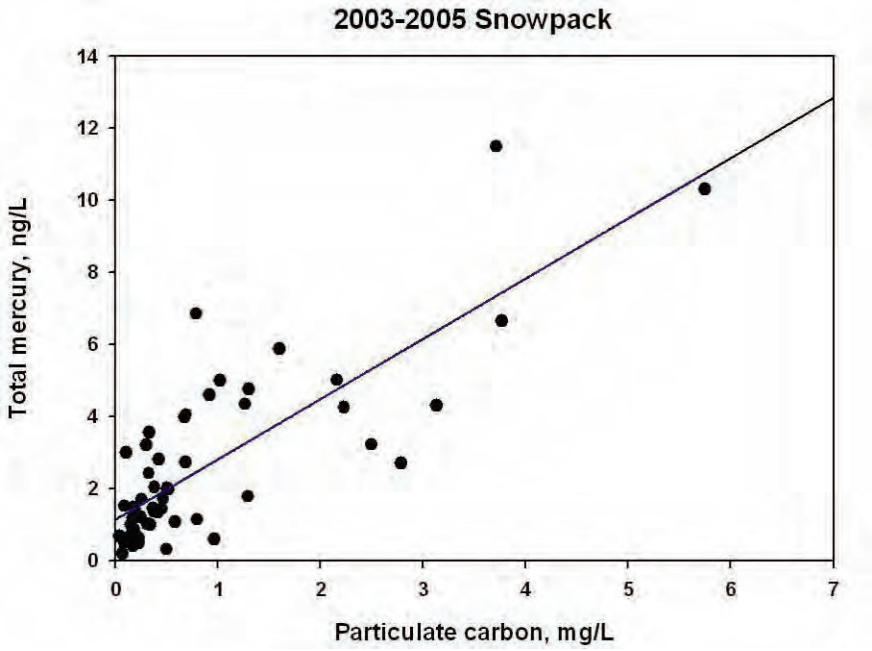

Figure 4-34. Unfiltered Total Mercury vs. Particulate Carbon Concentrations for All WACAP Snowpack Samples, 2003-2005.

Snow sampling crew digging a snow pit at the meadow site near Lake Irene in ROMO. The paired forest site is in the background.

Mexico, and Texas westward (excluding Hawaii), and all lichen species and elements targeted in WACAP parks.

To augment comparison data for the Arctic lichens, *Masonhalea richardsonii* and *Flavocetraria cucullata*, we added 2004 and 2005 data from the NPS Arctic Parks database from NOAT (Peter Neitlich, pers. comm.) to the resulting database. This combined WACAP Western States Lichen Element Database contains data for 7,953 lichen samples from 76 national forests, parks, and other federally managed lands for 60 elements representing all WACAP target lichens and includes the WACAP lichen element data. See Appendix 4A.15 for a list of public lands encompassed in the database.

To specifically examine the relative enhancement of nitrogen, sulfur, mercury, cadmium, nickel, and lead, we calculated the 0, 2.5, 10, 25, 50, 75, 90, 97.5 and 100% distribution quantiles by lichen genus and element for the WACAP Western States Lichen Element Database, excluding the WACAP data to determine background ranges that were independent of the WACAP data (Appendix 4A.14). Because not all parks are in pristine locations, we chose the 90% quantile, rather than a higher quantile, as the upper limit for background values. This limit is arbitrary, being based on a perusal of distribution histograms which indicate that values below the 90% quantile tend to follow a normal distribution typical of a background population. Ideally, comparisons at the species level would be desirable, but in this analysis, species in the WACAP target genera examined were similar morphologically and had similar element profiles, justifying assessment at the genus level. Also, comparing genera simplifies calculations by reducing the number of comparisons.

The same lichens that were best accumulators of SOCs—*Platismatia*, *Usnea*, *Xanthoparmelia*, and *Hypogymnia*—also accumulated larger concentrations of metals and nutrients, than did the poorer SOC accumulators—*Alectoria*, *Cladina*, *Flavocetraria*, and *Masonhalea* (compare 50% quantiles across species in Appendix 4A.14). This finding underscores the desirability of using a single species where possible, choosing species with similar element profiles, or overlapping target species sampling so that a system for comparison can be developed.

To evaluate how the samples in each park compared with background ranges for remote sites in the western United States, we expressed each sample as a percentage of the background range by dividing element concentrations of each WACAP sample by the upper limit of the background range for the relevant lichen genus and element. Results are presented as percent enhancement in Figure 4-35. The chief advantage of this approach is that it allows samples from different species within and across parks to be compared.

Overall, metals were not noticeably elevated in any of the WACAP parks (Appendix 4A.12). The GAAR site at Matcharak Lake had high concentrations of many of the rare earth elements [dysprosium (Dy), erbium (Er), europium (Eu), gallium (Ga), gadolinium (Gd), holmium (Ho), lanthanum (La), lutetium (Lu), neodymium (Nd), praseodymium (Pr), antimony (Sb), terbium (Tb), thulium (Tm), uranium (U), yttrium (Y), ytterbium (Yb)], compared to other WACAP core parks. Rare earth elements are typically associated with soils and probably represent local dust. Evidence of this association is the rather high aluminum concentrations in the *Flavocetraria cucullata* samples from GAAR. In general for lichen samples, the higher the aluminum and iron concentrations the higher the concentrations of the rare earth elements. Of the elements identified for comparison with other public lands of the western United States, mean concentrations of cadmium, nickel, and lead were well under thresholds at all parks (Figure 4-35).

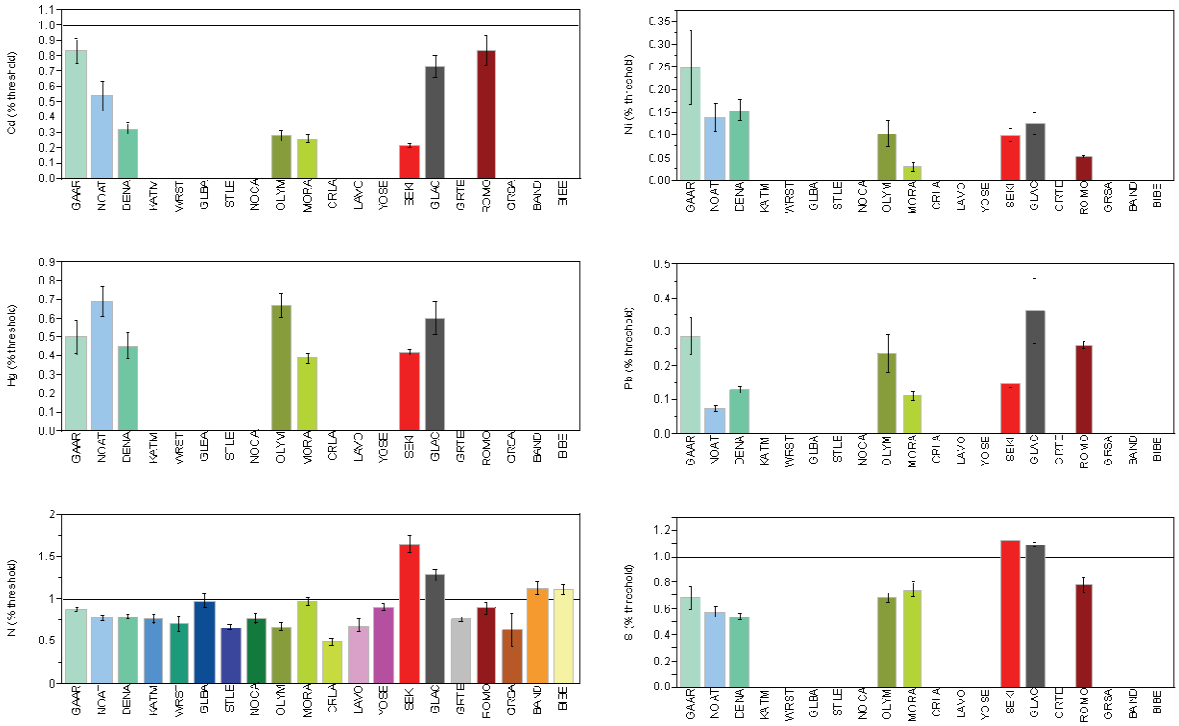

Figure 4-35. Comparison of Selected Elements in Lichens of WACAP Parks with Elements in Other National Parks and Forests in Western North America. Thresholds are the 90th percentile of element concentration distributions in lichens from remote sites. In general, lichen element concentrations indicate that metals were within expected ranges, sulfur deposition was elevated in SEKI and GLAC, and nitrogen deposition was elevated in SEKI, GLAC, BAND, BIBE. Error bars indicate one standard error.

Highest mercury concentrations in lichens among western parks in the NPElement database were measured in samples from BIBE in 2002: 39% of *Usnea* samples and 25% of *Xanthoparmelia* samples collected there in 2002 were above the 90% quantile of the background range for these species. (Lichen samples were collected at all WACAP parks and are currently archived at UMNRAL, but were analyzed only for sulfur, mercury, and metals at the core parks). Although mercury concentrations are not higher in the WACAP core parks than we would expect for western forests and parks, because the biomass of needles is so high on a per hectare basis, forest fire is a significant source of mercury release into the atmosphere (e.g., Friedli et al., 2003). Mercury is an emerging element in lichen biomonitoring of air quality, and historic data for trends analysis is nearly non-existent. The oldest data in NPElement and the USFS Lichens and Air Quality databases are from 1990 and 1995; only in recent years have researchers been more systematic about including mercury in lichen biomonitoring studies (Bennett, 2007; US Forest Service, 2007). On a global scale, mercury emissions are predicted to increase with increased human population and concomitant development of coal resources for energy production, especially in China. Continued monitoring of mercury in vegetation can assess the effects of implementing emission controls vs. increased energy production.

In contrast to mercury, most lichen elemental concentration studies on public lands have included measurements of lead and sulfur (Bennett, 2007; US Forest Service, 2007). Significant reductions have been observed in study areas where re-measurements have occurred. For example, lead concentrations in *Alectoria sarmentosa* collected in 1983 from Golden Lake in

MORA averaged 5.45 ± s.d. 2.62 ppm. WACAP samples of *A. sarmentosa* from Golden Lake collected in 2005 averaged 1.29 ppm ± s.d. 0.12 ppm. In SEKI, 27 samples of *Letharia vulpina* sampled at 8 sites in 1984 had concentrations ranging from 3.11 to 24.12 ppm (average 8.58). The 2004 WACAP samples of *L. vulpina* from Emerald Lake basin in SEKI ranged from 1.22 to 1.77 (average 1.39).

In summary, metal concentrations in WACAP core parks were within background ranges for remote sites in the western United States. Mercury is likely to be the metal of highest concern because it is re-released to the atmosphere during forest fires. Comparisons of WACAP data with historic data in the NPS lichen element database, NPElement (Bennett, 2007), indicate that lead is decreasing in MORA and SEKI. Although lichen sulfur and metal concentrations were not analyzed in the secondary parks, historic data from NPElement indicates mercury concentrations could be elevated in BIBE. Analysis of archived WACAP lichen samples could provide trends data for some secondary WACAP parks and establish baselines for parks currently lacking lichen data.

4.3.4 Mercury and Trace Metals in Fish

Unlike lipophilic SOCs (contaminants stored in lipids), Hg in fish is mainly in the form of methyl-Hg, which accumulates in muscle tissue (Munthe et al., 2007). Although fish Hg concentrations (shown in Figure 4-33) are measured in the whole fish, the bulk of the Hg is tied up in muscle tissue. Incorporation of Hg into the food web and into fish tissue is generally limited by rates of methylation, which in turn can be limited by nutrient availability (St. Louis et al., 2004). Therefore, some areas can have fairly high Hg deposition, but low methylation rates and hence low fish tissue Hg (Bloom, 1992). This limitation probably explains the fish concentration data at ROMO, where Hg flux to the snow and sediments is fairly high, yet fish Hg concentrations are fairly low (see Figure 4-33). Data from NOAT and GAAR show the opposite pattern—low Hg in snow and sediment fluxes, but high Hg concentrations in fish. On this basis, it appears that even though atmospheric deposition is a primary source of Hg to these ecosystems, the linkage between snow deposition and fish concentrations is weak. Other factors, as already mentioned, must also be important in explaining the Hg uptake and bioaccumulation in fish. More attention to this topic is given in Section 5.6 of Chapter 5.

The complex processes that control mercury accumulation in fish include atmospheric deposition, methylation and bioconcentration in the food web, and bioaccumulation as fish age.

In a comprehensive study at Voyageurs National Park in Minnesota, Wiener et al. (2006) investigated the factors associated with Hg concentrations in fish. These authors concluded that high dissolved sulfate, low lake water pH, and high organic carbon favored methyl-Hg accumulation in the fish. Lake temperature has also been implicated in methylation (Schindler et al., 1995; Lambertsson and Nilsson, 2006). These results indicate that we should not expect a direct relationship between Hg concentrations in vegetation, snow, and fish in the WACAP parks, and indeed we see no simple relationship.

For trace metals in fish, we analyzed concentrations in both fillets and livers. A comparison of concentrations in the fillets with those in the livers showed significantly higher concentrations in the livers. For Cd, Cu, Ni, Pb, and zinc (Zn), concentrations in the livers were elevated by factors

of 20, 60, 10, 900, and 230, respectively, compared to those in the fillets. On average, vanadium (V) did not show an enhancement. Because the concentrations in the fillets are very low, and close to the limit of detection for the various metals, small differences in concentration are not easily observed, whereas these changes are clearly indicated in the liver concentration data.

For all metals except V, the liver compositional analysis shows stronger influence from bioaccumulation than did the corresponding fillet tissue analysis.

Figure 4-36 shows the distribution of trace metals in the liver of fish from the core WACAP parks. The highest concentrations of lead in fish livers were observed in fish from Snyder Lake in GLAC (Figure 4-36). The next highest concentrations were observed for fish from Burial Lake (NOAT), Wonder Lake (DENA), and Emerald Lake (SEKI). There was always a significant difference in lead concentrations among lakes within a park, except at ROMO, where concentrations between Lone Pine and Mills Lakes were similar.

The Cd concentration in fish liver was highest in Emerald Lake (SEKI), followed by similar concentrations in Burial Lake (NOAT), Wonder Lake (DENA), Mills Lake (ROMO), and Pear Lake (SEKI). However, the fish specimens sampled in Burial and Wonder lakes were considerably older than specimens from the other lakes. Therefore, this observation could include an age/bioaccumulation effect or a species effect.

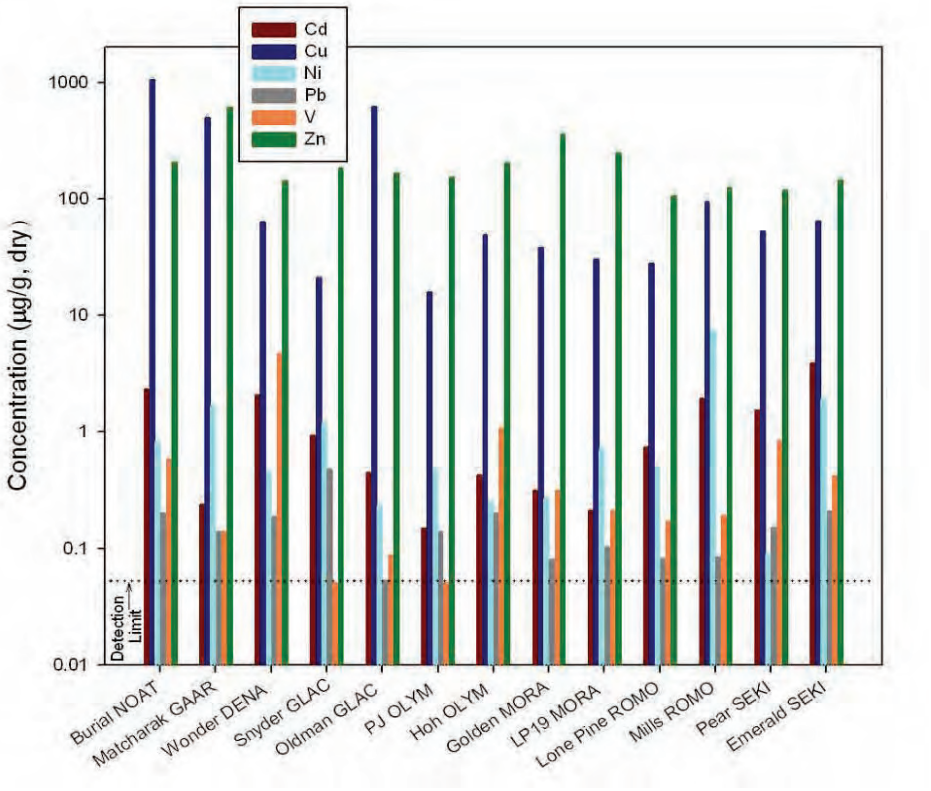

Figure 4-36. Trace Metals in Fish Liver. Distribution of Cd, Cu, Pb, Ni, V, and Zn average concentrations in fish livers from 2- to 8-year-old specimens collected from western national park lakes in GLAC, OLYM, MORA, ROMO, and SEKI, and 18- to 28-year-old specimens from lakes in NOAT, GAAR, and DENA. Because of the small sample size, no fish from McLeod Lake (DENA) were analyzed for trace metals.

Concentrations of Cu were highest in the livers of fish from Burial Lake, Matcharak Lake, and Oldman Lake, compared with fish livers from the other lakes studied. Copper concentrations in fish livers are similar in the other national park lakes, with the lowest concentration observed in PJ Lake (OLYM).

Concentrations of Zn in fish liver were highest in Matcharak Lake (GAAR), which represents older fish specimens that might exhibit bioaccumulation. The second highest concentration occurred in Golden Lake (MORA). Zinc concentrations were similar in magnitude in all other national park lakes—between 100 µg/g (dry basis) and 150 µg/g (dry basis).

All Ni and V concentrations in fish liver were below 10 µg/g (dry basis), with most below about 1 µg/g (dry basis). The detection limit for all metals was about 0.6 µg/g (dry basis).

4.3.5 Mercury, Trace Metals, and Spheroidal Carbonaceous Particles in Sediments

4.3.5.1 Mercury, Trace Metal, and SCP Focus-Corrected Fluxes

Temporal patterns of mercury, trace metals, and spheroidal carbonaceous particles (SCPs) were determined from the dated sediment profiles at the core parks. These have been corrected by the focusing factor as described in Chapter 3. Figures 4-37 to 4-43 show the focus-corrected fluxes for a selected set of metals and SCPs for both lakes in each park. In addition to atmospheric deposition, watershed processes influence the delivery of mercury to the lake sediments. Some of the more important factors are the watershed-to-lake area ratio, total organic carbon (TOC) in the lake water, and the wetland area associated with the lake (Wiener et al., 2006). In nearly all lakes, Hg fluxes are larger now, compared to pre-industrial values. The one exception is Hoh Lake, where the Hg flux showed a large increase between 1910 and 1930, and then decreased to pre-industrial values.

Figures 4-37 to 4-43 also show the focus-corrected fluxes for Ni, Cu, Pb, V, Zn, and Cd in $\mu g/m^2/yr$. These metals display a complex and closely matched pattern with some metals generally rising and falling together in the same lake. We know that many of these variations are related to watershed processes such as erosion, avalanches, and landslides, which is discussed in more detail later in this section. In most lakes, there were generally increasing fluxes of Pb and Cd toward the surface, which we believe to be associated with greater anthropogenic sources. But at some lakes, a different trend appeared, with metals increasing and decreasing together in a complex pattern. In most lakes in parks in the conterminous 48 states, the order of flux was approximately Zn > V > Pb > Cu > Ni > Cd > Hg. In a few sediment cores, V was greater than Zn. In the Alaska parks, Cu and Ni were much higher than the Pb flux. The highest flux for most metals was observed at PJ Lake (OLYM). PJ Lake shows a very complex pattern, with multiple peaks in the flux of all metals between 1920 and 1970. The Pb fluxes were highest in Snyder Lake (GLAC), Mills Lake (ROMO), and Emerald Lake (SEKI). These same lakes were also high in SCPs, suggesting a strong influence from regional combustion sources. Although the spatial pattern for Cd is similar to that of the other metals, the magnitude of the flux is lower than most other metals by a factor of 100 or more.

SCPs result from high temperature combustion of fossil fuels (see Chapter 3). Because SCPs range from 5 to 50 µm in diameter, transport of these large atmospheric particles is limited by their atmospheric lifetime (a few days to one week). Thus SCPs provide a measure of exposure to fossil fuel combustion within a range of a few hundred to approximately 1,000-2,000 km.

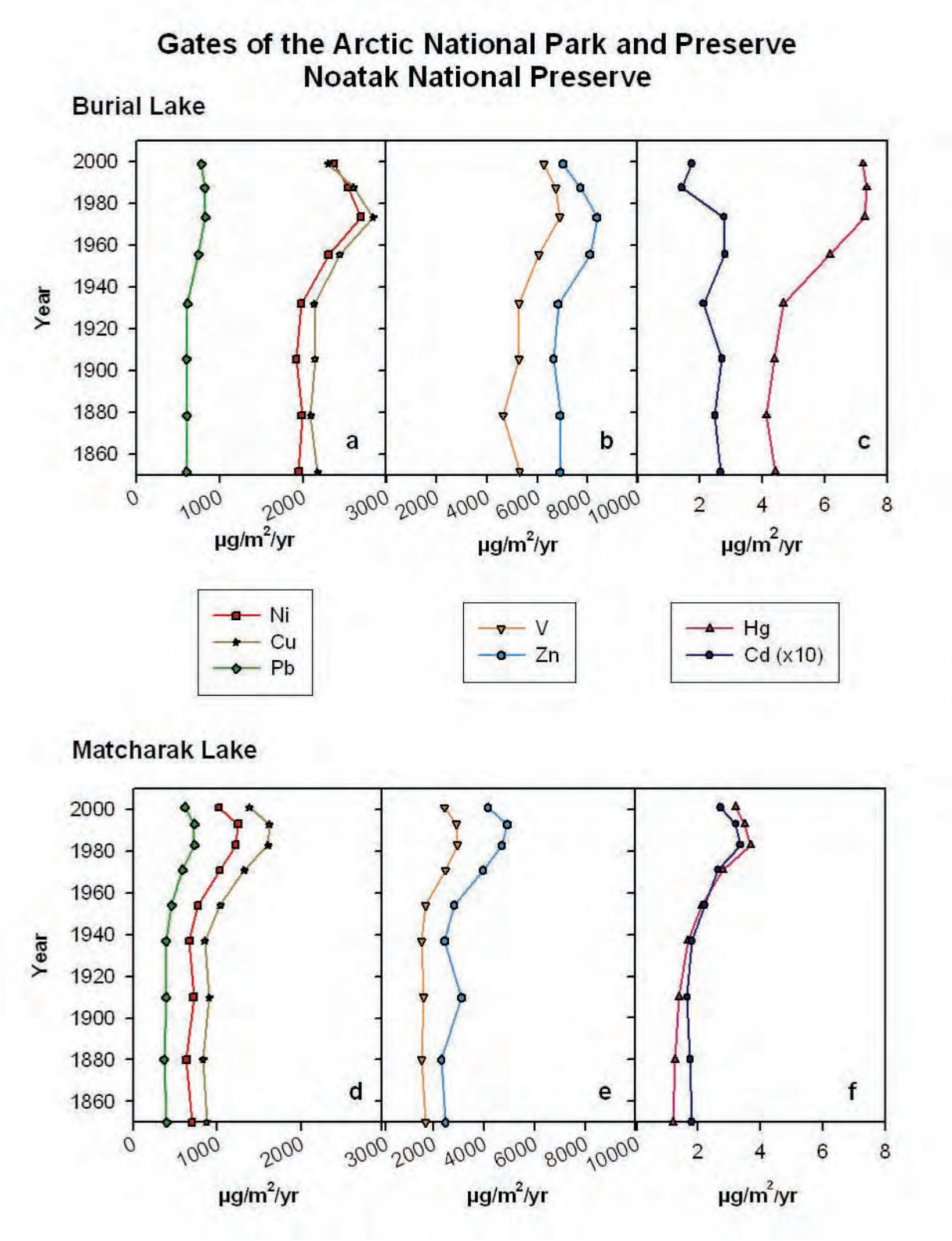

Figure 4-37. Focusing Factor-Corrected Flux of Ni, Cu, Pb, V, Zn, Cd, and Hg (µg/m^2/yr) in Sediment Cores from Burial Lake (NOAT) and Lake Matcharak (GAAR). Cd flux has been reduced by a factor of 10. No SCPs were detected in the sediment cores from these lakes.

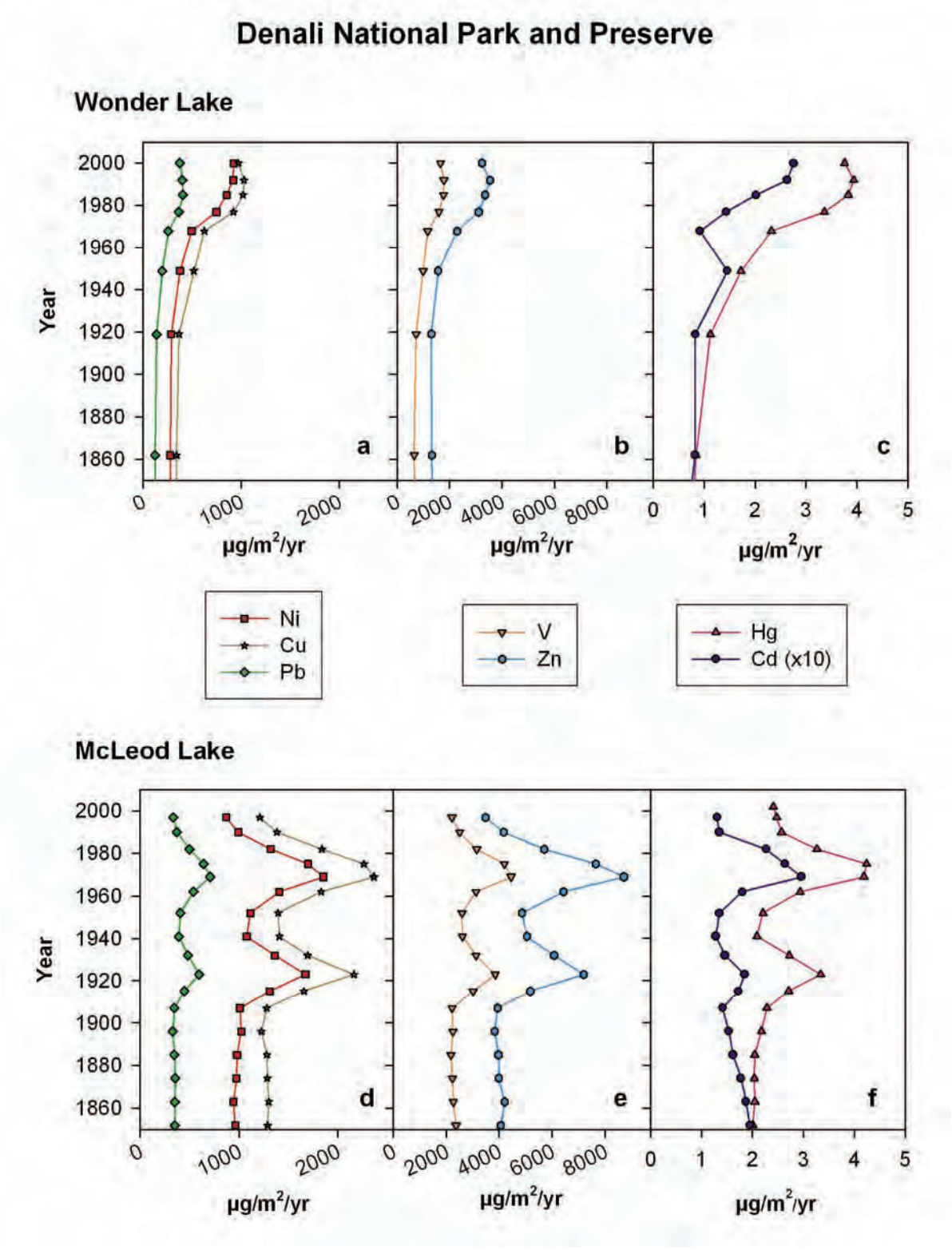

Figure 4-38. Focusing Factor-Corrected Flux of Ni, Cu, Pb, V, Zn, Cd, and Hg (µg/m^2/yr) in Sediment Cores from Wonder and McLeod Lakes (DENA). Cd flux has been reduced by a factor of 10. No SCPs were detected in the sediment cores from these lakes.

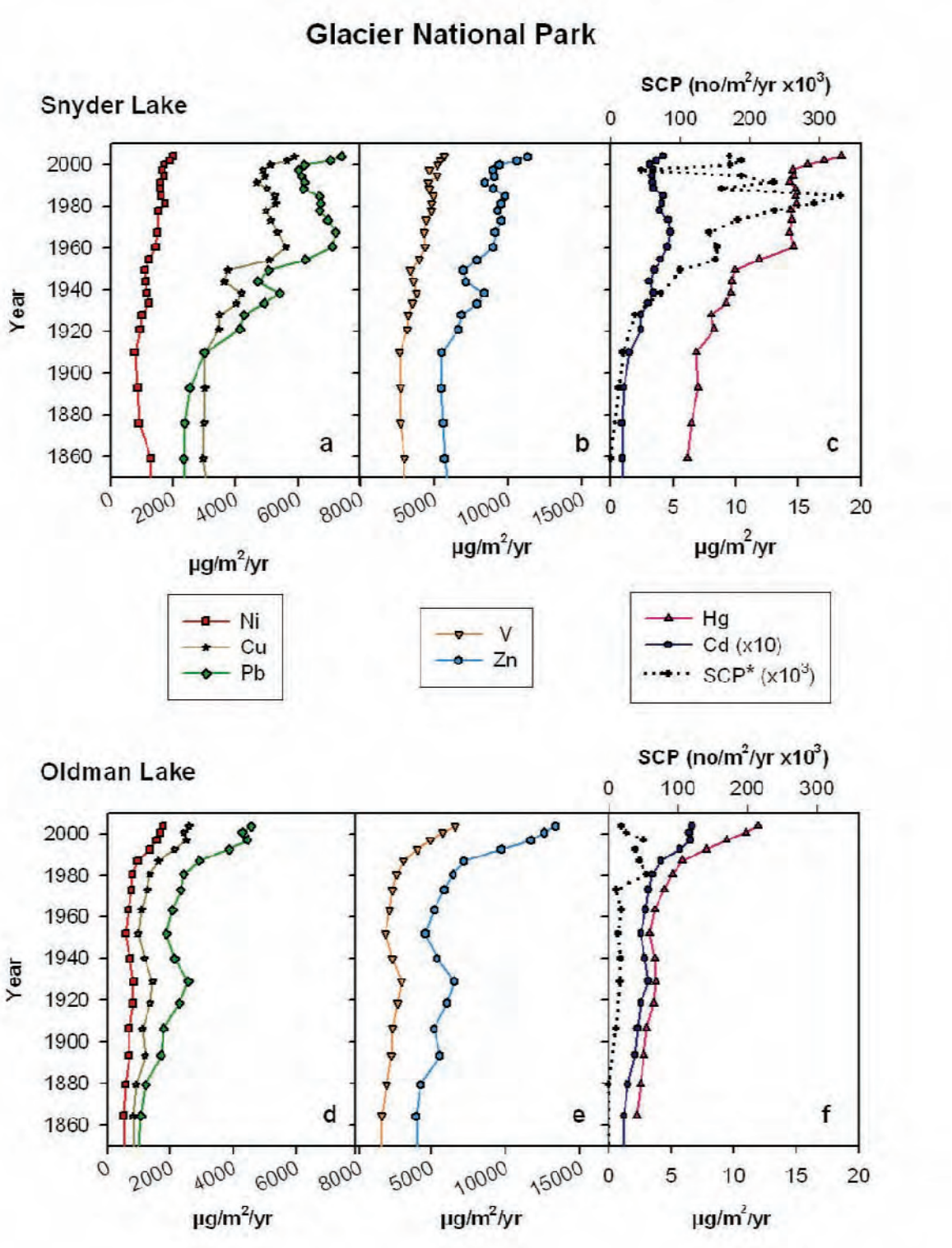

Figure 4-39. Focusing Factor-Corrected Flux of Ni, Cu, Pb, V, Zn, Cd, and Hg (µg/m^2/yr) and SCP (number/m^2/yr, reduced by a factor of 1,000 and shown in the top axis) in Sediment Cores from Snyder and Oldman Lakes (GLAC). Cd flux has been reduced by a factor of 10. SCP flux for Snyder Lake is from the secondary core from this lake.

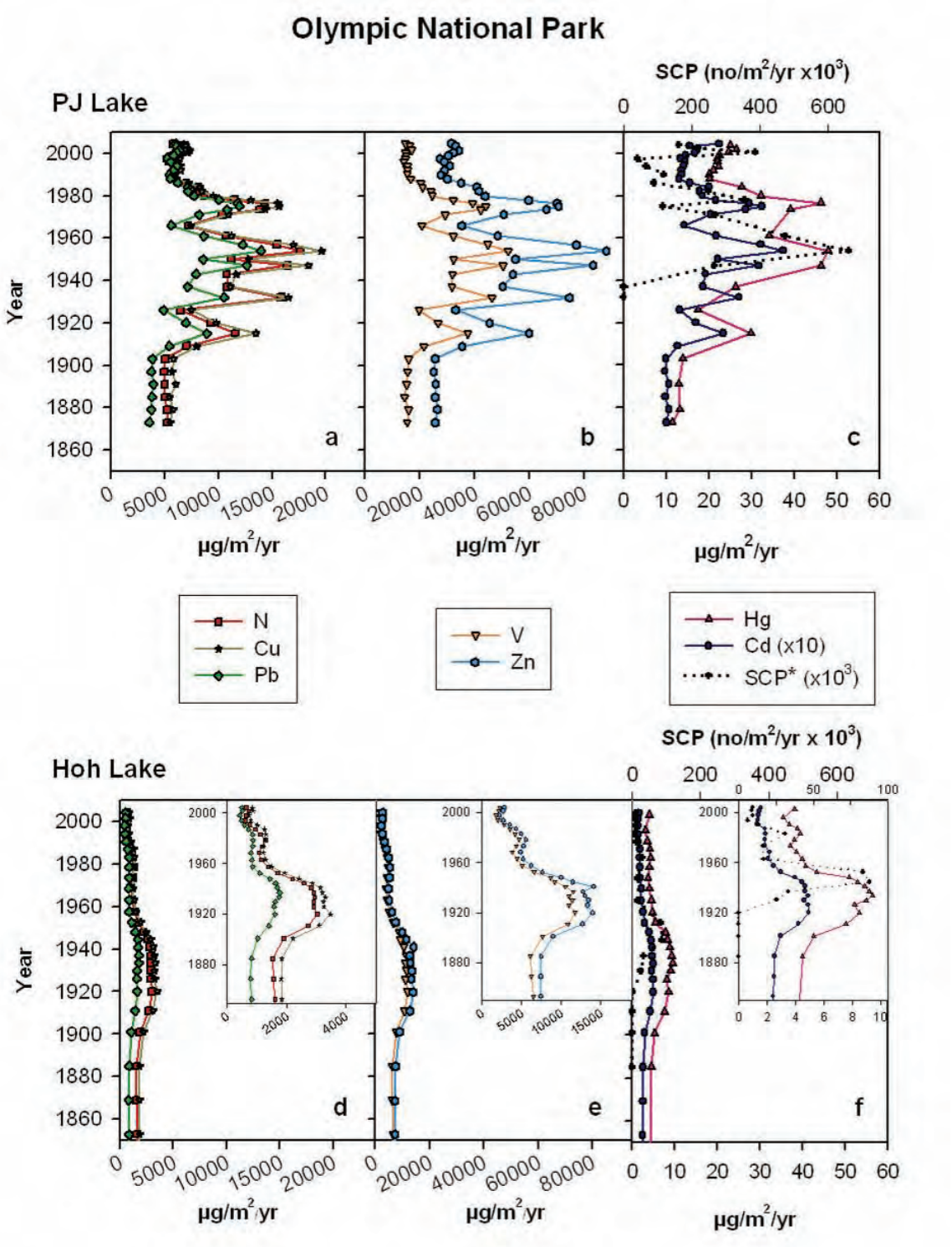

Figure 4-40. Focusing Factor-Corrected Flux of Ni, Cu, Pb, V, Zn, Cd, and Hg (µg/m^2/yr) and SCP (no/m^2/yr, reduced by a factor of 1,000 and shown in the top axis) in Sediment Cores from PJ and Hoh Lakes (OLYM). Cd flux has been reduced by a factor of 10. Inset boxes for Hoh Lake have expanded flux scale. SCP flux is from the secondary cores from these lakes.

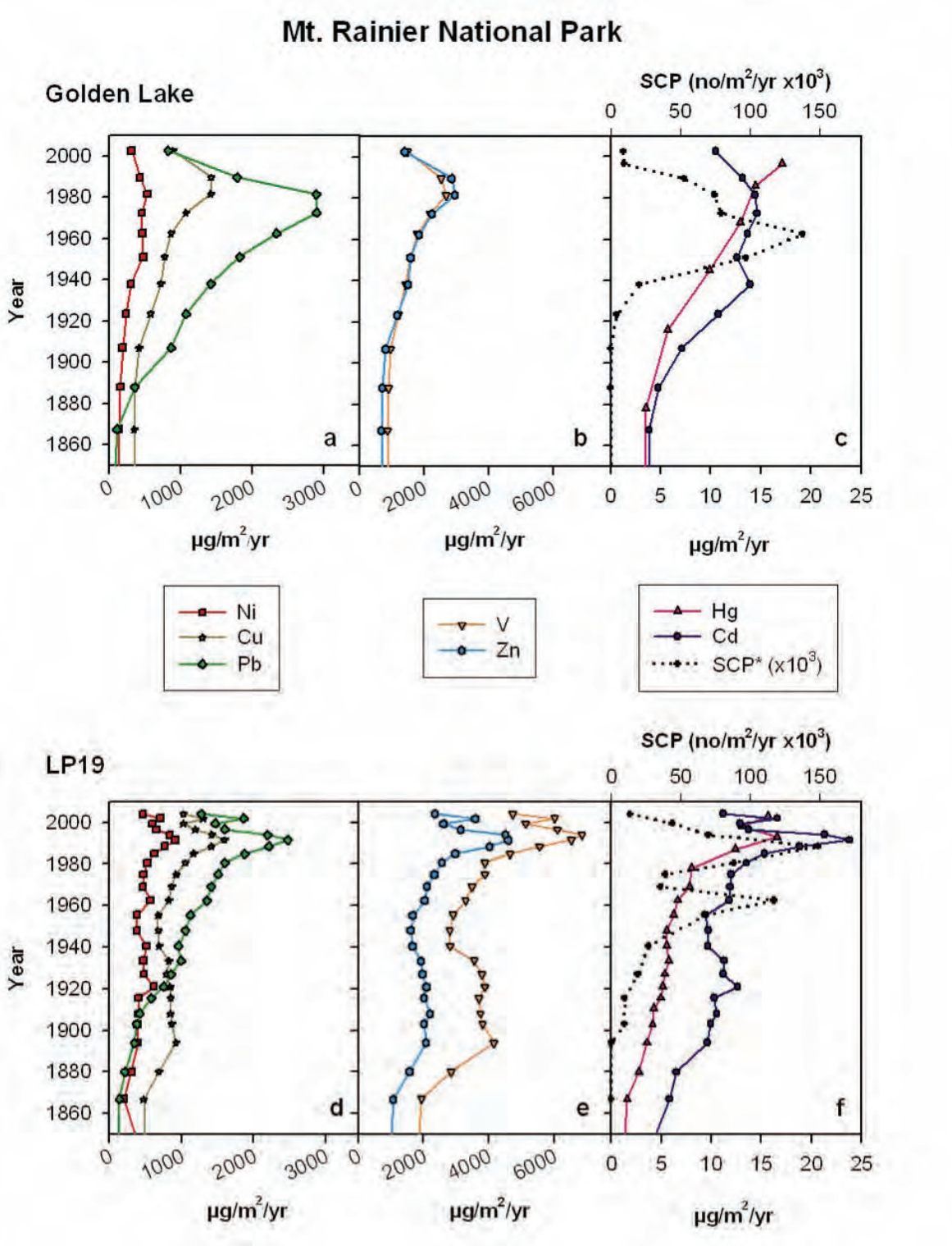

Figure 4-41. Focusing Factor-Corrected Flux of Ni, Cu, Pb, V, Zn, Cd, and Hg (µg/m^2/yr) and SCP (number/m^2/yr, reduced by a factor of 1,000 and shown in the top axis) in Sediment Cores from Golden Lake and LP19 (MORA). SCP flux is from the secondary cores from these lakes.

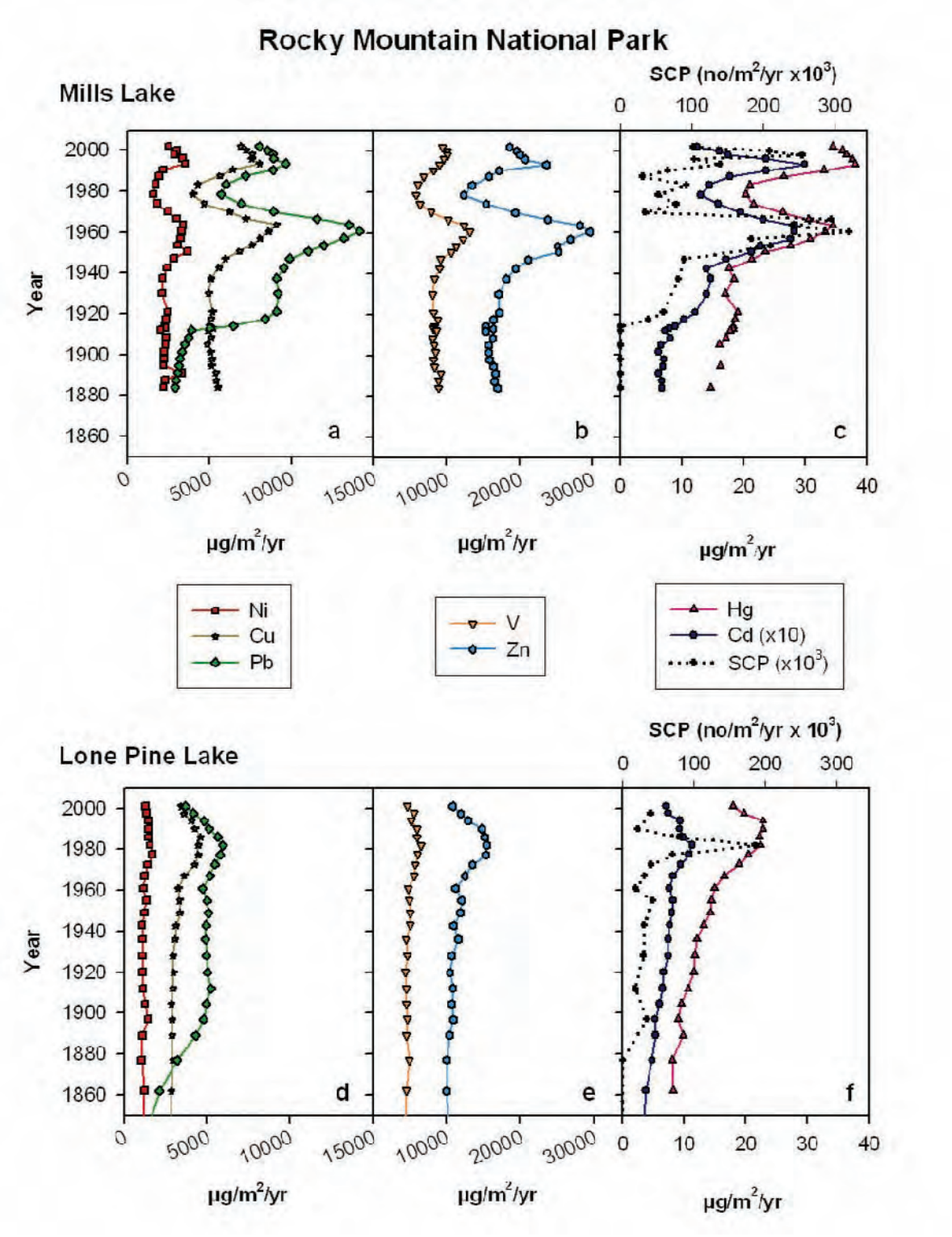

Figure 4-42. Focusing Factor-Corrected Flux of Ni, Cu, Pb, V, Zn, Cd, and Hg (µg/m^2/yr) and SCP (number/m^2/yr, reduced by a factor of 1,000 and shown in the top axis) in Sediment Cores from Mills and Lone Pine Lakes (ROMO). Cd flux has been reduced by a factor of 10.

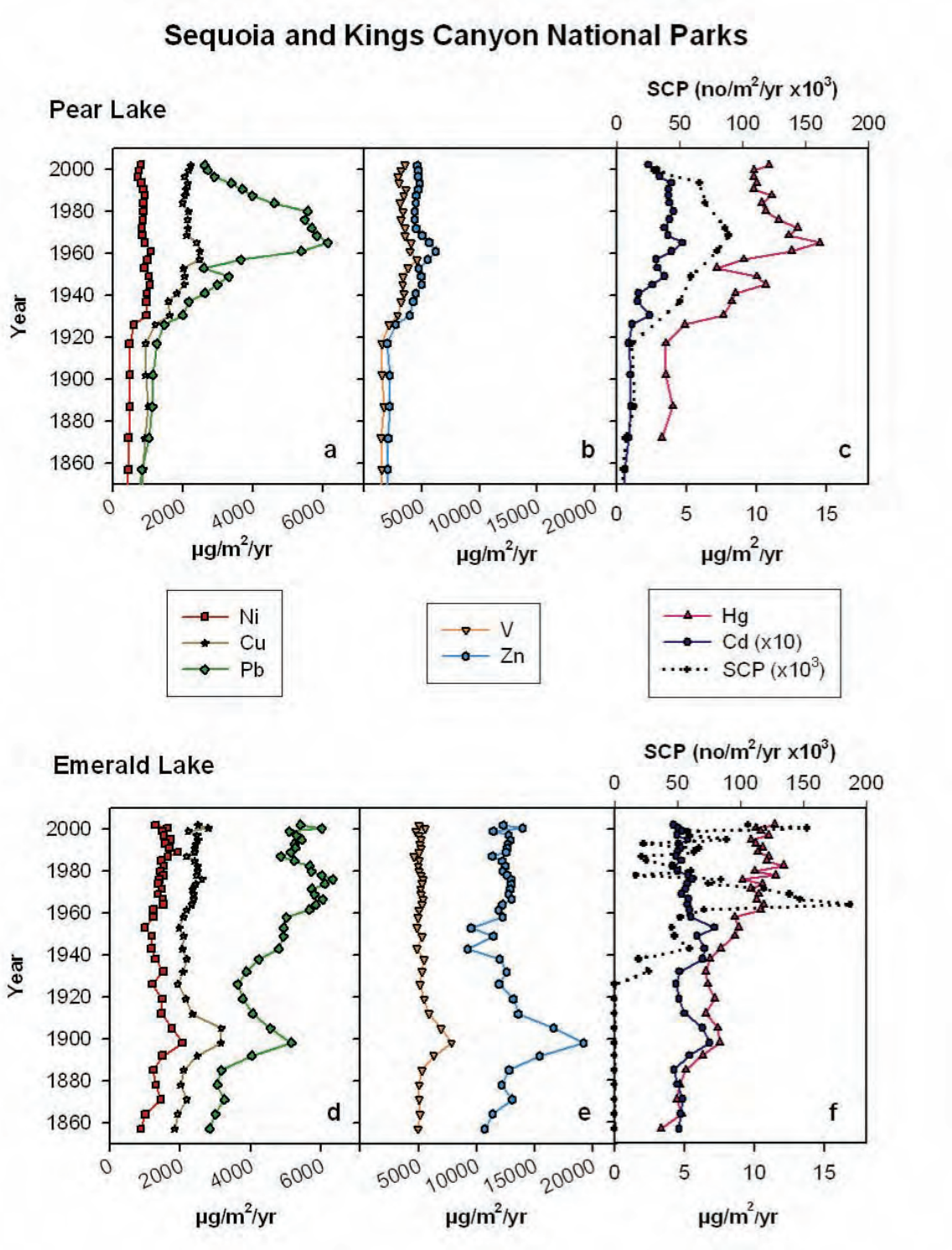

Figure 4-43. Focusing Factor-Corrected Flux of Ni, Cu, Pb, V, Zn, Cd, and Hg (µg/m^2/yr) and SCP (number/m^2/yr, reduced by a factor of 1,000 and shown in the top axis) in Sediment Cores from Pear and Emerald Lakes (SEKI). Cd flux has been reduced by a factor of 10.

Table 4-6 shows the accumulated SCP totals for each lake sediment core, in units of particles per $m^2 \times 10^5$. In terms of total deposition over the industrial period, the data show a general decline from south to north. Highest values occur for Emerald and Pear lakes in SEKI, while the four sites in Alaska are below the limits of detection. The results from sites in Alaska in themselves suggest very low concentrations of contamination from high-temperature combustion—equivalent to, or below, concentrations observed in sites in the European Arctic, the Falkland Islands, and even sites on the South Orkney Islands to the north of the Antarctic Peninsula (Rose, pers. comm., unpublished data). In GLAC, SCPs are higher at Snyder Lake than at Oldman Lake, which might be because of the proximity of regional sources (see Section 4.2.6). Similarly, PJ Lake (OLYM) shows considerably more SCP contamination than Hoh Lake, which might reflect greater local contamination. In terms of overall contamination, the SCP totals for SEKI are the highest among all WACAP parks and comparable to those observed in similarly affected European mountain lakes (in southern Spain, southern Norway, and the northwest UK (Rose, pers. comm. unpublished data).

Figures 4-37 to 4-43 also show the SCP flux profiles in the WACAP lake sediments (SCPs were not detected in the Alaskan lakes). In some cases, the SCPs were not analyzed on the same cores as the other compounds, but instead on parallel cores taken at the same time (in close proximity in the same lake). Although assumptions are made in transposing dates in this way, at present this is the best chronology available for SCPs in the sediment cores. It could explain some of the offsets seen in the SCP profiles, compared to the metals. The SCP dates can be updated when a better correlation between cores becomes available (e.g., with metal flux).

Table 4-6. Total Integrated SCPs in WACAP Lake Sediment Cores.

Park	Lake	Total Number of SCPs in the Core (x 10^5 m^{-2})[1]
NOAT	Burial	< DL
GAAR	Matcharak	< DL
DENA	McLeod	< DL
DENA	Wonder	< DL
GLAC	Oldman	100.4
GLAC	Snyder	143.3
OLYM	Hoh	51.3
OLYM	PJ	141.6
MORA	Golden	46.0
MORA	LP19	77.5
ROMO	Lone Pine	91.0
ROMO	Mills	168.6
SEKI	Emerald	193.8
SEKI	Pear	280.3

[1]This gives the total integrated number of SCPs in the entire core and can therefore be used to indicate the overall exposure to anthropogenic fossil fuel combustion over the entire temporal record of the sediment core.

4.3.5.2 Mercury and Trace Metal Enrichment Factors

The sediment profiles clearly indicate that watershed processes complicate the interpretation. Therefore, to better isolate and evaluate the human (anthropogenic) influence from atmospheric deposition over time, we normalized the sediment metal fluxes to titanium (Ti), a conservative element measured with high precision in the cores (Cowgill and Hutchinson, 1966; Engstrom, 1984). This procedure corrects for watershed disturbances and processes, such as catchment instability (e.g., avalanches, rapid snow melt) and erosion. The resulting enrichment is reported as the percent enrichment (PE) by subtracting the pre-industrial background concentrations from more recent metal concentrations as a modification of Kemp et al. (1976), as follows:

$$\text{Percent Sediment Enrichment} = \frac{(M_x/Ti_x) - (M_b/Ti_b)}{(M_b/Ti_b)} \times 100 \qquad [4\text{-}1]$$

where:

M_x = metal concentration (ng/g) at interval depth ×

Ti_x = titanium concentration (ng/g) at interval depth ×

M_b = metal concentration (ng/g) at interval closest to year 1870

Ti_b = titanium concentration (ng/g) at interval closest to year 1870

Figures 4-44 to 4-50 show the PE in the sediment cores for V, Cu, Zn, Pb, Cd, Ni, and Hg for each lake in the core WACAP parks. A PE value above zero indicates that that element is enriched in the sediment, relative to titanium and compared with the pre-industrial background (1870). For an element with a recent anthropogenic increase, we would expect its enrichment to go from zero (pre-industrial) to positive values after industrialization. Several patterns are apparent in the enrichment plots, compared to the un-normalized fluxes (Figures 4-37 – 4-43). All lakes in the conterminous 48 states show significant enrichment in Pb, Cd, and Hg. For all other metals, enrichment is either zero or fairly small. In the Alaska parks, there is recent enrichment in Hg at all lakes, but no other consistent patterns.

Atmospheric Pb is found primarily on fine particulate matter (less than 10 microns in diameter). Thus, deposition of Pb is related largely to sources within about 1,000-2,000 km. Pb deposition was heavily influenced by the introduction of leaded gasoline in the 1920s. Pb in gasoline was drastically reduced in the United States starting in the 1970s (Thomas, 1995). Other sources of lead to lake sediments shown to be important include lead mining, smelting, logging, and other industrial activities (see Table 3-4 in Chapter 3).

In the four Alaska lakes (Figures 4-44 and 4-45), only Wonder Lake shows a modest increase in Pb enrichment toward the surface, beginning in about 1920. In parks in the conterminous United States, Pb shows significant enrichment in all sediment profiles, and most of these lakes show a peak between 1960 and 1980, with a decrease afterwards. The PE values are by far the largest at both lakes in MORA. At LP19, Pb PE reached 400% and at Golden Lake, it reached 800%. At Mills Lake in ROMO, the Pb PE sharply increased in the early 1900s, possibly because of its proximity to historic lead mines and/or smelting operations. It is worth observing that the Omaha and Grant lead smelter was built in Denver in 1892 and the stack was the tallest structure in the world for some time thereafter.

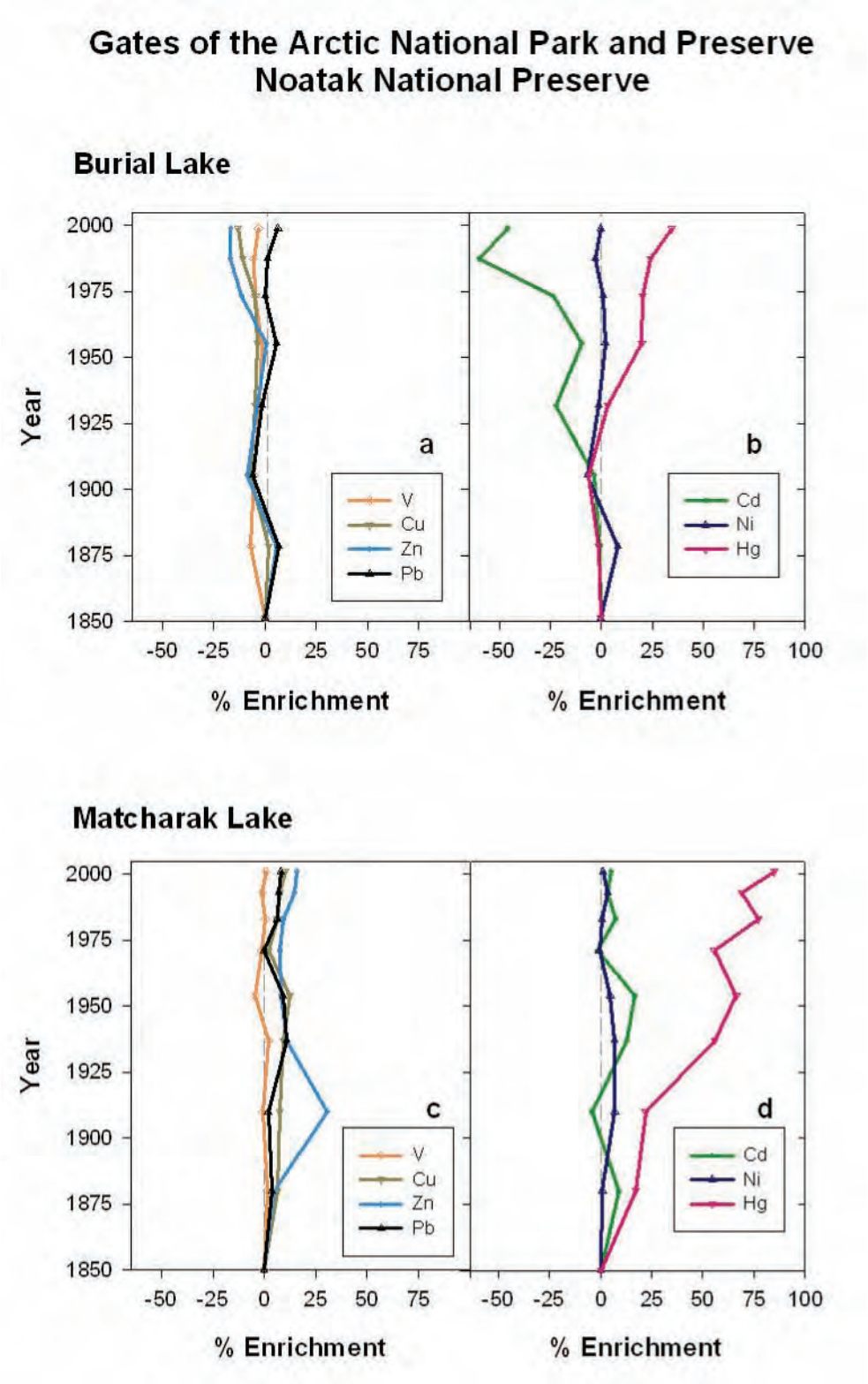

Figure 4-44. Percent Enrichment of V, Cu, Zn, Pb, Cd, Ni, and Hg in Sediment Cores from Burial Lake (NOAT) and Lake Matcharak (GAAR). Sediment Ti values were used to normalize to a conservative crustal element to reduce the effects of watershed processes on the contaminant profiles.

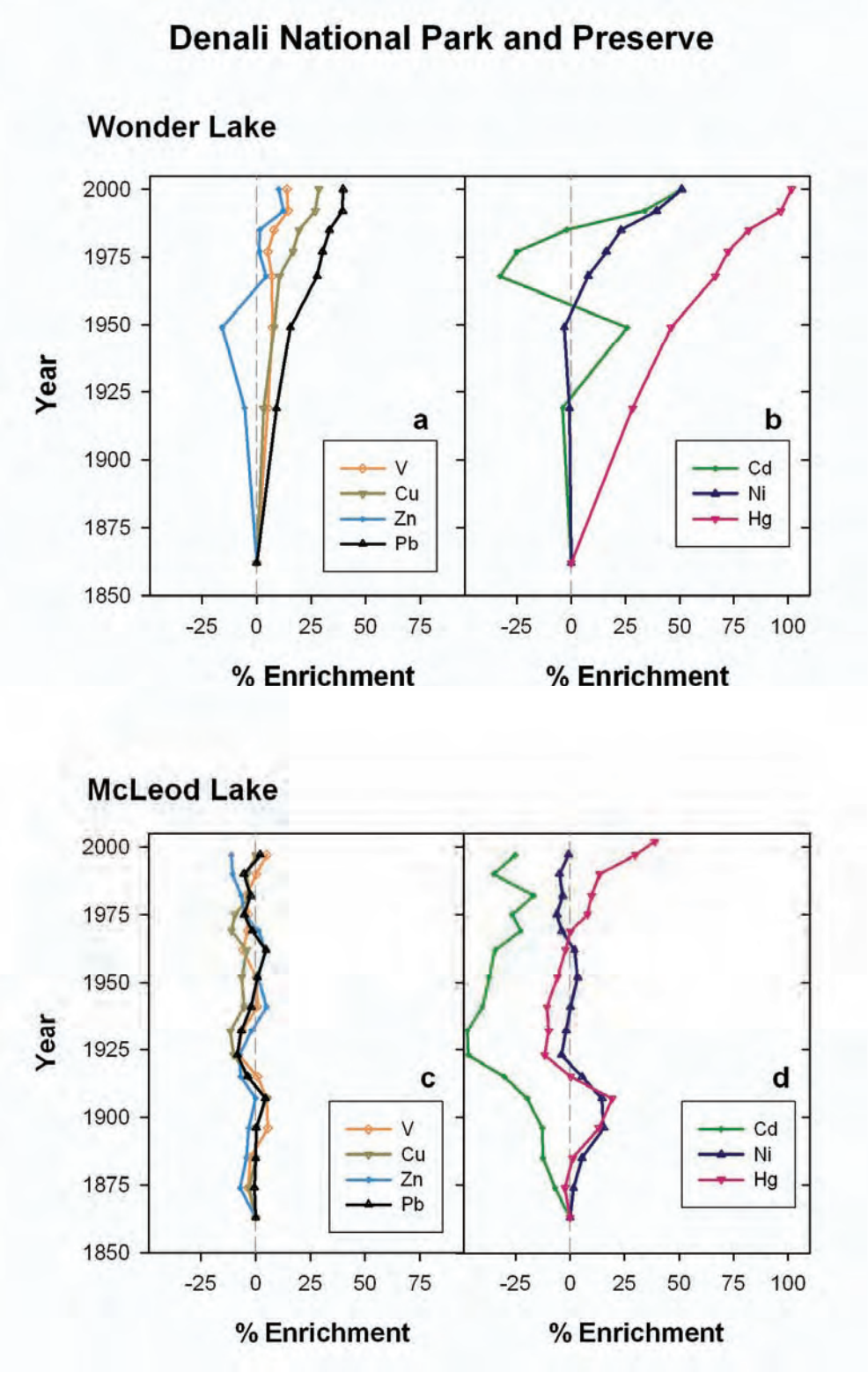

Figure 4-45. Percent Enrichment of V, Cu, Zn, Pb, Cd, Ni, and Hg in Sediment Cores from Wonder and McLeod Lakes (DENA). See Figure 4-44 for more information.

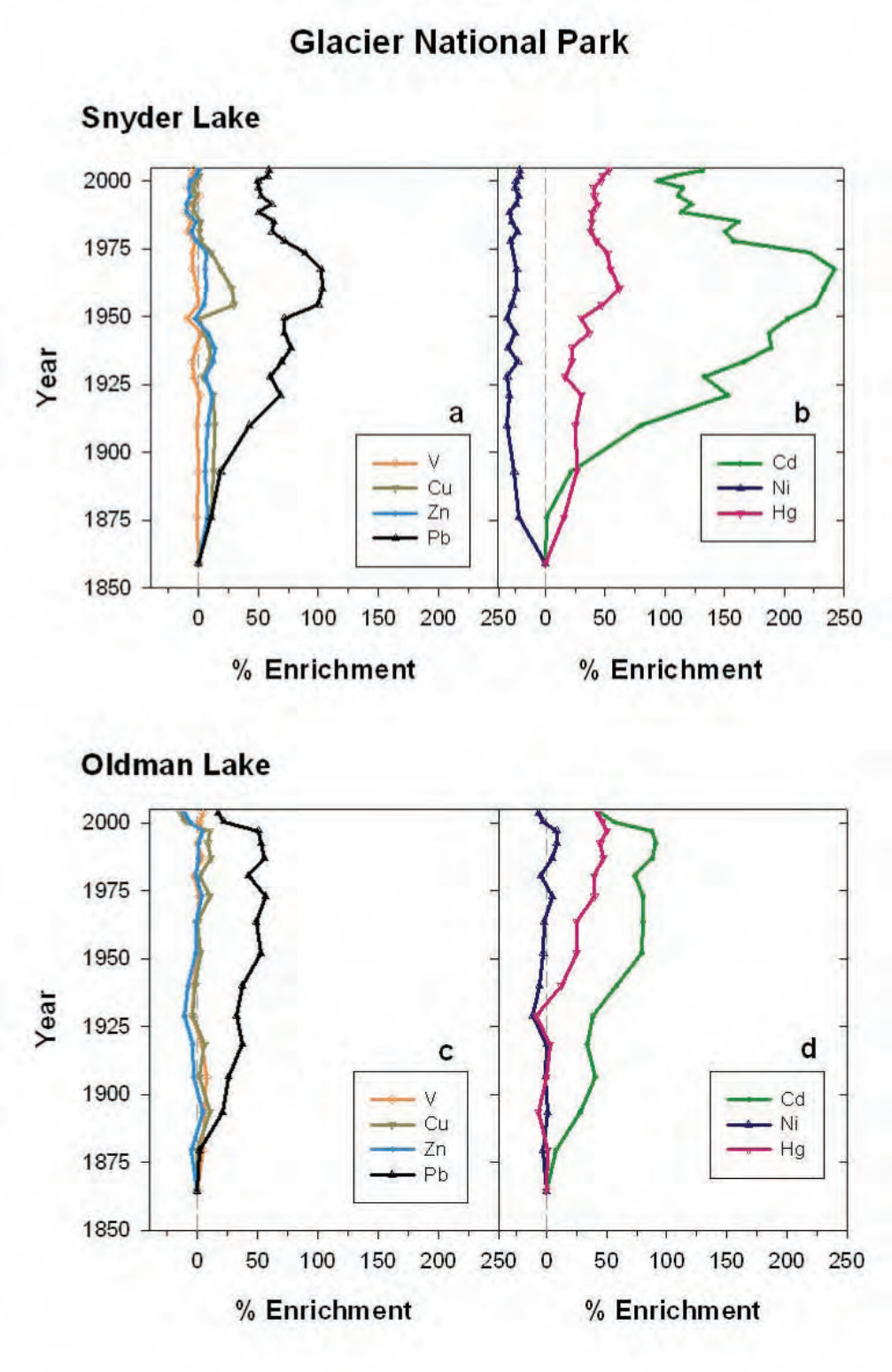

Figure 4-46. Percent Enrichment of V, Cu, Zn, Pb, Cd, Ni, and Hg in Sediment Cores from Snyder and Oldman Lakes (GLAC). See Figure 4-44 for more information.

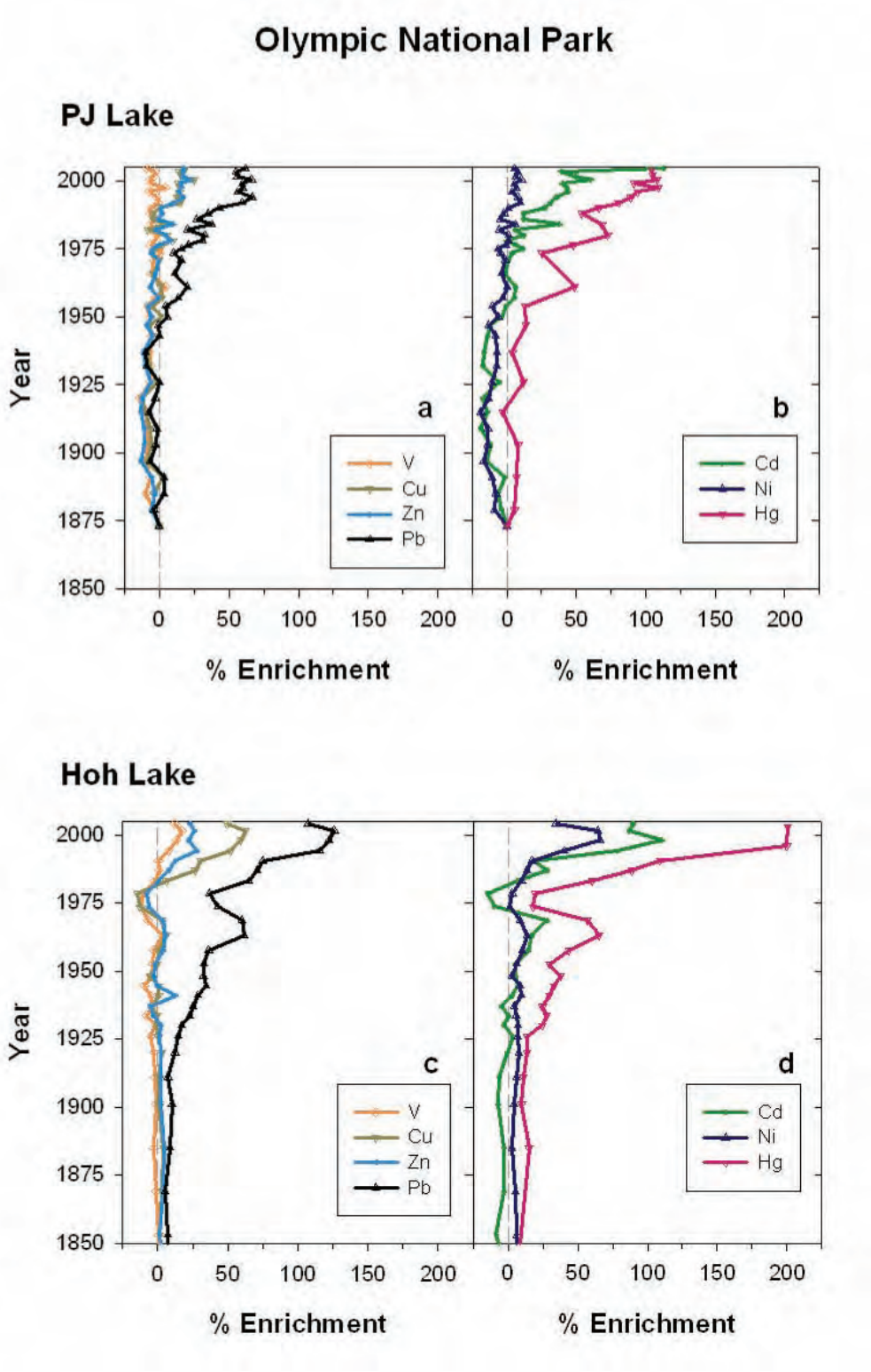

Figure 4-47. Percent Enrichment of V, Cu, Zn, Pb, Cd, Ni, and Hg in Sediment Cores from PJ and Hoh Lakes (OLYM). See Figure 4-44 for more information.

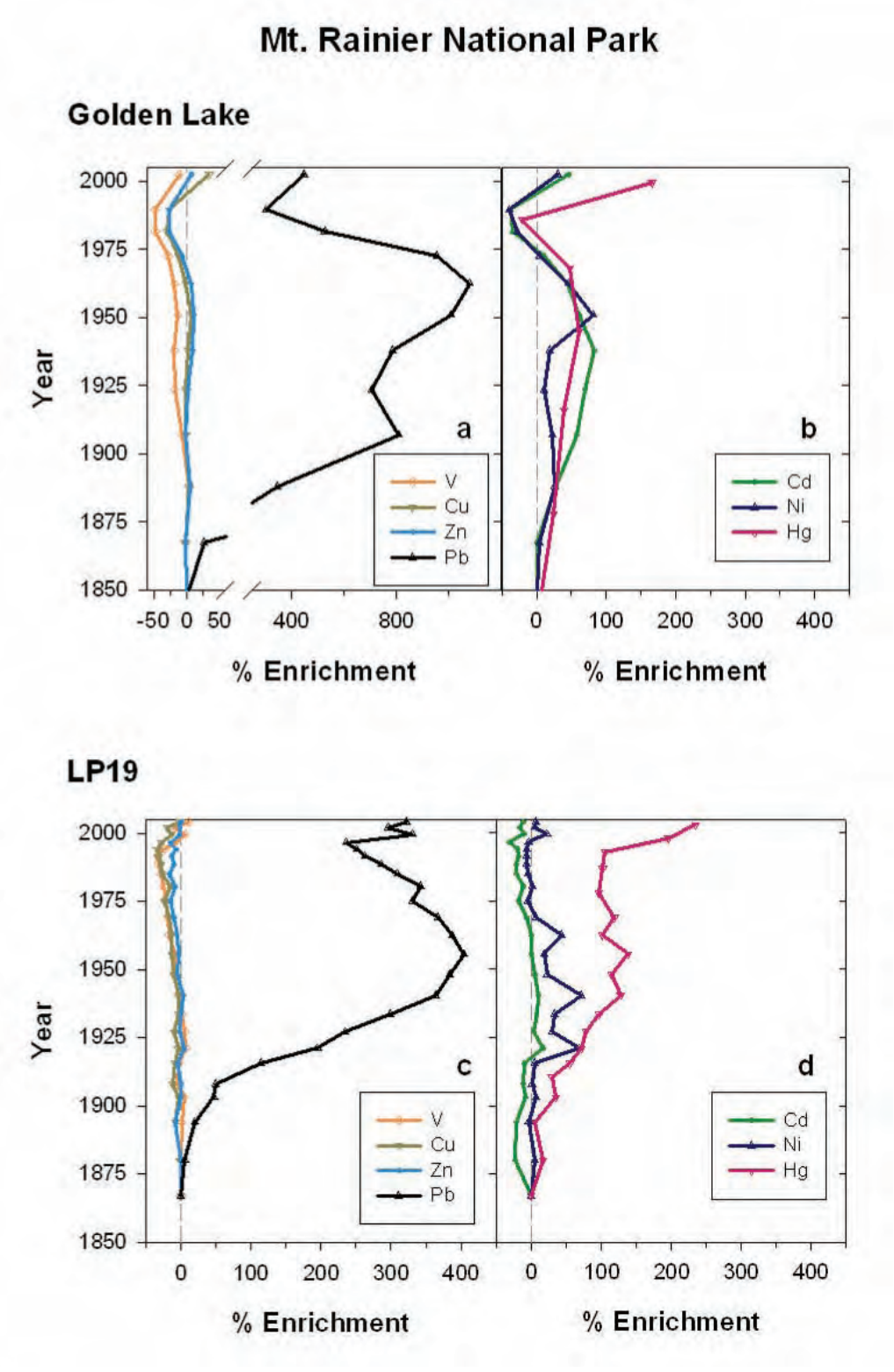

Figure 4-48. Percent Enrichment of V, Cu, Zn, Pb, Cd, Ni, and Hg in Sediment Cores from Golden Lake and LP19 (MORA). See Figure 4-44 for more information.

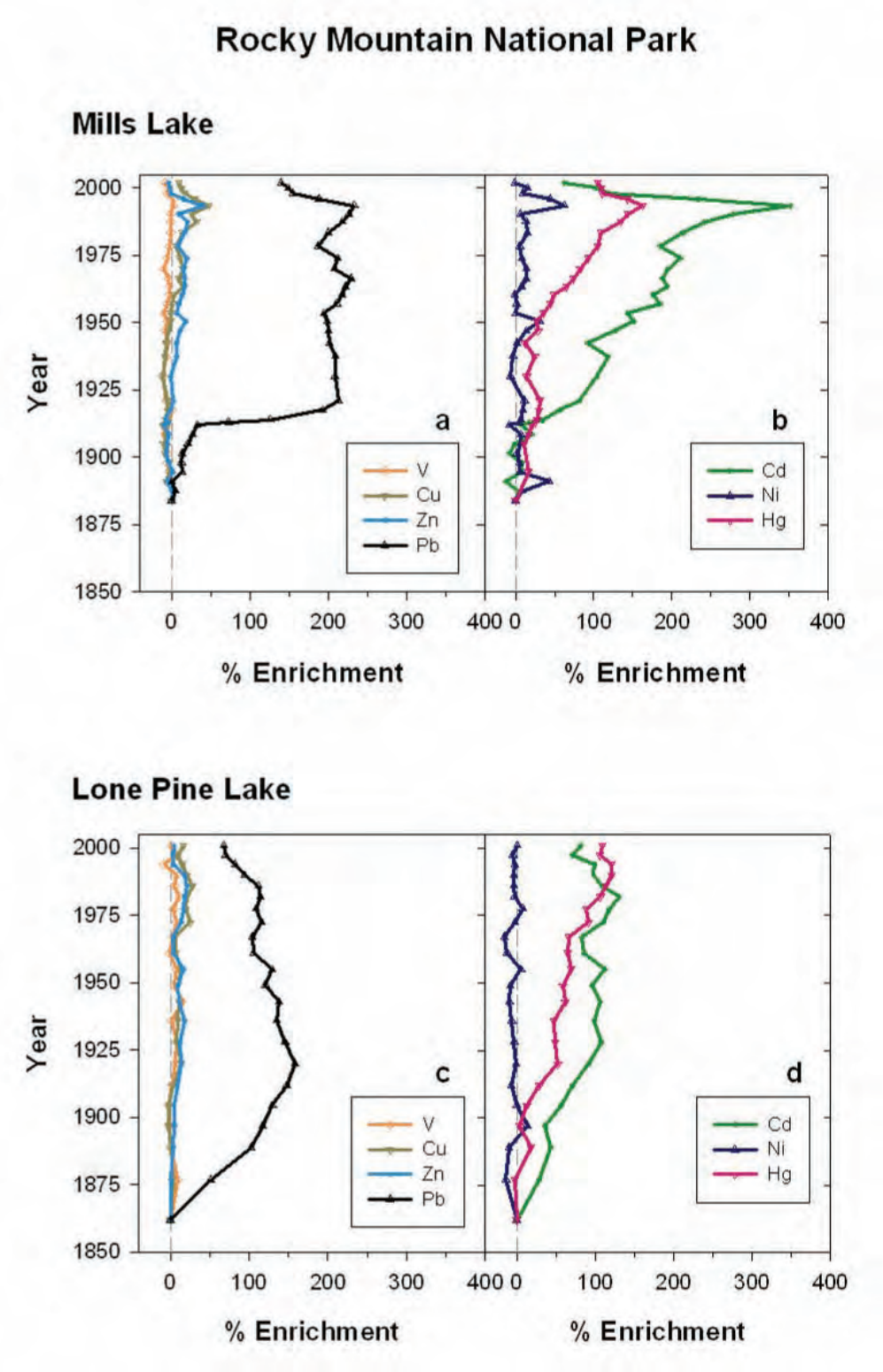

Figure 4-49. Percent Enrichment of V, Cu, Zn, Pb, Cd, Ni, and Hg in Sediment Cores from Mills and Lone Pine Lakes (ROMO). See Figure 4-44 for more information.

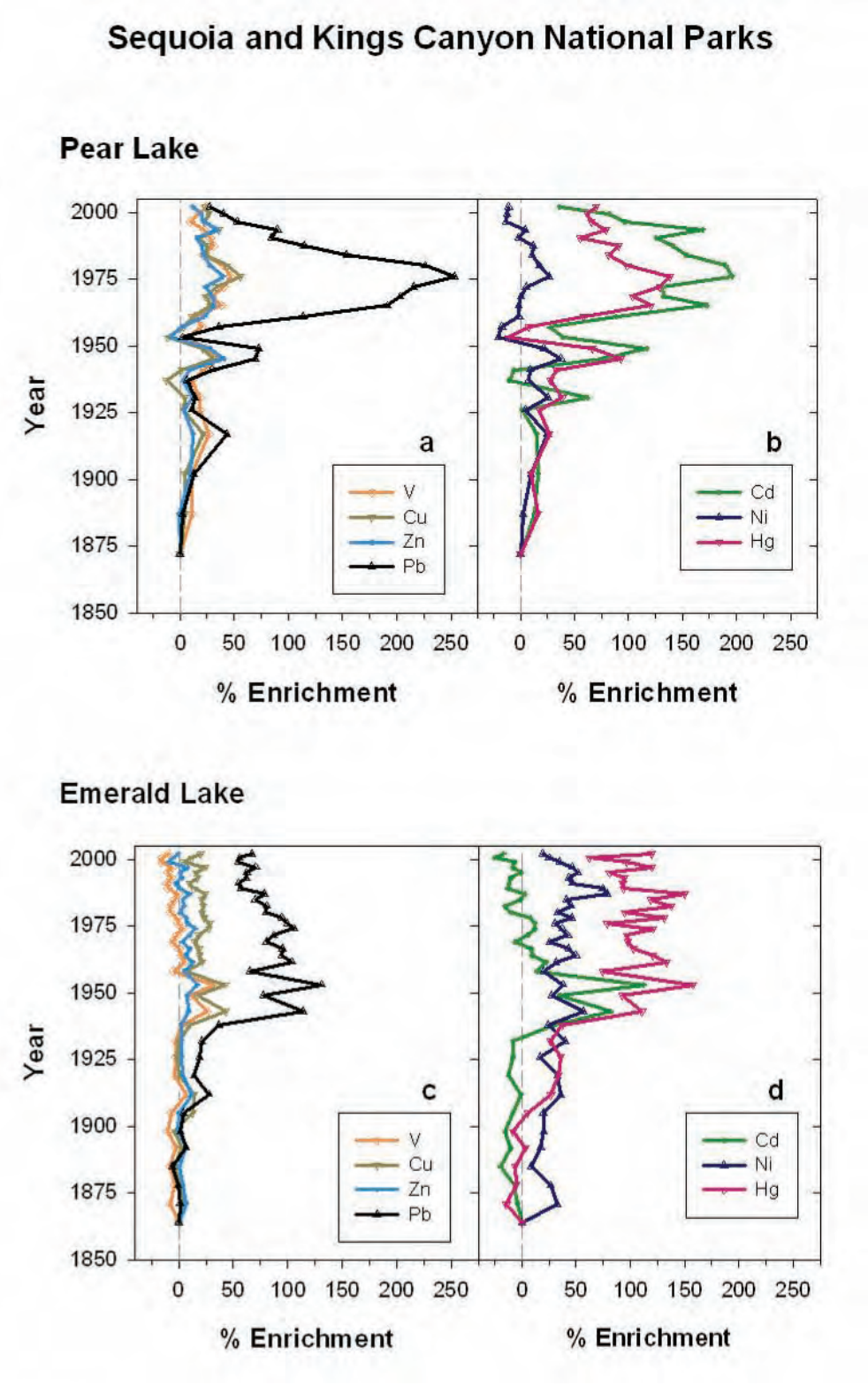

Figure 4-50. Percent Enrichment of V, Cu, Zn, Pb, Cd, Ni, and Hg in Sediment Cores from Pear and Emerald Lakes (SEKI). See Figure 4-44 for more information.

Like Pb, Cd is found on fine atmospheric particulate matter. The element is derived from many different anthropogenic and natural sources (see Table 3-4). Cd enrichment is a result of increasing anthropogenic sources of the metal. Significant Cd enrichment was not seen uniformly, but was seen at Snyder and Oldman Lakes (GLAC; Figure 4-46), PJ and Hoh lakes (OLYM; Figure 4-47), Mills and Lone Pine lakes (ROMO; Figure 4-49), and Pear Lake (SEKI; Figure 4-50). The largest PE increase for Cd was seen at Mills Lake (Figure 4-49), with a temporal pattern similar to that of Pb. Thus, sources associated with Pb mining and smelting in the area could be contributing both elements.

For mercury, all parks show an increase in PE starting around the late nineteenth or early twentieth century, which is consistent with other sediment and ice core data and is attributed to the increasing emissions of mercury from human sources. At most parks, the PE values reached 50-100% in the most recent sections of the sediment cores. At Hoh Lake (OLYM; Figure 4-47), Golden Lake (MORA; Figure 4-48), and LP19 (MORA; Figure 4-48)), PE was much higher in the last few (top) sediment layers. Some caution is needed, however, in interpreting these results, because for these lakes, the PE value was much lower and then rose significantly in the top one or two sediment sections. At Hoh Lake, although the PE value increased, the Hg flux values were low and generally decreasing.

For two of the Alaska lakes, Matcharak and Wonder (Figures 4-44 and 4-45), we see an increase in Hg PE beginning in the early 1900s that continues to the surface, with no leveling off or decline. Both lakes currently have Hg PE values of 85-100%. Burial and McLeod lakes (Figures 4-44 and 4-45) show a smaller increase in Hg PE, beginning in about 1970 for McLeod Lake and 1935 for Burial Lake. These two lakes had the lowest Hg PE (~35-40%) for recent sediments among all WACAP lakes. Because no SCPs were observed in any of the Alaska lake sediments, we suspect that these Hg increases result entirely from an increase in anthropogenic global background of Hg, rather than regional sources.

Oldman Lake and Snyder Lake (GLAC; Figure 4-46) show both differences and similarities in their Hg PE profiles. Hg in Snyder Lake began to rise in the late 1800s, along with Pb and Cd, whereas the Oldman Lake profile shows Hg PE beginning to increase about 1930, well after the increase in Pb and Cd. For both lakes, the Hg PE values increase steadily up to the surface, where values are fairly low, about 50%, similar to the Alaska lakes with the lowest values. At Snyder Lake, the SCP flux began earlier than it did at Oldman Lake, supporting the notion of a regional high temperature combustion source for the earlier rise in Hg PE. SCPs were higher at Snyder Lake, similar to the results for PAHs (see Section 4.2.6.2).

Both OLYM lakes (Figure 4-47) show similarity among Hg, Pb, Cd, Cu, and Zn PE profiles, suggesting that they might share a common source for all of these elements. The Hg focus-corrected fluxes for Hoh Lake were some of the lowest among all WACAP lakes, yet the PE values increased to very high values. For PJ lake, all metals had much higher fluxes (including Hg), yet the Hg enrichment values were not as high as those at Hoh Lake.

In the MORA lakes (Figure 4-48), the Hg PE profile for Golden Lake began a very slow increase in the late 1800s. At LP19, the increase began at about the same time, but the magnitude is much larger. At the surface, the PE values for LP19 were over 100% for most of the 1900s, and over 200% in the most recent sediment layers. As already mentioned, the top one or two sediment slices show significant enrichment in Hg, whereas SCPs are declining. This enrichment could be related to an increase in Hg deposition from global/Asian sources and decreasing SCPs as a

result of controls on particulate emissions associated with regional high temperature combustion sources.

In the ROMO lakes (Figure 4-49), recent Hg fluxes were some of the highest among all WACAP parks (20-40 μg/m^2/yr), and the PE profiles are broadly similar to one another. Hg PE values for Lone Pine Lake show an increase starting around 1900, whereas values for Mills Lake began to increase somewhat later. The PE value at both sites reached maximum values of 100-150% in the late twentieth century and have declined slightly since. At Mills Lake, the SCP profile is broadly similar to the Hg profile, but at Lone Pine Lake, the SCP profile is rather different. This early increase in Hg is mirrored by Cd and Pb in both Mills and Lone Pine lakes, suggesting a possible common source. In both lakes, the SCPs have declined considerably in the recent decades. These patterns are broadly consistent with a decrease in regional emissions from high temperature fossil fuel combustion, metal smelting, or other industrial sources. These patterns are also influenced by an increase in global background Hg concentrations, not associated with SCPs, that have supplanted the regional sources. An increase in global sources (e.g., Wu et al., 2006) could be replacing Hg deposition that was previously from regional sources.

In SEKI (Figure 4-50), both lakes show an increase in Hg PE in the early 1900s, reaching values of 100-150%. Hg PE values in Emerald Lake reached this value very quickly between about 1940 and 1955. The concentrations have declined only slightly since then. At Pear Lake, the values are more variable, peaking around 1975, and have dropped considerably since then. At both lakes, the Cd and Pb enrichment pattern is similar to the Hg pattern. In Pear Lake, this pattern is similar to the SCP profile, suggesting a role for regional fossil fuel sources. But in Emerald Lake, the SCPs have a different pattern, suggesting that the sources are more complex. The fact that SCPs and Hg in both lakes now appear to be moving in different directions suggests that other Hg sources (i.e., increasing global background, transpacific, local/regional sources not associated with SCP) are now affecting these sites.

4.3.6 Source Attribution for Mercury, Trace Metals, and SCPs

Most metals and SCPs reside on, and are transported with, other fine particulate matter. As mentioned previously, detectable SCPs are in the range of 5-50 μm in diameter. Metals are found primarily on particles less than 10 μm diameter. These particles are produced from a variety of sources, including fossil fuel combustion, metal smelting, and other industrial processes. SCPs are produced only from high temperature combustion. Transport of the fine and larger particulate matter is generally limited to distances of no more than about 1,000-2,000 km. Starting in the late 1970s, the Clean Air Act mandated controls on many industrial sources in the United States. These controls initially applied only to new sources, but over time, nearly all large sources have installed, or are in the process of installing, scrubbers or other technologies to capture most particulate matter. Over the same time frame, Pb in gasoline was also phased out in the United States. Thus for SCPs, Pb, and Cd, we see a clear decline in fluxes to the sediments for nearly all WACAP sites in the conterminous 48 states. In Alaska, the SCPs were non-detectable and Pb and Cd were generally much lower than at sites in the conterminous 48 states; thus we do not observe the same decline in the Alaska sediment cores.

For Hg, source attribution is more complex. There are both natural and industrial sources and, once deposited, Hg can be re-emitted to the atmosphere. Mercury can be transported to the WACAP parks, both on fine particulate matter as well as via several gaseous compounds. While

particulate mercury and gaseous Hg(II) compounds have short atmospheric lifetimes, gaseous elemental mercury [Hg(0)] has a lifetime up to one year or more, which results in a fairly uniform global reservoir of elemental mercury in the atmosphere. Gaseous elemental mercury is slowly oxidized to Hg(II), which is then quickly removed via wet or dry deposition. The oxidation is believed to be driven by UV light, which results in a latitudinal gradient in the depositional flux (Selin et al., 2007). Thus, in regions with significant industrial sources of particulate Hg or gaseous Hg(II) compounds, such as from coal combustion or waste incineration, there can be a significant contribution to regional deposition. The complexity of the Hg cycle suggests that the relative contribution from global vs. regional sources for any location is complex, and depends on numerous factors. In addition, there are large uncertainties in the sources and overall cycling of Hg in the atmosphere (Lindberg et al., 2007).

Mercury in the WACAP parks comes from both regional and global sources. As a result of the Clean Air Act, scrubbers and other control technologies were installed for removal of particulate matter, sulfur dioxide (SO_2), and nitrous oxides (NO_x) beginning in the 1970s. As an unintended benefit, these scrubbers also remove some of the mercury, mainly particle bound and Hg(II) compounds. These forms of Hg are also the forms that are most important for regional deposition. Gaseous elemental Hg is much more difficult to remove from the waste stream. According to the USEPA, between 1990 and 1999, US industrial emissions of Hg dropped by 44%, from 220 tons to 115 tons per year (see http://www.epa.gov/mercury/control_emissions/emissions.htm).

Using both global (Selin et al., 2007) and regional models (Seigneur et al., 2004), several groups have simulated Hg deposition patterns. Although there are significant uncertainties, these two models get broadly similar results: US industrial sources dominate Hg deposition in the eastern United States, whereas natural and global sources dominate deposition in the western United States. This largely reflects the greater emissions from coal-fired plants in the eastern United States. The WACAP results are broadly consistent with this current understanding, but they also demonstrate the complex biogeochemical pathways of Hg that result in our observations in sediments, vegetation, snow, and fish.

For the four Alaska WACAP lakes, the average Hg flux to the sediments since 1950 was 4.8 $\mu g/m^2/yr$, whereas the mean highest flux determined for WACAP lakes in the conterminous 48 states during the same period of accumulation was approximately 21 $\mu g/m^2/yr$. Thus, in the last 50 years, WACAP lakes in the conterminous 48 states accumulated approximately four times more Hg in their sediments. This large difference in Hg flux probably results from a combination of factors, including greater regional anthropogenic sources in the conterminous 48 states and enhanced oxidation of atmospheric Hg(0) at lower latitudes (Selin et al., 2007).

The overall impact is that the aquatic environment in the WACAP lakes in Alaska appears to receive 80% less Hg from atmospheric sources than WACAP lakes in the conterminous 48 states. This finding is also confirmed by the snowpack Hg flux (see Section 4.3.1). Nonetheless, fish from the Alaska lakes had the highest Hg concentrations among fish from all WACAP sites, reflecting the poor relationship between atmospheric deposition and fish bioaccumulation in aquatic ecosystems, which probably reflects mainly the complexity of food web transfer of mercury and methylation, both of which play key roles in bioaccumulation.

Winter deposition of Hg to the snowpack in the Alaska, Washington, and California parks is probably dominated by the global pool of atmospheric Hg, because of relatively low Hg(0) oxidation rates and subsequent deposition during the winter months (Selin et al., 2007).

However, the high SCP flux in SEKI lakes suggests Hg from regional high temperature combustion sources is also a likely source. For MORA, some Hg deposition from the coal-fired power plant in Centralia Washington is also likely. At ROMO, local and regional upwind emissions sources, principally coal combustion, might also contribute. As seen in the sediment patterns (Figures 4-41 and 4-48), both lakes in ROMO are undergoing recent declines in Hg flux to the sediments, probably because of reductions in regional emissions. The Hg flux to the snowpack in OLYM was fairly high (see Figure 4-33), but this probably reflects a very high snowpack amount, as well as the fact that the average is calculated from only a few samples collected in a single year.

In summary, the WACAP data show that regional sources of Hg have declined, consistent with reductions in US emissions of Hg. The WACAP data also suggest that global sources are now contributing an ever increasing share of the total Hg deposition. Because of the potential for continuing increases in global mercury emissions (Wu et al., 2006), the NPS should continue to monitor mercury in some forms within the western parks.

4.4 Nutrient Nitrogen and Sulfur

4.4.1 Spatial Distributions of Nitrogen and Sulfur in Lichens

Mean dry weight (dw) concentrations of nitrogen and sulfur in lichens in the core and secondary WACAP parks are shown in Figure 4-35 (see Section 4.3.3). Lichen data are reported in Appendices 4A.12 and 4A.13, as well as in the WACAP database. Lichen nitrogen and sulfur concentrations indicate that deposition of atmospheric pollutants containing nitrogen and sulfur is enhanced in some WACAP parks. Mean nitrogen and sulfur concentrations were well above the upper limit for the background range for public lands in the western United States at SEKI and GLAC, and nitrogen concentrations were also above these background ranges at BAND and BIBE (see Section 4.3.3 and Appendix 4A.14 for a description of how the background ranges were calculated). WACAP field lichenologists remarked in their notes that nitrophytic (nitrogen-loving) lichen species were abundant at these latter two parks. Because ammonium sulfate is a dominant fine particulate at the BIBE IMPROVE site, it is likely that sulfur deposition is also elevated in BIBE relative to other remote parks and forests in the western United States. Analysis of lichen samples collected during WACAP and currently archived at the University of Minnesota Research Analytical Laboratory could provide corroborative evidence.

4.4.2 Source Attribution for Nitrogen

Lichens generally accumulate nitrogen from atmospheric sources in the following order of preference: gaseous ammonia, particulate ammonium, particulate nitrates, gaseous nitric acid, and gaseous nitrogen oxides. Therefore, lichen nitrogen is highly responsive to agricultural sources, especially ammonia, as well as NO_x emissions from fossil fuel combustion. High N deposition is associated with adverse effects to vegetation. NO_x-nitrogen emissions come mainly from fossil fuel combustion, although there is a small natural contribution from lightning and soils. NH_3-nitrogen sources are associated with agricultural applications (fertilizers), animal wastes, and industrial sources. Natural sources are much smaller. Thus nitrogen sources are fairly ubiquitous in the western United States. SEKI probably gets the greatest contributions from both NH_3 and NO_x sources, because of its proximity to large urban areas, agriculture, and animal husbandry.

4.5 Atmospheric Transport

(Refer to Section 3.4.1 in Chapter 3 for a discussion of the interpretation of atmospheric trajectories and the methods used.) Figures 4-51 to 4-57 show the air mass back-trajectory cluster plots for all sites. The back-trajectories for each park were generated by the NOAA-Hysplit trajectory model for the period 1998-2005. Clusters were generated with 1-, 5-, and 10-day back trajectories, which represent the airsheds of the WACAP parks at different scales of atmospheric motion. These differences represent local, regional, and long-range atmospheric transport and the climatology of each cluster, as shown by two parameters: precipitation and seasonal distribution of transport patterns. Although the WACAP parks cover a wide geographic range, many of them share similar climatological drivers (and similar patterns within the clusters). OLYM, MORA, SEKI, and GLAC all have winter precipitation maxima and summer minima that are driven by the Aleutian low pressure and Pacific high pressure systems, respectively.

The annual average precipitation at MORA was about 275 cm. For the 1-day clusters, ~50% of this amount comes from winter-dominated clusters E and F, whereas these same clusters contain only ~17% of the total trajectories (see Figure 4-55). Conversely, summer-dominated clusters A and C are responsible for ~17% of the precipitation, with ~45% of the trajectories. Although the 1-day clusters capture the climate of the Pacific Coast, the seasonality and precipitation graphs for the 5- and 10-day clusters show that the percentage of trajectories per cluster and the percentage of precipitation per cluster are similar. These longer clusters do a poorer job of describing regional flow patterns at MORA, a trend that was also seen at OLYM, GLAC, and SEKI. Precipitation patterns at these sites occur on a scale of a few hundred kilometers. The standard deviations about the cluster means are very high in this region for the 5- and 10-day clusters, suggesting that longer clusters do not accurately describe regional phenomena. This result implies that the longer transport patterns do not accurately reflect the transport of regional emissions to the parks. Instead, the 1-day clusters do a better job of describing the nearby transport pathways.

As demonstrated in Chapter 3 (SOCs), 50-100% of historic- and current-use pesticide concentrations in snow are believed to result from regional transport of less than 300 km. The 1-day clusters represent trajectories with lengths ranging from ~250 km for the shortest clusters and ~1,200 km for the longest clusters, indicating that the 1-day clusters are most representative of regional transport to the WACAP parks. The remainder of the transport occurs on scales ranging up to ~7,500 km within 5 days, and ~17,000 km within 10 days. For contaminants with long enough atmospheric lifetimes, such a distance implies that trans-Pacific sources are possible.

ROMO has a precipitation regime unique amongst the WACAP sites. It receives nearly equal amounts of precipitation in each season. The percentage of trajectories in each cluster is nearly the same as the percentage of precipitation from each cluster, regardless of season (see Figure 4-56). Winter precipitation comes from the Pacific, and summer precipitation from the Gulf of Mexico. The cluster plots for ROMO reflect this pattern, especially summer-dominated cluster A in the 10-day clusters. In addition to bringing precipitation from the Gulf of Mexico, cluster A could be responsible for transport of SOCs from the more heavily contaminated southeastern United States. Higher SOC concentrations are observed in multiple media on the east side of the Continental Divide at ROMO, with different atmospheric sources the likely culprit (see Sections 4.2.1 and 4.2.6). In addition, 1-day cluster A suggests significant local/regional influence during summer.

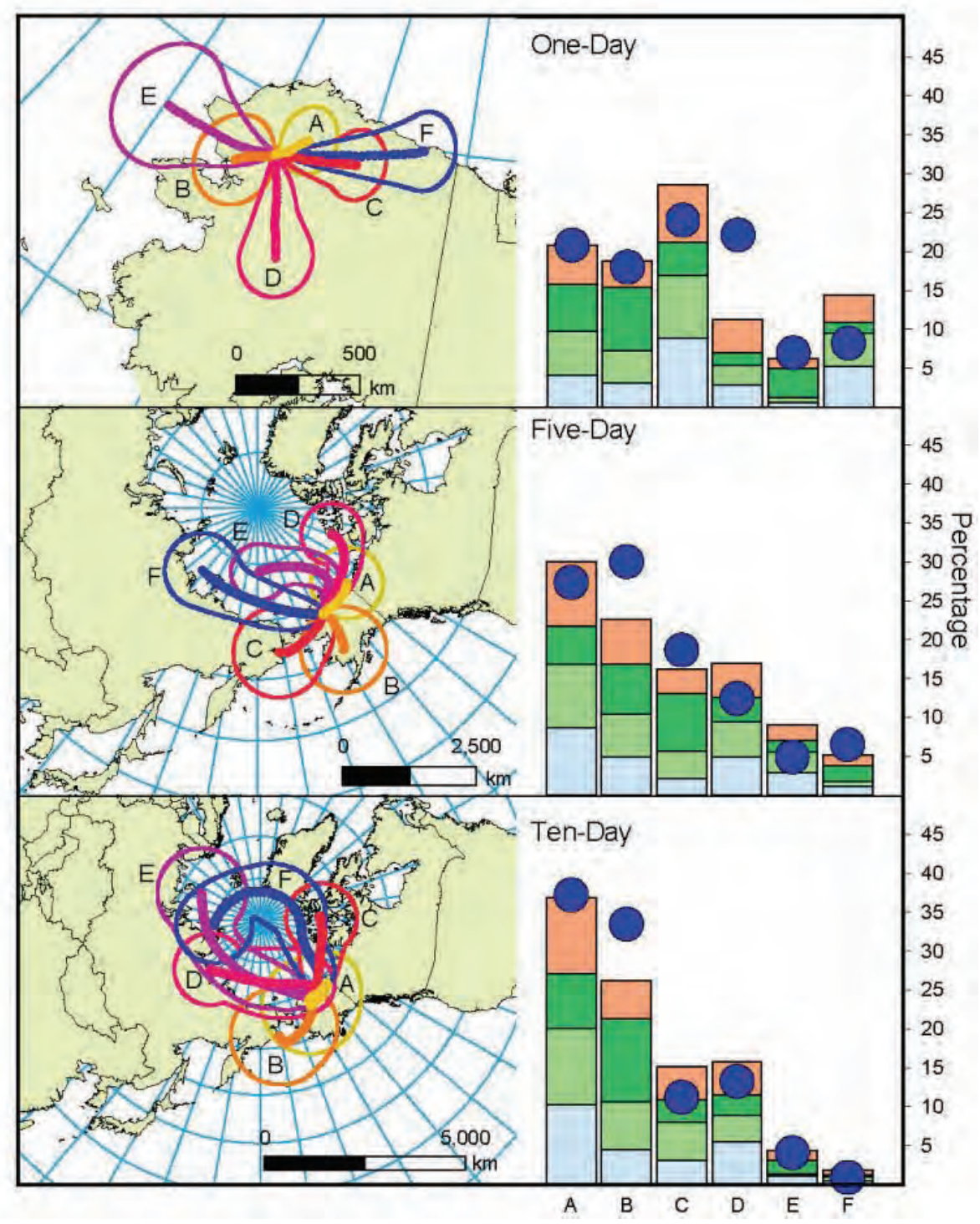

Figure 4-51. 1-, 5-, and 10-Day Cluster Plots for NOAT and GAAR. Each cluster represents the average transport pathway for a group of individual trajectories. Clusters are sorted shortest to longest, A–F. Bars represent the percent of trajectories by season in each cluster out of 2,922 total (1998-2005). Light blue = winter; light green = spring; dark green = summer; orange = autumn. The dark blue dot is the percent of total precipitation for which each cluster is responsible.

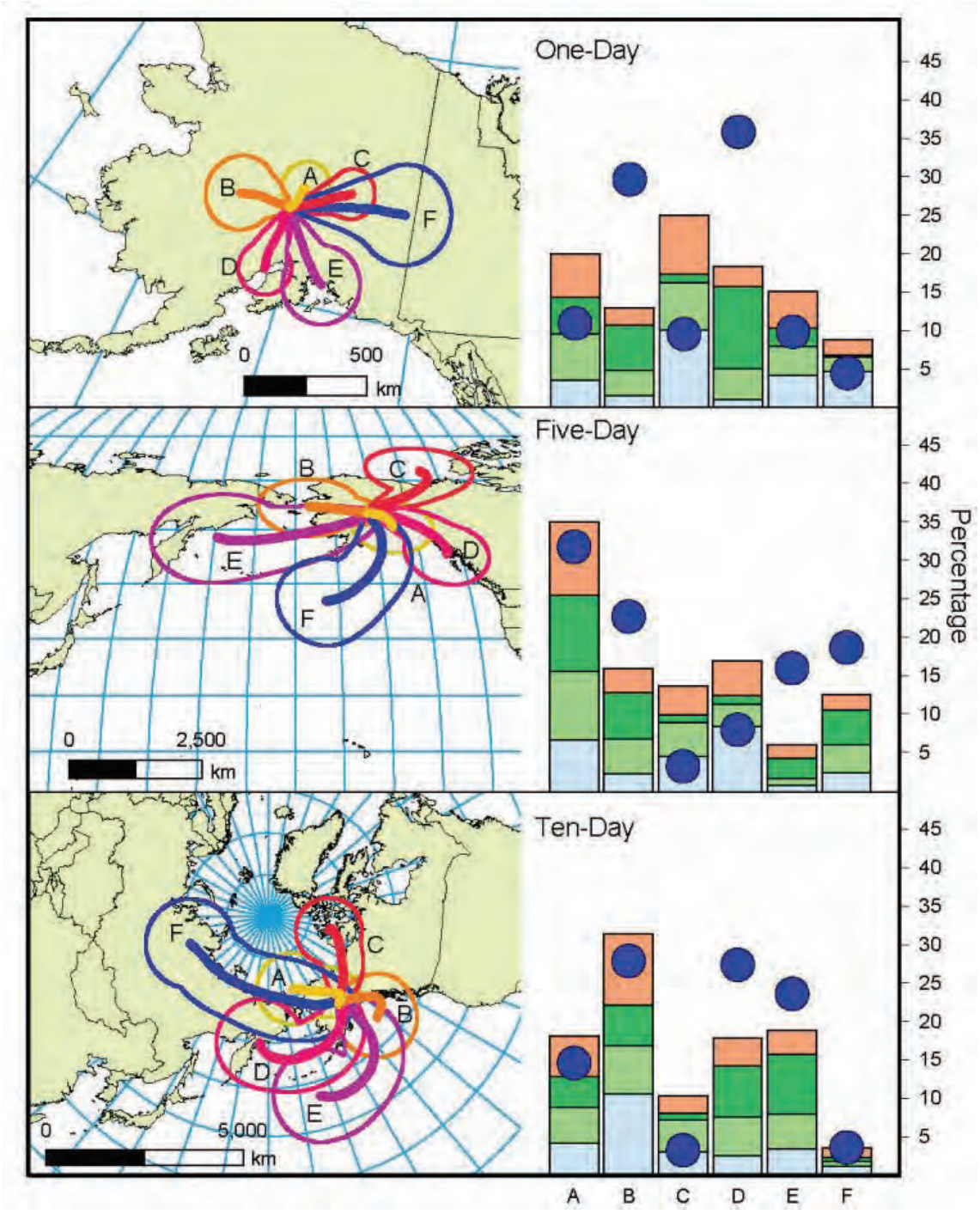

Figure 4-52. 1-, 5-, and 10-Day Cluster Plots for DENA. Each cluster represents the average transport pathway for a group of individual trajectories. Clusters are sorted shortest to longest, A–F. Bars represent the percent of trajectories in each cluster out of 2,922 total (1998-2005). Light blue = winter; light green = spring; dark green = summer; orange = autumn. The dark blue dot is the percent of total precipitation for which each cluster is responsible.

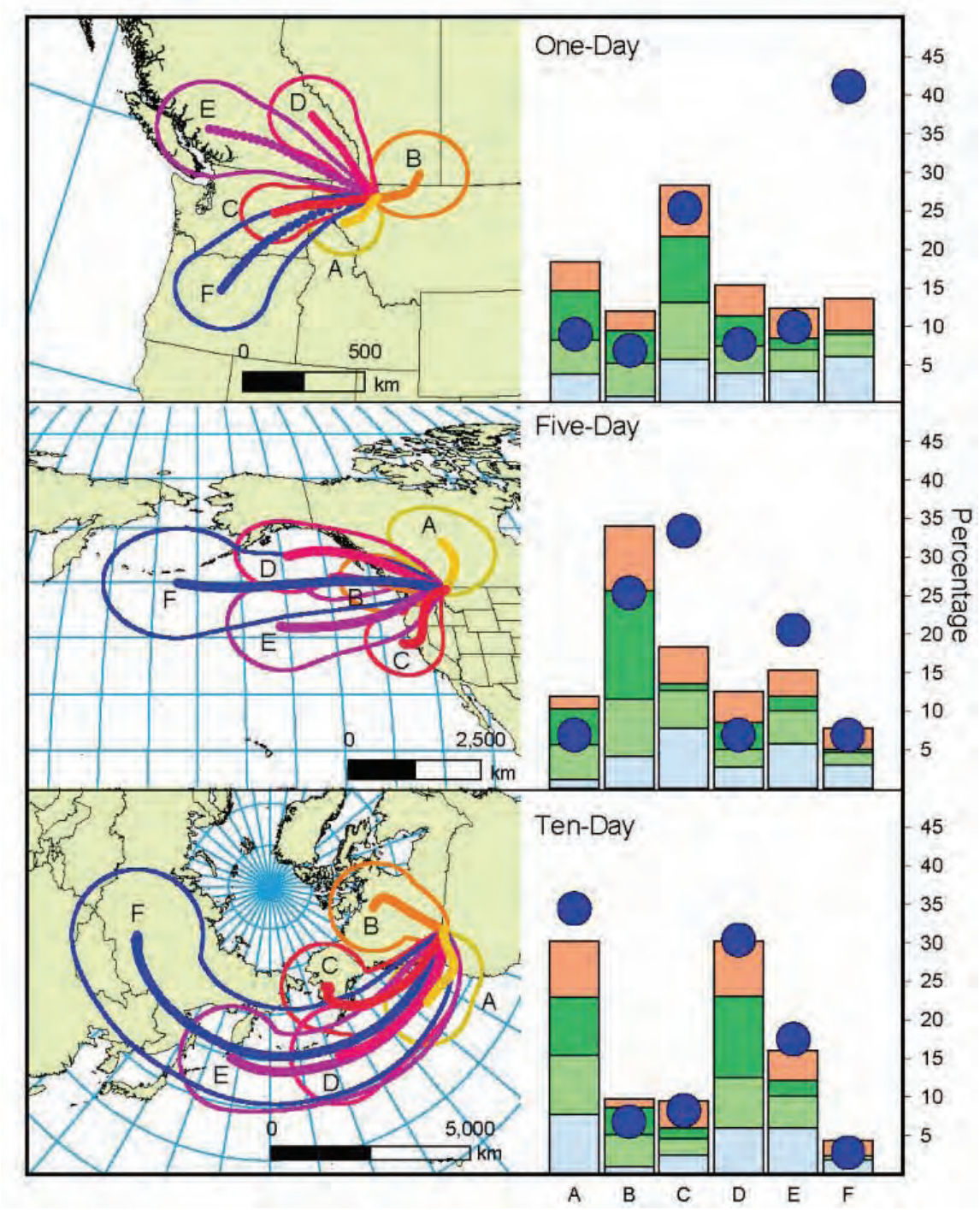

Figure 4-53. 1-, 5-, and 10-Day Cluster Plots for GLAC. Each cluster represents the average transport pathway for a group of individual trajectories. Clusters are sorted shortest to longest, A–F. Bars represent the percent of trajectories in each cluster out of 2,922 total (1998-2005). Light blue = winter; light green = spring; dark green = summer; orange = autumn. The dark blue dot is the percent of total precipitation for which each cluster is responsible.

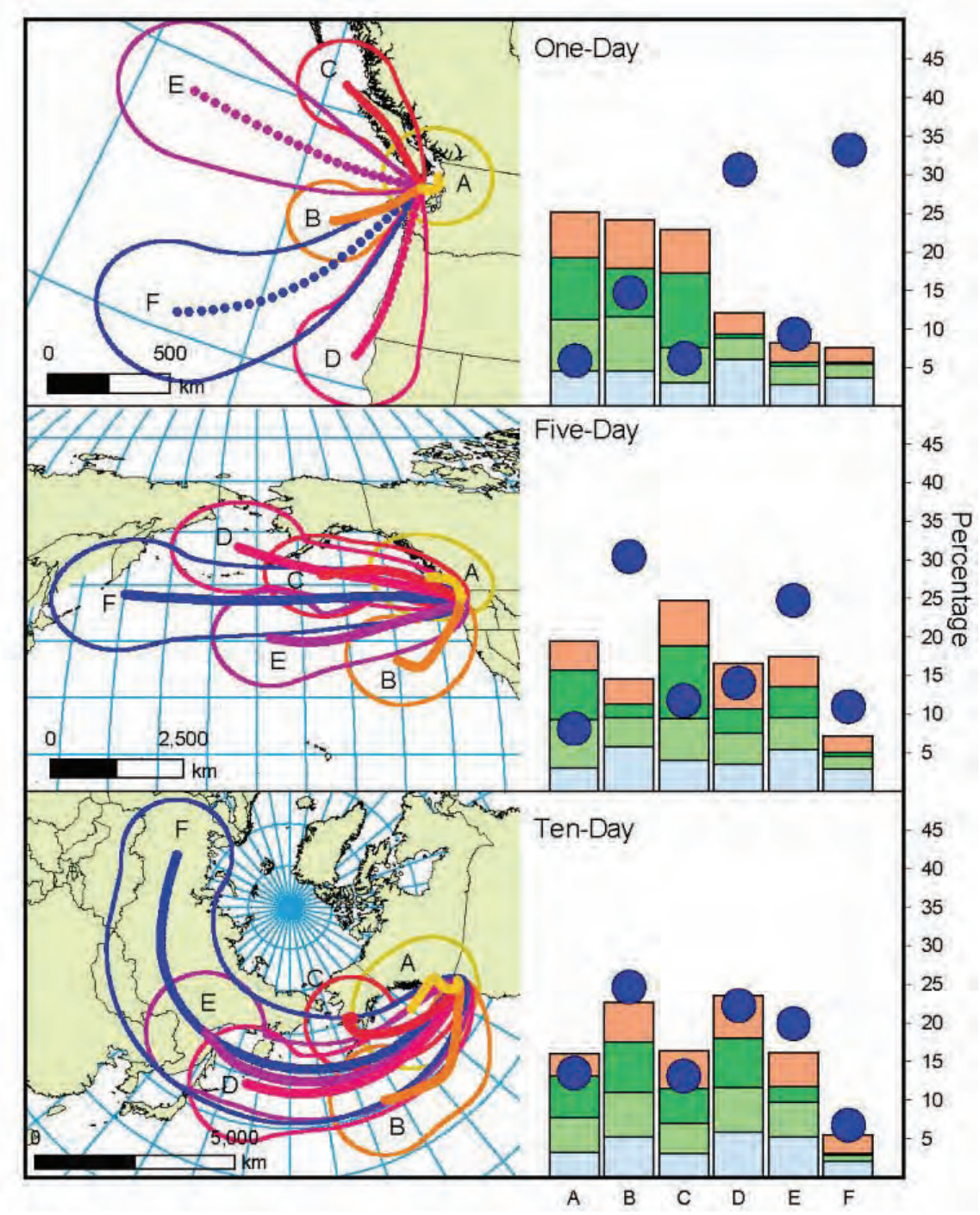

Figure 4-54. 1-, 5-, and 10-Day Cluster Plots for OLYM. Each cluster represents the average transport pathway for a group of individual trajectories. Clusters are sorted shortest to longest, A–F. Bars represent the percent of trajectories in each cluster out of 2,922 total (1998-2005). Light blue = winter; light green = spring; dark green = summer; orange = autumn. The dark blue dot is the percent of total precipitation for which each cluster is responsible.

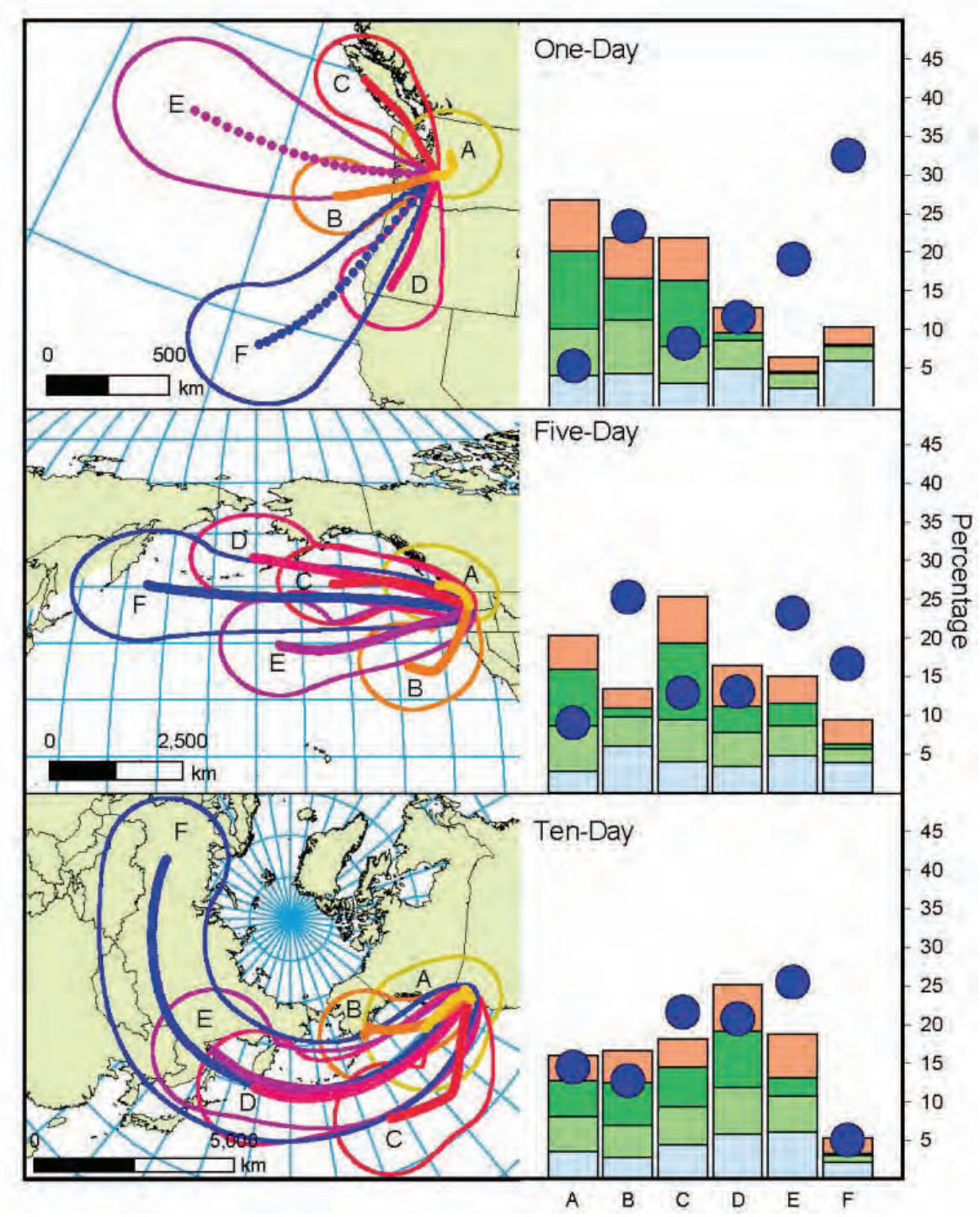

Figure 4-55. 1-, 5-, and 10-Day Cluster Plots for MORA. Each cluster represents the average transport pathway for a group of individual trajectories. Clusters are sorted shortest to longest, A–F. Bars represent the percent of trajectories in each cluster out of 2,922 total (1998-2005). Light blue = winter; light green = spring; dark green = summer; orange = autumn. The dark blue dot is the percent of total precipitation for which each cluster is responsible.

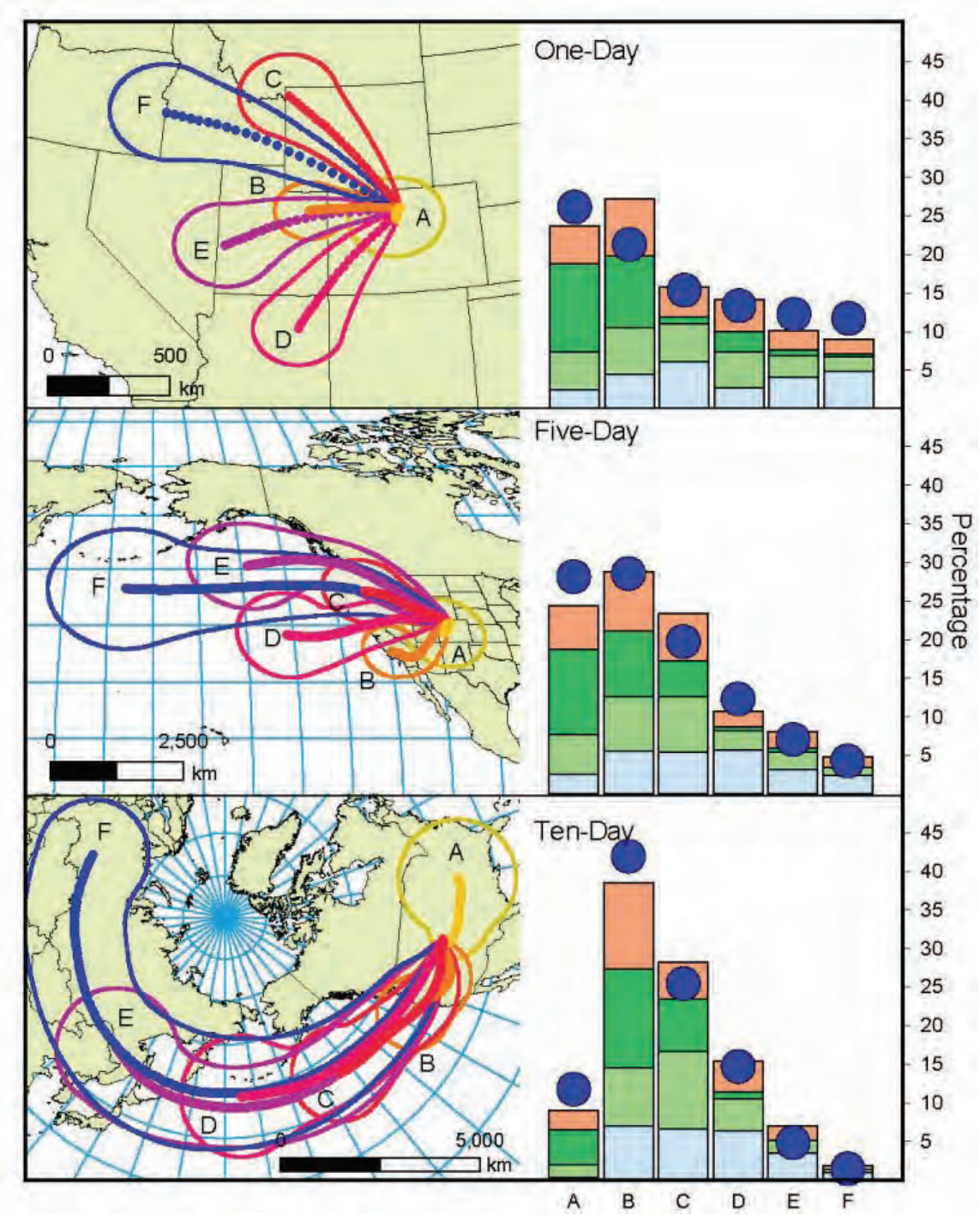

Figure 4-56. 1-, 5-, and 10-Day Cluster Plots for ROMO. Each cluster represents the average transport pathway for a group of individual trajectories. Clusters are sorted shortest to longest, A–F. Bars represent the percent of trajectories in each cluster out of 2,922 total (1998-2005). Light blue = winter; light green = spring; dark green = summer; orange = autumn. The dark blue dot is the percent of total precipitation for which each cluster is responsible.

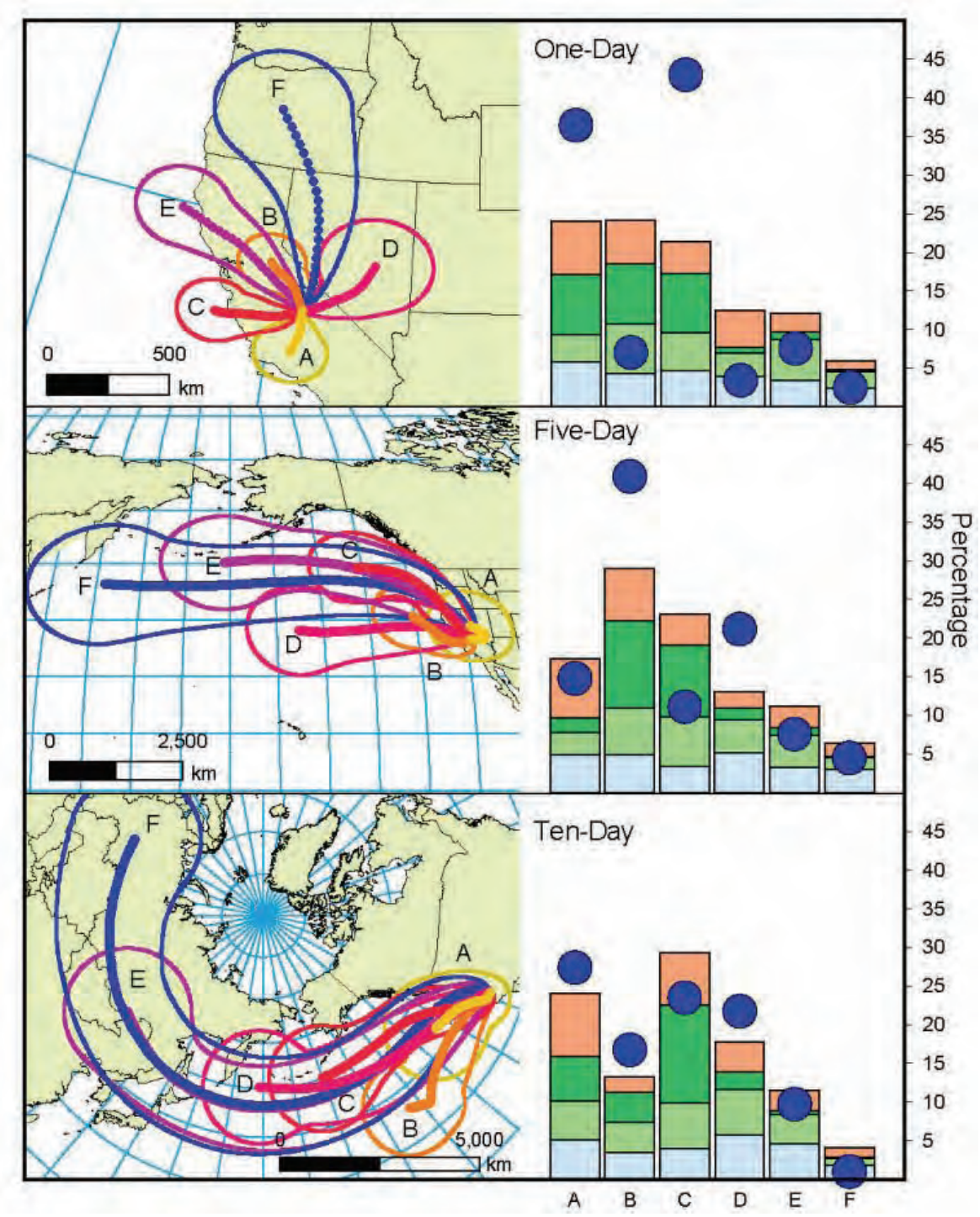

Figure 4-57. 1-, 5-, and 10-Day Cluster Plots for SEKI. Each cluster represents the average transport pathway for a group of individual trajectories. Clusters are sorted shortest to longest, A–F. Bars represent the percent of trajectories in each cluster out of 2,922 total (1998-2005). Light blue = winter; light green = spring; dark green = summer; orange = autumn. The dark blue dot is the percent of total precipitation for which each cluster is responsible.

SOCs measured in Alaska are attributed to background sources or long-range transport. Figure 4-52 shows the clusters for DENA. Within 5 days, likely sources include Siberia and coastal British Columbia. An important aspect of the Alaska clusters is that they are the shortest among clusters for all the sites. The WACAP sites at DENA and NOAT and GAAR are at low elevations, so these trajectories were calculated at ground level. The result was slower moving, less distinguishable air masses.

4.6 Summary

WACAP conducted extensive sampling in 8 core and 12 secondary parks in the western United States from 2003 to 2006. In the core parks, samples of lake water, snow, air, vegetation (lichen and conifer needles), fish, and lake sediments were collected from two watersheds in each park, except the Arctic parks NOAT and GAAR, where one watershed was sampled in each park. In the secondary parks, only lichen, conifer, and air samples were collected in 4-6 sites along an elevational gradient. Samples were analyzed for SOCs (current-use and historic-use pesticides, industrial compounds, and PAHs), mercury, and other metals. Lichen samples were also analyzed for nitrogen content. The data are presented and analyzed in this chapter. From these observations, we have drawn a number of conclusions, as follows:

1. Total SOC concentrations in snow were highest in interior (GLAC and ROMO) and in California (SEKI) parks. The highest SOC concentrations in vegetation were measured at SEKI, GLAC, YOSE, and GRSA.

2. At parks with the highest SOC concentrations in vegetation, the total SOC concentration was dominated by current-use pesticide residues, notably endosulfans and dacthal.

3. Lichen concentrations of PCBs and the pesticides chlorpyrifos, dacthal, endosulfans, HCB, a-HCH, g-HCH, chlordanes, and DDTs increased with elevation at most of the WACAP parks for which there were sufficient data, suggesting that these compounds are undergoing cold fractionation. Concentrations of PAHs decreased with elevation at most parks.

4. Similar SOC concentrations were detected in lichens and conifer needles, but lichens had concentrations 2-9 times greater, except for a-HCH and g-HCH, for which concentrations were similar. Despite lipid normalization, different species of lichens and conifers accumulated different concentrations of SOCs; sampling a single species aids site-to-site comparisons.

5. The magnitude of SOC concentrations in the seasonal snowpack varied substantially year to year, but the percent contribution of each SOC was fairly consistent from year to year for a given park.

6. Concentrations of flame retardants (PBDEs) and historic-use pesticides in WACAP fish were approximately 3 times higher and 2-9 times lower, respectively, than concentrations in fish from similar alpine environments in Europe. Concentrations of dieldrin in fish at some parks (notably ROMO and SEKI) were significantly elevated compared with concentrations in fish from similar Canadian studies.

7. At parks in the conterminous 48 states, good correlations were observed between concentrations of CUPs in snow and vegetation versus percent cropland within 150 km and, in the

case of vegetation, ammonium nitrate concentrations in ambient fine particulates measured by IMPROVE. Based on this relationship, we conclude that most of the CUP deposition comes from regional agricultural sources.

8. For some compounds (e.g., dacthal), pesticide application data are missing for significant regions of the western United States, limiting the ability to accurately identify sources.

9. PAH concentrations in snow, sediment, and vegetation in the Snyder Lake watershed at GLAC were higher than concentrations in the Oldman Lake watershed and in other WACAP parks. Several lines of evidence point to the aluminum smelter in Columbia Falls, Montana, as the most likely source.

10. The evidence suggests that SOC and Hg deposition to Mills Lake, on the east side of the Continental Divide in ROMO, is higher than deposition to Lone Pine Lake, on the west side. This finding might be because the Continental Divide serves as a topographic barrier for transport of SOCs and Hg from populated areas on the east side of ROMO to the west side. SOC concentrations in air, conifer needles, and fish show no clear evidence of an east side enhancement.

11. Snow, lake sediment, and vegetation data indicate that Hg flux to parks in the conterminous 48 states is greater than flux to the parks in Alaska. Despite this observation, fish in the Alaska parks had the highest concentrations of Hg. This finding could be a result of several factors, including fish age, Hg methylation rate, watershed biogeochemical characteristics, and foodweb efficiency as it relates to bioaccumulation.

12. Temporal records from sediment cores indicate that in nearly all parks, Hg deposition increased in the twentieth century because of anthropogenic sources. At some parks, Hg deposition fluxes have declined somewhat since the 1970-1980 time period, although at other parks, the Hg flux appears still to be increasing. This finding reflects a complex array of decreasing regional sources combined with increasing global contributions, complicated by the effects of watershed processes on the sedimentation record.

13. Pb, Cd, and SCPs indicate regional fossil fuel combustion sources. SCPs in lake sediments clearly show increasing contributions from industrial sources in the conterminous 48 states during the late twentieth century. In recent decades, Pb, Cd, and SCPs have declined substantially, reflecting source reductions resulting from the Clean Air Act and regulations on lead in gasoline. Lead concentrations in lichens at SEKI and MORA have decreased 5- to 6-fold since the 1980s.

14. In the Alaska lake sediments, SCPs were non-detectable and Pb and Cd showed little signs of a twentieth century increase. Only the Hg flux showed a consistent increase in the Alaska lake sediments, reflecting a primary contribution from global sources.

15. Nitrogen concentrations in lichens from SEKI, GLAC, BAND, and BIBE were elevated, indicating enhanced nitrogen deposition in these parks. Lichen sulfur concentrations indicated enhanced S deposition at SEKI and GLAC.